SUPPORTING INFORMATION

Standardized excitable elements for scalable engineering of far-from-equilibrium chemical networks

Table of Contents

1. Genelet design and network assembly workflow

1.1 Node species and reactions

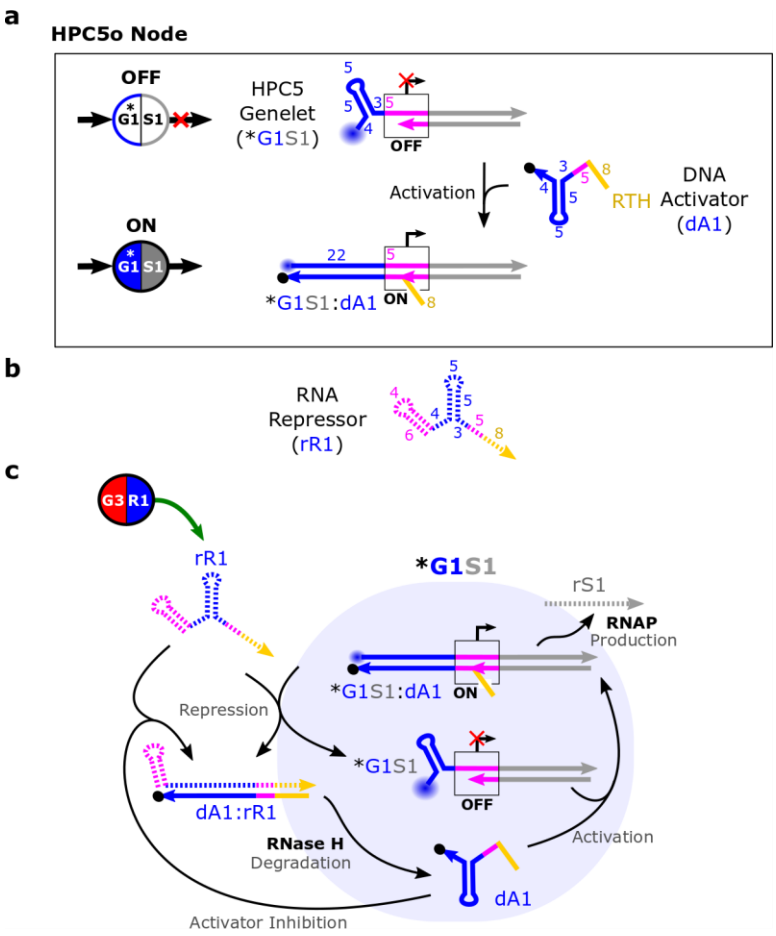

Supplementary Figure 1 | The species that make up a HPC5o node, the RNAs that regulate node activity, and the designed reactions for HPC5o node regulation. (**a**) A HPC5o genelet and DNA activator. HPC5o genelets are denoted with a * through the text. r and d prefixes denote RNA and DNA species, respectively. Numbers indicate domain lengths in nucleotides. (**b**) RNA regulators of an HPC5o node. (**c**) Designed HPC5o reactions by which the *G1S1 node can be repressed by the production of rR1 by an upstream node with output domain R1 (such as G3R1, shown here).

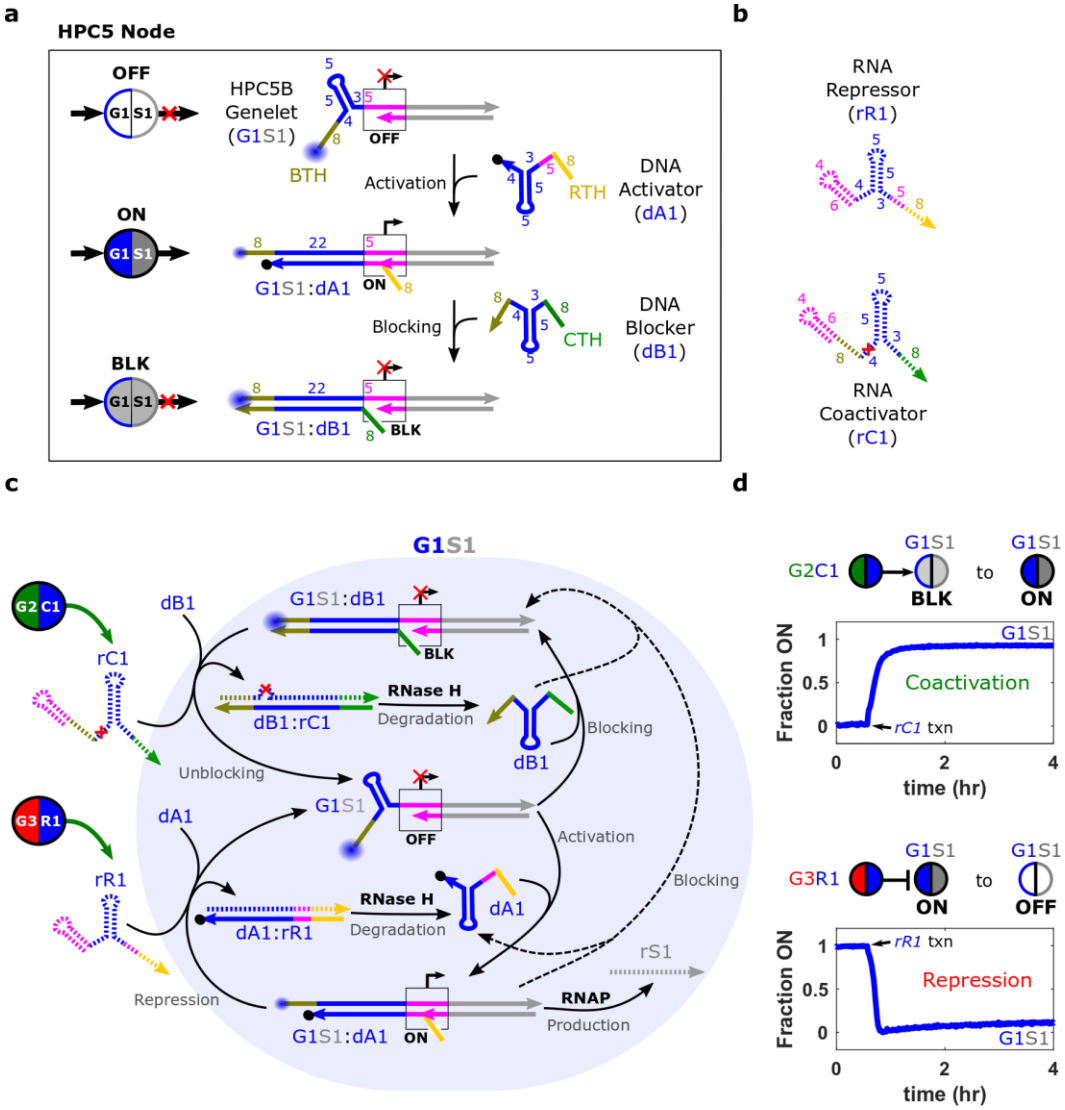

Supplementary Figure 2 | The species that make up a HPC5 node, the RNAs that regulate node activity, and the designed reactions for HPC5 node regulation. (**a**) A HPC5 genelet, DNA activator and DNA blocker. r and d prefixes denote RNA and DNA species, respectively. Numbers indicate domain lengths in nucleotides. (**b**) RNA regulators of an HPC5 node. (**c**) Designed genelet reactions by which the G1S1 node can be coactivated by rC1, which could be produced by an upstream node with output domain C1 (such as G2C1, shown here) or repressed by the production of rR1 by an upstream node with output domain R1 (such as G3R1, shown here). Dashed lines for the arrows showing the reaction between G1S1:dA1 and dB1 where the blocker displaces the activator, reversing the activation reaction are used to visually distinguish these reaction arrows from overlapping ones. (**d**) Normalized G1S1 activation levels before, during and after transcriptional coactivation (top) or repression (bottom). Induced by adding the active upstream transcriptional templates (G2C1 or G3R1) were added at the times pointed to by the arrows. Reactions were conducted as described in the Methods of the main text with all genelets at 25 nM and dA1 at 250 nM.

1.2 Protocol for combining sequences and strands together to assemble genelets

Supplementary Table 1 enumerates the sequences for the library of 11 standardized nodes developed in this work. To aid in the reuse of these nodes in other networks, nodes are separated into input (I) and output (O) domain sequences that can be combined to produce the desired nodes for an arbitrary network. All of the exact sequences used in the networks presented in the main text are tabulated in the networks' corresponding Supplementary Sections.

Here we describe how to combine the sequences in Supplementary Table 1 to produce the strands for a given genelet node. Each genelet is composed of a non-template (nt) and a template strand (t). Each non-template (nt) strand is split into an input and an output domain (Supplementary Figure 3a, left). The input domain sequences of the 11 standardized nodes we identified in Supplementary Section 4 are labeled G1 through G11 in Supplementary Table 1. The sequences of each genelet's DNA activator and blocker are tabulated with the corresponding input domain number, *i.e* dA1 and dB1 are the activator and blocker of G1, respectively. Two nodes can be connected by choosing an output domain for the first genelet that produces either the RNA repressor or the RNA coactivator of the second genelet. The sequences of the output domains for the 11 standardized nodes are tabulated with corresponding numbers, *i.e.* R1-nt encodes the RNA repressor for G1 and C4-nt encodes the RNA coactivator for G4 and so on. To design a genelet that regulates another genelet, the output domain sequence of the genelet to be regulated should be appended to the 3' end of the input domain sequence of the genelet directing the regulation. Merging these two sequences produces the non-template strand of the desired genelet. For example, to design G2C5-nt, the sequence of C5-nt would be added to the 3' end of the G2 sequence in Supplementary Table 1 (Supplementary Figure 3b *1.*).

To form genelets from their component strands, the non-template strand should be annealed with the corresponding template strand to produce a genelet in the OFF state, *i.e.* G2C5-nt would be annealed with the C5-t strand. Genelets can also be annealed with their corresponding blocker strand to produce a blocked genelet, *i.e.* G2C5-nt and C5-t would be annealed with dB2 (Supplementary Figure 3b *2.*).

For the reporting nodes (GiD) the GiD-nt strand is annealed with the universal-t stand to produce an OFF GiD reporting node. To produce a BLK GiD reporting node, the GiD-nt, universal-t, and the corresponding blocker strand should be annealed together *i.e.* for BLK G1D, the G1D-nt, universal-t, and dB1 should be annealed together.

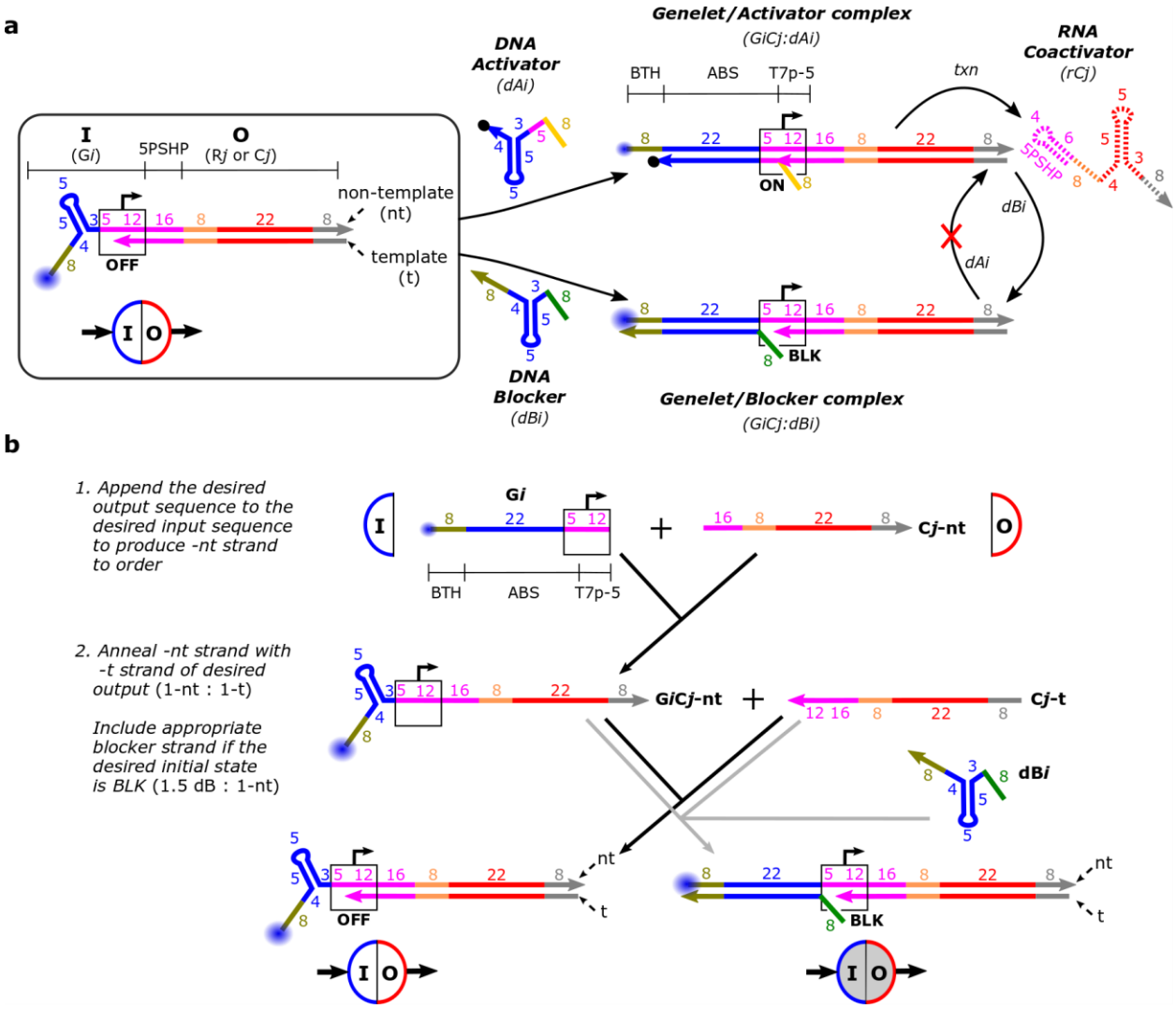

Supplementary Figure 3 | HPC5 genelet design and node assembly. (**a**) Each genelet is composed of two strands of DNA, a non-template strand (nt) that encodes the sequence of the RNA to be transcribed and a template (t) strand that T7 RNAP reads 3' -> 5' to produce a complementary RNA transcript. A genelet that is connected within a network has both an input (I) domain (G*i*) and an output (O) domain. The output domain can produce the RNA repressor (R*j*) or RNA coactivator (C*j*) or another genelet. (**b**) Schematic depicting how to assemble a genelet in either the OFF or BLK state. For reference, each input domain is comprised of three sub-domains: BTH – the 8-base toehold domain for the blocker, ABS – the 27-base activator binding site, and T7p-5 – the T7 RNAP promoter sequence missing the first five bases. The same procedure is followed to produce OFF or BLK GiD reporting nodes. Sequences are in Supplementary Table 1.

Supplementary Table 1 | Sequence motifs for assembling genelets and the sequences of the genelets' respective activators and blockers. Bidirectional regulation kinetic data for all domains is presented in Supplementary Section 4.4. Non-template and template strands of genelets are labeled with -nt and -t, respectively. All strands were ordered from Integrated DNA Technologies, Inc (IDT). Most of the activators and -nt and -t strands were ordered HPLC purified. The sub-domains of the (I)nput domains are separated and labeled below. Strands with N/A sequences correspond to nodes that only transcriptionally repressed or coactivated but not both. An "m" in front of a base designates the base as 2' methylated RNA. The truncated "dummy genelets" were used to monitor genelet states in some networks. * indicates that genelets lack the 8-base BTH at the 5' end of the -nt strand. The universal-t strand was the template strand for all dummy genelet complexes.

(I)NPUT DOMAINS	**BTH** **ABS** **T7p-5**
G1	5'TCCTTCCA TGCACGCCAAACCGTGGCGACGTAATA CGACTCACTATA
G2	5'AGCCAAGA TTCAGGTCAATAAGTGACCAAGTAATA CGACTCACTATA
G3	5'GAAGATGA AGGTGTACCGTATAGGTACTAGTAATA CGACTCACTATA
G4	5'GCTCTCCA TCTTCCAGGTACACCCTGGCTCTAATA CGACTCACTATA
G5	5'TCTCTTAC CCTCGCTCGTCCTCCGAGCCTCTAATA CGACTCACTATA
G6	5'CCAACCTA CTCTGCCGTTCCATACGGCTCCTAATA CGACTCACTATA
G7	5'CCACTTCA CCTTGTCGGCATTTCCGACTCCTAATA CGACTCACTATA
G8	5'GAATAGAA CAGAGGGTTAGCAGAACCCAGATAATA CGACTCACTATA
G9	5'CCAACTAC CTATGACTGTAACCCAGTCTCTTAATA CGACTCACTATA
G10	5'GATAAATA GAGAGCCGCACAGAGCGGCAGATAATA CGACTCACTATA
G11	5'GTCCAATT CCACGGCTCGTCAAGAGCCACCTAATA CGACTCACTATA
ACTIVATORS	
dA1	5'TCCAGCTCTATTACGTCGCCACGGTTTGGCGTGCA/3IABkFQ/
dA2	5'CATCCCACTATTACTTGGTCACTTATTGACCTGAA/3IABkRQSp/
dA3	5'CCGACAAATATTACTAGTACCTATACGGTACACCT/3IABkRQSp/
dA4	5'TGCGAGGATATTAGAGCCAGGGTGTACCTGGAAGA/3IABkFQ/
dA5	5'GGGACGAATATTAGAGGCTCGGAGGACGAGCGAGG/3BHQ_1/
dA6	5'GGAGATAATATTAGGAGCCGTATGGAACGGCAGAG
dA7	5'AGCGCAGATATTAGGAGTCGGAAATGCCGACAAGG/3IABkRQSp/
dA8	5'GTCGCGTGTATTATCTGGGTTCTGCTAACCCTCTG/3IABkRQSp/
dA9	5'AGCAGAAGTATTAAGAGACTGGGTTACAGTCATAG/3IABkRQSp/
dA10	5'TGTGCAATTATTATCTGCCGCTCTGTGCGGCTCTC
dA11	5'GTGCGTGTTATTAGGTGGCTCTTGACGAGCCGTGG/3IABkFQ/
BLOCKERS	
dB1	5'GAGTAGGTCGTCGCCACGGTTTGGCGTGCATGGAAGGA
dB2	5'GGTGTACGCTTGGTCACTTATTGACCTGAATCTTGGCT
dB3-2omR	5'GCTCGTTCCTAGTACCTATACGGTACmAmCmCmUmUmCmAmUmCmUmUmC
dB4	5'GGTAGGGTGAGCCAGGGTGTACCTGGAAGATGGAGAGC
dB5	5'GTAGTGTGGAGGCTCGGAGGACGAGCGAGGGTAAGAGA
dB6	5'GGTAGTGTGGAGCCGTATGGAACGGCAGAGTAGGTTGG
dB7	N/A – COACTIVATION SLOW FOR THIS NODE
dB8-2omR	5'CCTCGTCCTCTGGGTTCTGCTAACCCmUmCmUmGmUmUmCmUmAmUmUmC
dB9	5'GATGGGCGAGAGACTGGGTTACAGTCATAGGTAGTTGG
dB9-2omR	5'GATGGGCGAGAGACTGGGTTACAGTCmAmUmAmGmGmUmAmGmUmUmGmG
dB10-2omR	5'CCTCCCGCTCTGCCGCTCTGTGCGGCmUmCmUmCmUmAmUmUmUmAmUmC
dB11	N/A – COACTIVATION SLOW FOR THIS NODE

Continued...

REPRESSOR (O)UTPUT-nt	5PSHP A-linker R_i
R1-nt	5′GGGAGATTCGTCTCCC A TGCACGCCAAACCGTGGCGACGTAATAGAGCTGGA
R2-nt	5′GGGAGATTCGTCTCCC A TTCAGGTCAATAAGTGACCAAGTAATAGTGGGATG
R3-nt	5′GGGAGATTCGTCTCCC A AGGTGTACCGTATAGGTACTAGTAATATTTGTCGG
R4-nt	5′GGGAGATTCGTCTCCC A TCTTCCAGGTACACCCTGGCTCTAATATCCTCGCA
R5-nt	5′GGGAGATTCGTCTCCC AAA CCTCGCTCGTCCTCCGAGCCTCTAATATTCGTCCC
R6-nt	N/A – REPRESSION SLOW FOR THIS NODE
R7-nt	5′GGGAGATTCGTCTCCC AAA CCTTGTCGGCATTTCCGACTCCTAATATCTGCGCT
R8-nt	5′GGGAGATTCGTCTCCC AAA CAGAGGGTTAGCAGAACCCAGATAATACACGCGAC
R9-nt	N/A – REPRESSION SLOW FOR THIS NODE
R10-nt	N/A – REPRESSION SLOW FOR THIS NODE
R11-nt	5′GGGAGATTCGTCTCCC AAA CCACGGCTCGTCAAGAGCCACCTAATAACACGCAC
REPRESSOR (O)UTPUT-t	
R1-t	5′TCCAGCTCTATTACGTCGCCACGGTTTGGCGTGCATGGGAGACGAATCTCCCTATAGTGAGTCG
R2-t	5′CATCCCACTATTACTTGGTCACTTATTGACCTGAATGGGAGACGAATCTCCCTATAGTGAGTCG
R3-t	5′CCGACAAATATTACTAGTACCTATACGGTACACCTTGGGAGACGAATCTCCCTATAGTGAGTCG
R4-t	5′TGCGAGGATATTAGAGCCAGGGTGTACCTGGAAGATGGGAGACGAATCTCCCTATAGTGAGTCG
R5-t	5′GGGACGAATATTAGAGGCTCGGAGGACGAGCGAGGTTTGGGAGACGAATCTCCCTATAGTGAGTCG
R6-t	N/A – REPRESSION SLOW FOR THIS NODE
R7-t	5′AGCGCAGATATTAGGAGTCGGAAATGCCGACAAGGTTTGGGAGACGAATCTCCCTATAGTGAGTCG
R8-t	5′GTCGCGTGTATTATCTGGGTTCTGCTAACCCTCTGTTTGGGAGACGAATCTCCCTATAGTGAGTCG
R9-t	N/A – REPRESSION SLOW FOR THIS NODE
R10-t	N/A – REPRESSION SLOW FOR THIS NODE
R11-t	5′GTGCGTGTTATTAGGTGGCTCTTGACGAGCCGTGGTTTGGGAGACGAATCTCCCTATAGTGAGTCG
COACTIVATOR (O)UTPUT-nt	5PSHP A-linker C_i
C1-nt	5′GGGAGATTCGTCTCCC AAA TCCTTCCATGAACGCCAAACCGTGGCGACGACCTACTC
C2-nt	5′GGGAGATTCGTCTCCC AA AGCCAAGATTAAGGTCAATAAGTGACCAAGCGTACACC
C3-nt	5′GGGAGATTCGTCTCCC A GAAGATGAAGATGTACCGTATAGGTACTAGGAACGAGC
C4-nt	5′GGGAGATTCGTCTCCC A GCTCTCCATCCTCCAGGTACACCCTGGCTCACCCTACC
C5-nt	5′GGGAGATTCGTCTCCC A TCTCTTACCCACGCTCGTCCTCCGAGCCTCCACACTAC
C6-nt	5′GGGAGATTCGTCTCCC AAA CCAACCTACTATGCCGTTCCATACGGCTCCACACTACC
C7-nt	N/A – COACTIVATION SLOW FOR THIS NODE
C8-nt	5′GGGAGATTCGTCTCCC A GAATAGAACAAAGGGTTAGCAGAACCCAGAGGACGAGG
C9-nt	5′GGGAGATTCGTCTCCC AA CCAACTACCTCTGACTGTAACCCAGTCTCTCGCCCATC
C10-nt	5′GGGAGATTCGTCTCCC A GATAAATAGAAAGCCGCACAGAGCGGCAGAGCGGGAGG
C11-nt	N/A – COACTIVATION SLOW FOR THIS NODE
COACTIVATOR (O)UTPUT-t	
C1-t	5′GAGTAGGTCGTCGCCACGGTTTGGCGTTCATGGAAGGATTTGGGAGACGAATCTCCCTATAGTGAGTCG
C2-t	5′GGTGTACGCTTGGTCACTTATTGACCTTAATCTTGGCTTTGGGAGACGAATCTCCCTATAGTGAGTCG
C3-t	5′GCTCGTTCCTAGTACCTATACGGTACATCTTCATCTTCTGGGAGACGAATCTCCCTATAGTGAGTCG
C4-t	5′GGTAGGGTGAGCCAGGGTGTACCTGGAGGATGGAGAGCTGGGAGACGAATCTCCCTATAGTGAGTCG
C5-t	5′GTAGTGTGGAGGCTCGGAGGACGAGCGTGGGTAAGAGATGGGAGACGAATCTCCCTATAGTGAGTCG
C6-t	5′GGTAGTGTGGAGCCGTATGGAACGGCATAGTAGGTTGGTTTGGGAGACGAATCTCCCTATAGTGAGTCG
C7-t	N/A – COACTIVATION SLOW FOR THIS NODE
C8-t	5′CCTCGTCCTCTGGGTTCTGCTAACCCTTTGTTCTATTCTGGGAGACGAATCTCCCTATAGTGAGTCG
C9-t	5′GATGGGCGAGAGACTGGGTTACAGTCAGAGGTAGTTGGTTGGGAGACGAATCTCCCTATAGTGAGTCG
C10-t	5′CCTCCCGCTCTGCCGCTCTGTGCGGCTTTCTATTTATCTGGGAGACGAATCTCCCTATAGTGAGTCG
C11-t	N/A – COACTIVATION SLOW FOR THIS NODE

Continued...

DUMMY GENELETS	BTH	ABS
G1D-nt	/56-FAM/ TCCTTCCA	TGCACGCCAAACCGTGGCGACGTAATA CGACTCACTATAGGGAGA
G2D-nt	/5TYE665/AGCCAAGA	TTCAGGTCAATAAGTGACCAAGTAATA CGACTCACTATAGGGAGA
G4D-nt	/5HEX/ TGCTCTCCA	TCTTCCAGGTACACCCTGGCTCTAATA CGACTCACTATAGGGAGA
G5D-nt	/56-FAM/ TCTCTTAC	CCTCGCTCGTCCTCCGAGCCTCTAATA CGACTCACTATAGGGAGA
G8D-nt	/5Cy5/ GAATAGAA	CAGAGGGTTAGCAGAACCCAGATAATA CGACTCACTATAGGGAGA
*G1D-nt	/56-FAM/	TGCACGCCAAACCGTGGCGACGTAATA CGACTCACTATAGGGAGA
*G3D-nt	/5TEX615/	AGGTGTACCGTATAGGTACTAGTAATA CGACTCACTATAGGGAGA
*G4D-nt	/5HEX/	TCTTCCAGGTACACCCTGGCTCTAATA CGACTCACTATAGGGAGA
*G7D-nt	/5TEX615/	CCTTGTCGGCATTTCCGACTCCTAATA CGACTCACTATAGGGAGA
*G8D-nt	/5Cy5/	CAGAGGGTTAGCAGAACCCAGATAATA CGACTCACTATAGGGAGA
*G11D-nt	/5HEX/	CCACGGCTCGTCAAGAGCCACCTAATA CGACTCACTATAGGGAGA
universal-t	5'TCTCCCTATAGTGAGTCG	
S1-t	5'GTCACTGTCTGGTTAATCTGTATGTCTATAGTGAGTCG	

1.3 A summary of genelet design considerations useful when assembling networks

A full description of the genelet design process can be found in Supplementary Section 3; below are some features of the designs of genelets that can be helpful to understand when assembling genelet networks from the genelets synthesized in this work, which are listed in Supplementary Table 1.

As described in Supplementary Section 4, some of the nodes could be efficiently coactivated by upstream transcripts but not efficiently repressed by RNA transcripts, or vice versa. For example, G6, G9, and G10 can be coactivated by upstream RNA transcription but take over 4 hours to repress with transcription. G7 and G11 can be repressed by upstream RNA transcription but take over 4 hours to coactivate with transcription. Thus, these nodes should only be used at positions in networks where the nodes need only to be either coactivated or repressed. The coactivator or repressor sequences for nodes that cannot either be effectively coactivated or repressed by RNA transcripts are not listed in Supplementary Table 1 – an "N/A" label is there instead along with a description of the observed activation or repression behavior.

For nodes that will only be repressed in a network, the blocking toehold sub-domain (BTH) of the input domain is optional and the HPC5o genelet design can be used (Supplementary Figure 1). For example, a node in a network that will only ever be repressed and will never be coactivated does not need the BTH sequence or a DNA blocker. Thus, in the TSN, which is composed of only repression reactions, the HPC5o design that does not include the BTH sequence was used for all the nodes in this network. Additionally, the bi-stable module nodes (nodes with G7 or G8 input domains) in the BS_IFFL1|2 network used the HPC5o design without BTH sequences. The BTH sequences were left out because they were unnecessary, and their exclusion meant that the genelet's non-template strand was <100 bases and thus cheaper to synthesize by IDT. All sequences and nodes that use the HPC5o design without the BTH domains are denoted with a * in subsequent sections and in the main text.

The 5' end of each RNA coactivator and repressor contains a hairpin structure (5PSHP in Supplementary Table 1) followed by an adenine or poly-adenine linker (A-linker in Supplementary Table 1). This hairpin structure was included in every transcript sequence because we observed that sequences containing the hairpin could regulate their target nodes more efficiently (Supplementary Figure 10). The poly-A linkers were included to prevent the formation of secondary structure within the RNAs if any additional

guanines were added spuriously to the 5' end of the RNAs during transcription, as has been reported previously[1].

The 3' ends of the non-template sequences that are >100 bases in length can be truncated to produce sequences less than 100 bases so they can be ordered as regular oligonucleotides from IDT, rather than ultramers. This truncation still produces the full transcript as T7 RNAP reads through the 5' single-stranded overhang of the template strand[2]. We did find, as reported previously[3], that extensively truncating the 3' end of non-template strand can reduce the rate of transcription for certain sequences (Supplementary Figure 12), so excessive truncation should be avoided if possible.

Genelet autoactivation can occur for some genelets when their DNA blocker strands are present. To prevent autoactivation, the last 12 bases of the 3' ends of these problematic blockers were changed to 2' methylated RNA, which prevented this phenomenon (Supplementary Section 8). Such DNA blocker sequences are denoted with the suffix -2omR in Supplementary Table 1 and the methylated RNA bases are listed with "m"s in front of them. It is recommended that the methylated RNA version of blocker strands whose 2' methylated RNA version is listed in Supplementary Table 1 be used when assembling networks.

2. An HPC genelet variant with reduced autoinhibition

In previous work we identified an undesired genelet autoinhibition reaction, a phenomenon where some genelets incubated with T7 RNAP in transcription conditions could turn themselves off[4]. Autoinhibition was partially due to non-specific initiation of transcription at the single-stranded 3' repression toehold on the DNA activators bound to the genelets. Such initiation of transcription by T7 RNAP at single-stranded 3' ends has been previously reported in the literature[3,5]. We found that this autoinhibition reaction was prevalent both for the genelet design developed by Kim, White, and Winfree (KWW)[6] and the hairpin clamp genelet design we previously developed[4], which we refer to as HPC3 genelets. We hypothesized that we could move the 3' repression toehold on the DNA activators to the 5' end of the DNA activators to mitigate genelet autoinhibition for future genelet designs.

We first assessed whether moving the toehold would significantly change the rate of transcription from a genelet:activator complex. The KWW genelets have an incomplete T7 RNAP promoter sequence that is completed by the 5' end of a genelet's DNA activator. In such a design, a genelet bound to its activator has a nick in the promoter region. Transcription is roughly 50% slower from the resulting complex than from a promoter without a nick[6]. Moving the 3' repression toehold of a DNA activator to the 5' end of the activator would introduce a 5' single-stranded domain that extends out from the nick in the promoter region, potentially decreasing the rate of transcription further or completely preventing transcription. We tested whether a DNA activator with a 5' repression toehold could be used to activate genelet transcription by comparing the transcription rate from a genelet bound to an activator that had a 3' repression toehold to the transcription rate from a genelet bound to an activator that had a 5' repression toehold. Genelets with both activator designs were successfully transcribed; using the activator with a 5' repression toehold did slow down transcription by a factor of two compared to the activator with a 3' repression toehold (Supplementary Figure 4).

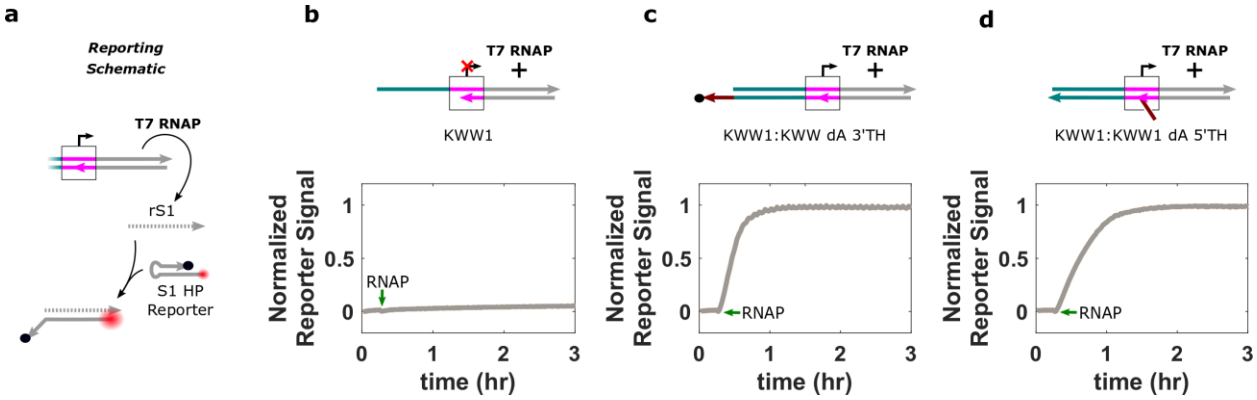

Supplementary Figure 4 | Rates of transcription from genelets bound to activators with 3' *vs* 5' repression toeholds. (**a**) Reporting scheme used to measure the amount of RNA produced by the KWW1 genelet. (**b**) Normalized reporter signal during transcription of the KWW1 node without a DNA activator. (**c**) Normalized reporter signal during transcription of the KWW1 node using a DNA activator with a 3' repression toehold. (**d**) Normalized reporter signal during transcription of the KWW1 node using a DNA activator with a 5' repression toehold. Transcription reactions conducted as described in the Methods of the main text with [S1 HP reporter] = 125 nM, [KWW 1] = 17.5 nM, [DNA activators] = 1 µM, [T7 RNAP] = 2.86 U/µL, and no other enzymes present. Excess of a DNA version of S1 was added at the end of the experiment to obtain an internal maximum reporter fluorescence signal for normalization. Sequences for the reporter, genelet, and activator strands are in Supplementary Table 2.

Since our goal was to build scalable genelet networks using genelet elements with low potential for crosstalk with other network components, we next sought to merge the 5' repression toehold activator design with our previously developed hairpin clamp (HPC3) genelets. The use of hairpins in the HPC3 design minimized the lengths of domains that were exposed and thus could participate in crosstalk reactions. However, we found that merely moving the repression toehold from the 3' end to the 5' end of the activators (HPC5_08 variant) dramatically decreased the rate of genelet activation (Supplementary Figure 5a,b).

To speed up the activation kinetics for DNA activators with 5' repression toeholds, we modified the HPC5_08 activator design so that the activation reaction would have two initiation toeholds, one on each side of the hairpin duplex. We tried two different designs, one with 4 and 8 base toeholds and another with 7 and 5 base toeholds (HPC5o and HPC5_75, respectively, in Supplementary Figure 5c,d). Both designs improved activation kinetics, allowing activation to occur as quickly as the HPC3 activator design. Additionally, the HPC5o and HPC5_75 variants had fast repression kinetics (Supplementary Figure 5c,d).

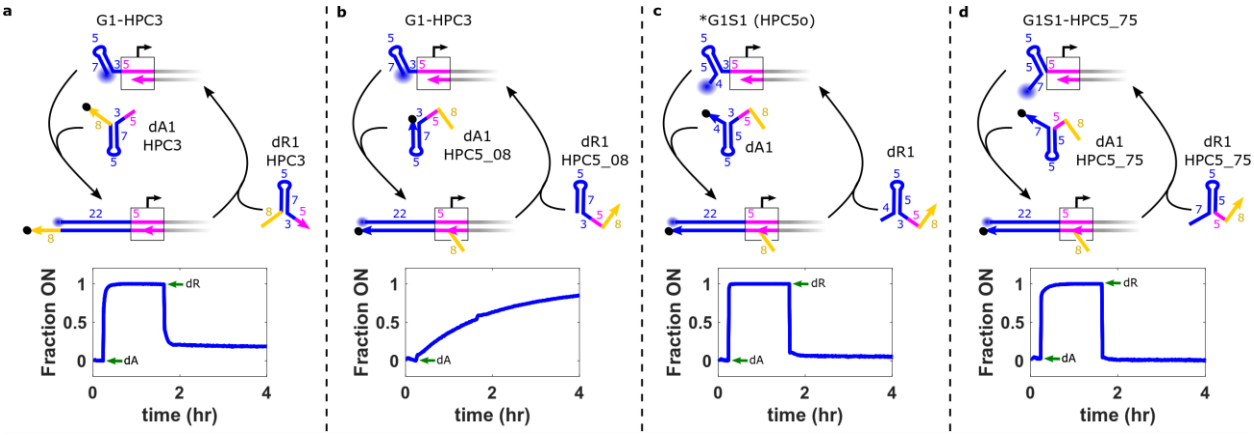

Supplementary Figure 5 | Kinetics of DNA activation and DNA repression of HPC genelet variants. (**a-d**) Normalized activation levels during activation and repression of HPC genelet variants using a DNA activator containing (**a**) a 3' repression toehold (3'TH) and 0-base 3' and 8-base 5' activation toeholds, (**b**) a 5' repression toehold (5'TH) 0-base 3' and 8-base 5' activation toeholds, (**c**) a 5' repression toehold (5'TH) and 4-base 3' and 8-base 5' activation toeholds, (**d**) a 5' repression toehold (5'TH) and 7-base 3' and 5-base 5' activation toeholds. Reactions were conducted as described in the Methods of the main text in the absence of enzymes with [Genelets] = 100 nM, [Activators] = 500 nM, [Repressors] = 1000 nM. Sequences are in Supplementary Table 2.

We next measured the amount of autoinhibition exhibited by the HPC5o and HPC5_75 variants when incubated with T7 RNAP in transcription conditions. We first tested autoinhibition of the genelet:activator complexes without excess DNA activator and found that both the HPC5o and HPC5_75 designs exhibited significantly less autoinhibition compared to the HPC3 design (Supplementary Figure 6a). The genelet:activator complexes in both the HPC5o and HPC5_75 designs lack single-stranded 3' overhangs, which likely prevents significant autoinhibition. However, the unbound activators in these designs have 4-base and 7-base single-stranded 3' overhangs, respectively. These overhangs could facilitate initiation of promoter-independent transcription when excess activator is present, potentially resulting in autoinhibition[4,5,7]. We thus tested whether autoinhibition occurred for these designs when excess activator was present (4-fold excess activator compared to genelet). Both the HPC5o and HPC5_75 designs exhibited significantly less autoinhibition than the HPC3 design when excess activators were present. The HPC5o design exhibited slightly less autoinhibition than the HPC5_75 design (Supplementary Figure 6b). Based on these results, and the fact that the HPC5o design has only a 4-base single-stranded 3' overhang, we selected the HPC5o design to move forward with for further characterization. All genelets and nodes with the HPC5o design are denoted with a * throughout the text.

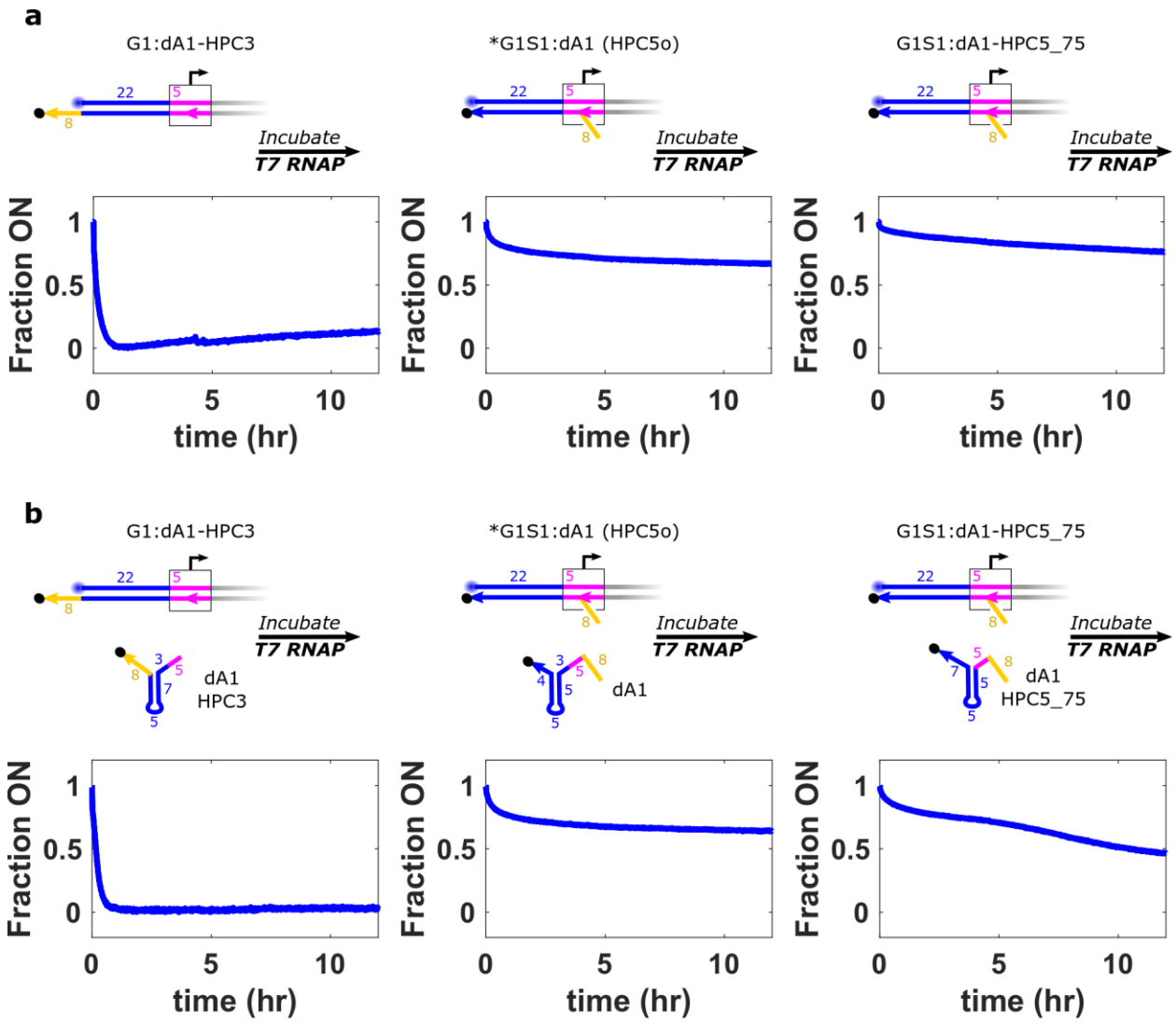

Supplementary Figure 6 | Characterization of the amount of autoinhibition exhibited by different HPC genelet variants. (**a**) Normalized activation levels of genelet:activator complexes during incubation with T7 RNAP in transcription conditions without excess activator. Genelet:activator variants are each shown above their plots of autoinhibition kinetics. Transcription reactions were conducted as described in the Methods of the main text with [Genelets] = 100 nM, [Activators] = 100 nM, [T7 RNAP] = 3.57 U/μL, and no other enzymes present. Sequences are in Supplementary Table 2. (**b**) Normalized activation levels of genelet:activator complexes and excess activators during incubation with T7 RNAP in transcription conditions. Genelet and activator variants are each shown above their respective plots of autoinhibition kinetics. Transcription reactions were conducted as described in the Methods of the main text with [Genelets] = 100 nM, [Activators] = 500 nM, [T7 RNAP] = 7.14 U/μL.

3. Design and characterization of HPC5 genelets with bidirectional regulation

The final HPC5o genelets designed in Supplementary Section 2 can be turned off (repressed) *via* transcription of an RNA repressor that sequesters the DNA activator. However, these genelets lack a mechanism to be turned on *via* transcription of an RNA signal. This section describes the process of designing such an RNA activation mechanism for the HPC5o genelets, thus allowing upstream transcription to both up- and down- (bidirectionally) regulate HPC5o genelet activity.

Since an RNA strand cannot directly serve as the activator for a genelet[8], we needed to design nodes such that genelets would not interact with their DNA activators until another strand was transcribed or added that changes the conformation of a node to allow activation to occur. In the designs we developed, we refer to nodes in a state in which they do not interact with their DNA activators as blocked (BLK) nodes.

There are two different ways to design BLK nodes. In one design, a genelet's DNA activator is sequestered in a DNA-DNA duplex and can only be freed for binding by the transcription or addition of an activator release (dAR or rAR) strand (Supplementary Figure 7a,b). In the other design, the input domain of a genelet is bound to a DNA blocker strand that prevents the DNA activator from binding to the genelet. The genelet can be freed for DNA activator binding by the transcription or addition of a coactivator (dC or rC) strand that displaces the blocker from the genelet (Supplementary Figure 8a,b).

Two important criteria were considered when developing a design for HPC genelets that can be bidirectionally regulated. First, the design should minimize off target hybridization interactions between components (crosstalk). Second, the RNA activation process must be reversible, *i.e.* if the RNA signal that triggers a BLK node to turn on is sequestered or degraded, then the node should return to the BLK state. This reversibility is key for building dynamic networks that can actuate multiple times. Crosstalk between node components was important to consider during design, as the ability to both up- and downregulate node activation introduces additional complementary sequence domains across components that could interfere with the activation process.

3.1 Constructing BLK nodes by sequestering DNA activators

To allow bidirectional regulation, we initially considered a BLK node design inspired by the mode of bidirectional regulation developed for KWW genelets[9]. In that design, the DNA activator of a genelet is bound to another DNA strand (dAB) to block the DNA activator from interacting with the genelet (Supplementary Figure 7a). An activator release strand (AR) can free the DNA activator from this complex *via* a toehold-mediated nucleic acid strand displacement. After release, the DNA activator can then bind to and activate its target genelet. We adopted this scheme for the HPC5P genelets (Supplementary Figure 7b). To ensure that release of the DNA activator by an AR strand was reversible, the DNA activator binding strand (dAB) was designed to have domains complementary to the 5' repression toehold of the DNA activator – the dAB strand could, by binding to this toehold, remove the DNA activator from the genelet:activator complex. Thus, if a BLK node is turned on by an AR strand and then the AR strand is subsequently sequestered or degraded, the free dAB strand will convert the ON node back to a BLK node.

A problem with this design is that the AR strand (for testing we used a DNA version of the activator release strand, dAR) that releases the DNA activator can also bind to the input domain of the genelet, as

the dAR strand has exactly the same sequence as the DNA activator – both are complementary to dAB. The binding of the AR strand to the genelet would block the DNA activator from binding to the genelet (Supplementary Figure 7c). In the case where the AR strand is RNA, the AR strand bound to the genelet domain would prevent transcription from occurring[8].

We thus created a series of modified designs for the dAB and AR strands in an attempt to address this problem. Although the AR strands would be RNA in networks, for testing purposes we used DNA versions. The undesired reaction between the AR strand and the genelet would occur *via* a 4-way branch migration process facilitated by two short toehold domains on either side of the AR strand's hairpin (Supplementary Figure 7c, right panel). If the AR design shown in Supplementary Figure 7c were used, then the AR strand and the DNA activator would bind to the genelet at the same rate. To slow down the kinetics of this potential side reaction, we created a variant of the AR strand (dARm) that had a single base mismatch with the genelet in one of the 4-way branch migration toeholds (Supplementary Figure 7d). We found that only 33% of the genelets bound to DNA activator when 1 μM of the dARm strand was added (Supplementary Fig. 7e), presumably because the dARm strand could still bind to the genelet rapidly. To decrease the rate of this undesired reaction further, we designed two more dARm variants with corresponding dAB variants that had 2 or 4 less complementary bases with the 3' end of the DNA activators (dARm2 and dAB1_2 or dARm4 and dAB1_4, respectively in Supplementary Fig. 7f,g) These dARm variants thus have less complementarity with the input domain of the genelet and should react with the genelet less quickly than a free DNA activator. With the dAB1_2 variant as the strand sequestering the DNA activator, addition of 1 μM of dABm2 resulted in 66% of *G1S1 bound to DNA activator, suggesting there was still some interaction between dARm2 and the genelet (Supplementary Fig. 7g). With the dAB1_4 variant as the strand sequestering the DNA activator, addition of 1 μM of dABm4 resulted in nearly 100% of *G1S1 bound to its DNA activator, but incubation of the dA1:dAB1_4 complex prior to the addition of dARm4 exhibited some leak activation of *G1S1 (Supplementary Fig. 7h). Thus, none of these variants were deemed a successful design for a BLK node using a sequestered DNA activator.

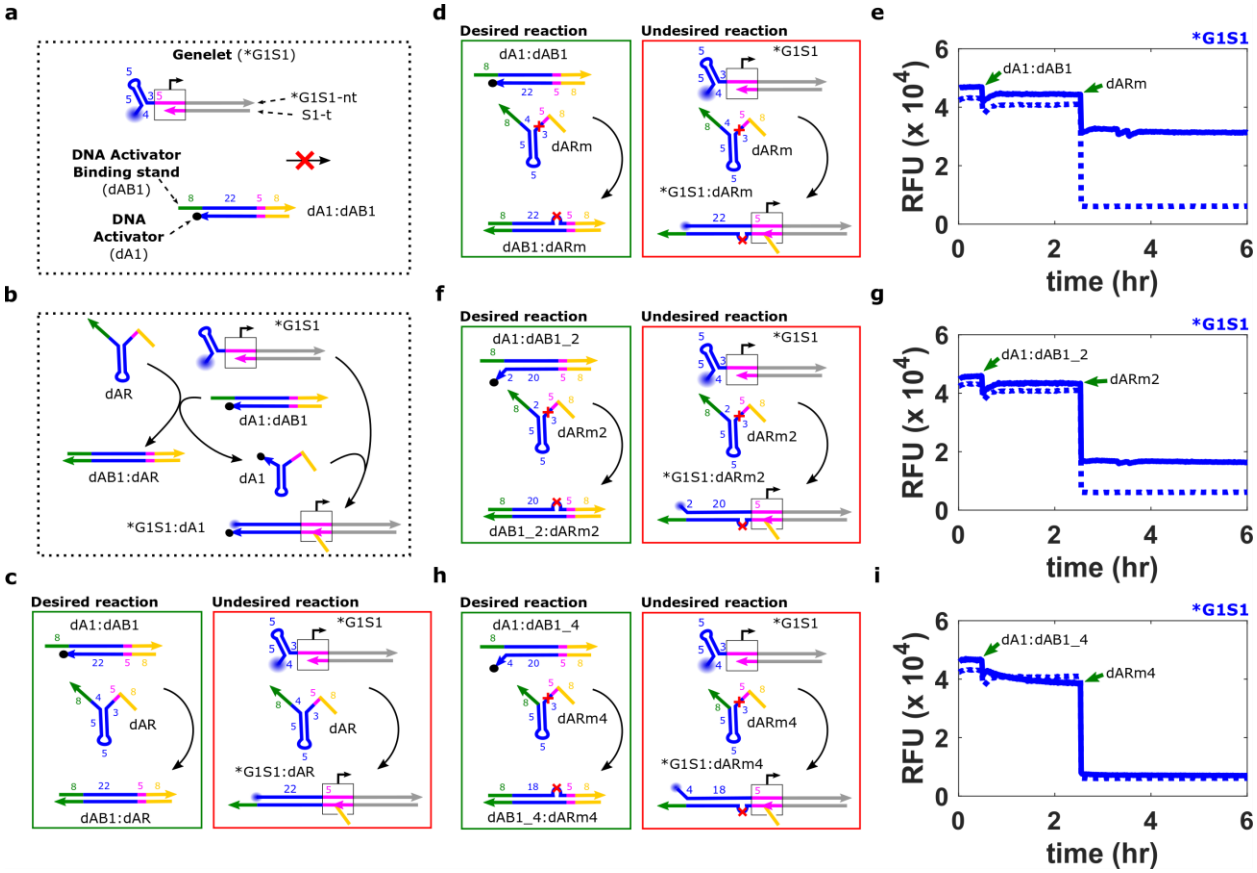

Supplementary Figure 7 | Characterization of blocked DNA activator designs inspired by the mechanism for bidirectional regulation of KWW genelets. (**a**) General design of a genelet and its blocked DNA activator using a DNA version dAR of the activator release strand for testing. The DNA activator (dA1) is sequestered by a DNA activator binding strand (dAB1) which prevents the DNA activator from binding to the genelet. (**b**) Reaction schematics of 1) DNA activator release by an upstream activator release strand (dAR) and 2) the binding of the released DNA activator to the genelet. (**c**) Schematics of the desired DNA activator release reaction and the undesired reaction between the DNA activator release strand and the genelet. If the AR strand were RNA, as a signal transcribed by an upstream genelet would be, this reaction would prevent transcription and would also prevent interaction with the DNA activator. The undesired reaction therefore would act to repress, rather than activate, transcription of the target genelet. dAR contains the entire sequence of dA1 so it binds as strongly to the genelet's input domain as the DNA activator does, thus, we never tested such a design. (**d**) Schematics of a desired reaction between an activator release strand variant (dARm) possessing a single base mismatch (indicated with a red x) and the DNA activator binding strand:activator complex (left) and an undesired reaction between this activator release strand variant and the genelet (right). The base mismatch was introduced to slow down the rate of the undesired reaction between dARm and the genelet. (**e**) Kinetic fluorescence data of *G1S1 after the addition of 500 nM of the dA1:dAB1 complex and 1 μM of the dARm strand (solid line). The dashed line is a control where dA1 was added to a sample containing *G1S1 at the time when dARm was added to the other sample. Significant suppression of *G1S1-dA1 binding is observed with the addition of dARm as full activation should result in fluorescence values comparable to the minimum of the control, the direct addition of DNA activator (dashed line). (**f**) Schematics of a desired reaction between a DNA activator binding strand variant:activator complex and a dARm strand variant (dARm2) with 2 fewer bases on its 3' end than the design in (c) (left), reducing its extent of complementarity with the input strand of the genelet in the undesired reaction (right). These 2 bases were removed from the activator release strand to further slow the rate of the undesired reaction between dARm2 and the genelet. (**g**) Kinetic fluorescence data of *G1S1 after the addition of the dA1:dAB1_2 complex and the dARm2 strand (solid line). The dashed line is the same control as in (**e**). Suppression of *G1S1-dA1 binding is still observed with the addition of dARm2. (**h**) Schematics of a desired reaction between a DNA activator binding strand variant:activator complex and a dARm strand variant (dARm4) with 4 fewer bases on its 3' end than the design in (c) (left), reducing its extent of complementarity with the input strand of the genelet in the undesired reaction (right). These 4 bases were removed from the activator release strand to further slow the rate of the undesired reaction between dARm4 and the genelet. (**i**) Fluorescence data

of *G1S1 after the addition of the dA1:dAB1_4 complex and the dARm4 strand (solid line). The dashed line is the same control as in (**e**). All of *G1S1 is able to bind to dA1 after dARm4 is added, but some dA1 binding also occurs after the dA1:dAB1_4 complex is added but before dARm4 is added. This indicates a leak reaction between dA1:dAB1_4 and *G1S1. Reactions were conducted as described in the Methods of the main text in the absence of enzymes with *G1S1 at 100 nM, 500 nM of the blocked DNA activator complexes, and 1 μM of the DNA activator release strands. Each blocked DNA activator complex was annealed 90°C to 20°C (-1°C/min) with 25% excess of the DNA activator binding strand. For the controls, the free DNA activator was added to a final concentration of 500 nM. Sequences are in Supplementary Table 2.

3.2 Constructing BLK nodes by blocking genelet input domains (HPC5 nodes)

Since we could not develop a design for bidirectional regulation based on sequestering the DNA activator, we investigated another BLK node design where the input domain of the genelet is bound to a DNA blocker strand (dB) that prevents the DNA activator from binding. Such a blocked genelet can be activated by sequestering the DNA blocker strand, because sequestering DNA blocker strand allows the DNA activator to bind the genelet to turn the node on. In this scheme, the DNA blocker's binding to the genelet must be thermodynamically favored over the binding of the DNA activator. To make such a preference possible, the 5' end of the genelet input domain was extended by 8 bases and the DNA blocker was designed to be complementary to all but the 5 bases of the missing T7 promoter sequence on the genelet's input domain (Supplementary Figure 8a). The DNA activator strand is not complementary to these 8 bases at the 5' end of the input domain, so even though the DNA activator binds to the 5 bases of the T7 promoter and the DNA blocker does not, the DNA blocker's binding is still favored by 3 bases. We term this the HPC5 genelet design.

We designed a coactivator strand that unblocks a blocked genelet by binding and removing the blocker strand from the genelet *via* a toehold-mediated nucleic acid strand displacement reaction. Supplementary Figure 8b shows how an example DNA coactivator, dC FC, sequesters a blocker strand bound to a genelet and how the resulting unblocked genelet can bind with its target DNA activator. If the coactivator is degraded (if the coactivator is RNA, this degradation is RNase H-induced) or otherwise removed from the blocker, the DNA blocker will be freed. A free blocker can remove the DNA activator from the genelet by a second toehold-mediated strand displacement reaction; the 8-base extension on the 5' end of the genelet's input domain serves as a toehold for this reaction. Thus, if a BLK node is turned on by the introduction of the coactivator strand and the coactivator is subsequently degraded or otherwise removed, the free dB strand will convert the ON node back to a BLK node.

One potential issue with this design is that the coactivator strand may interact with the DNA activator as these two molecules have significant sequence complementarity (Supplementary Figure 8c). If the coactivator were to bind to the DNA activator, it would sequester the DNA activator, thus preventing the DNA activator from binding to the genelet. This undesired reaction between the coactivator and the DNA activator would occur *via* a 4-way branch migration process facilitated by two short toehold domains on either side of the DNA activator's hairpin (Supplementary Figure 8c, left panel). To slow down the kinetics of this potential side reaction, we created a variant of the coactivator that had a single base mismatch with the DNA activator in one of the 4-way branch migration toeholds (Supplementary Figure 8c, right panel). We found that the coactivator that was fully complementary to the DNA blocker strand (dC1 FC) and the coactivator with the mismatch (dC1) could both unblock the genelet without significant suppression of activation when they were added at low concentrations (500 nM). However, when the coactivator was added at higher concentrations (5 μM) dC1 FC activated the genelet only

partially while 5 µM of dC1 activated the genelet fully. The kinetics of coactivation were similar for both coactivator designs (Supplementary Figure 8d and e, respectively).

The blocked genelet design showed no detectable activation when incubated with the DNA activator in the absence of the coactivators (Supplementary Figure 8d,e). Since the blocked genelet architecture with a coactivator containing a single mismatch (dC1) showed no genelet activation in the absence of coactivator and exhibited minimal suppression of activation upon the addition of high concentrations of coactivator, we selected this architecture as our BLK node design.

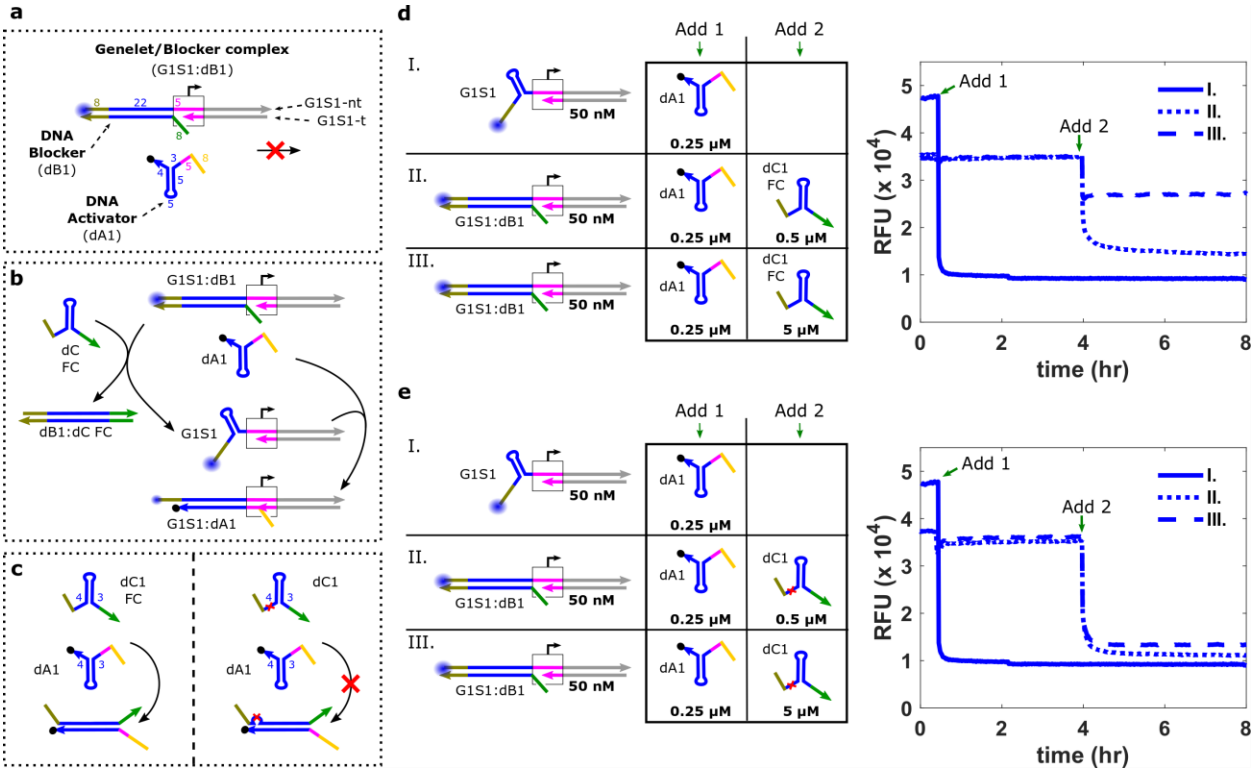

Supplementary Figure 8 | Development of the blocked genelet designs for bidirectional regulation and their initial characterization. (**a**) General design of a blocked genelet with its DNA activator. The input domain of the genelet is sequestered by a DNA blocker strand which prevents the DNA activator from binding the genelet. The DNA blocker strand is still missing 5 bases of the T7 RNAP promoter sequence so transcription cannot occur (Supplementary Figure 13a). (**b**) Schematic of a genelet being unblocked by an upstream input (termed a coactivator - dC) that is fully complementary (FC) to the DNA blocker. This enables the activator to bind. (**c**) Left panel: Possible undesired reaction between the coactivator that is fully complementary to the DNA blocker (dC-FC) and the DNA activator. The coactivator is partially complementary to the DNA activator and can hybridize to the activator through a 4-way branch migration process initiated with two short toehold domains (4 and 3 bases in length). Right panel: An alternative coactivator design with a mismatch in the 4-base toehold (indicated with a red x) which should decrease the reaction rate with the DNA activator. (**d**) Kinetic fluorescence data of genelet activation for the free genelet with dA1 (I.) and the blocked genelet after the addition of dA1 and a DNA coactivator that is fully complementary to the DNA blocker strand (II. and III.). Activation of the blocked genelet is significantly suppressed with the addition of 5 µM of dC1 FC (III.). (**e**) Kinetic fluorescence data of genelet activation for the free genelet with dA1 (I.) and the blocked genelet after the addition of dA1 and a DNA coactivator that has a single mismatch in the DNA blocker strand (II. and III.). Activation of the blocked genelet is not suppressed even when 5 µM of dC1 is added. Reactions were conducted as described in the Methods of the main text in the absence of enzymes with the concentrations of the DNA components shown in the tables to the left of the plots. The blocked genelet complexes were annealed as described in the Methods of the main text with 50% excess of the DNA blocker strand. Sequences are in Supplementary Table 2.

We next tested whether the coactivation reaction was reversible, *i.e.* a node that is turned on *via* addition of a coactivator will be converted back to a BLK state if the coactivation strand is removed or degraded (Supplementary Figure 9a). We found that an active genelet could be blocked by the addition of the DNA blocker strand (Supplementary Figure 9b) and unblocking by a coactivator could be reversed by the addition of the DNA blocker strand in excess of the coactivator (Supplementary Figure 9c). Further, unblocking the genelet with an RNA coactivator could be reversed by degradation of the RNA coactivator with RNase H (Supplementary Figure 9d). These results indicate that the coactivation reaction is reversible upon removal of the coactivator strand. We refer to nodes with this genelet design and DNA blocker strands as simply HPC5 nodes moving forward.

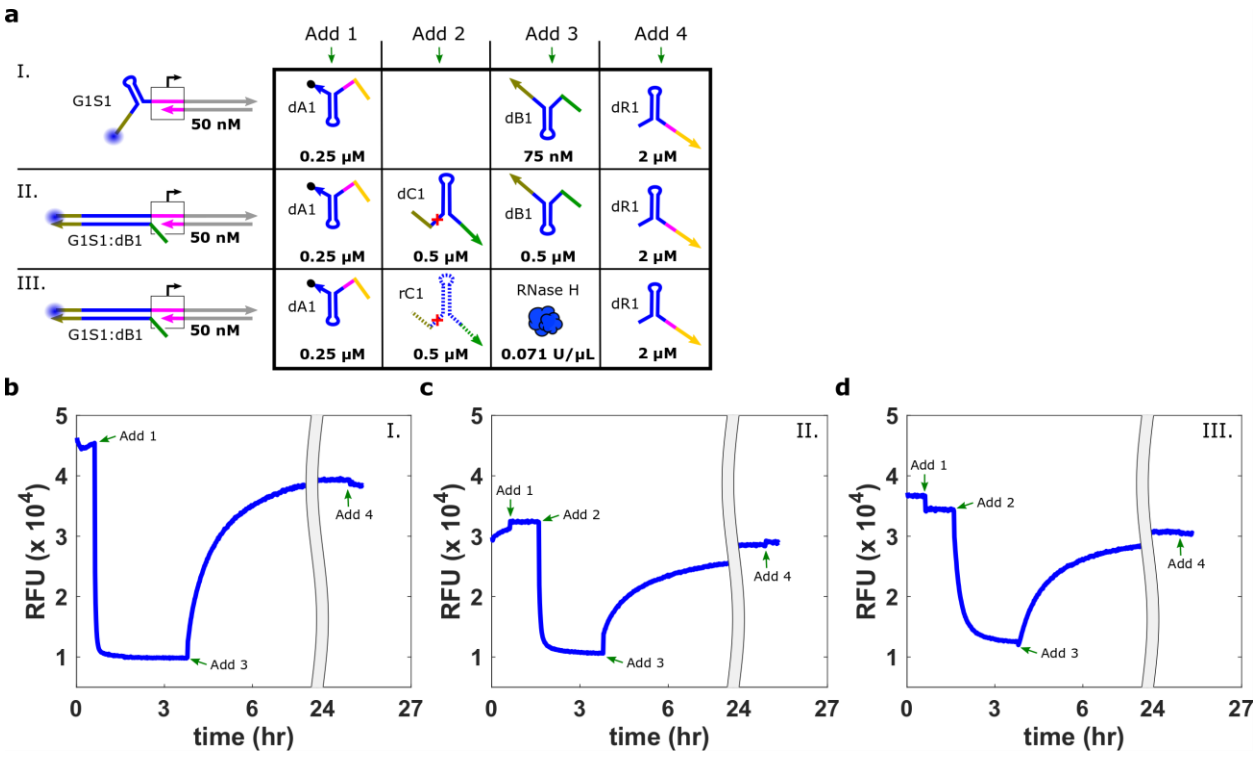

Supplementary Figure 9 | Characterization of reversibility of blocked genelet activation. (**a**) Table depicting the experiments conducted in (**b-d**). (**b**) Kinetic fluorescence data of genelet activation and blocking. A free genelet (in its off state) was activated by the addition of its DNA activator (Add 1) and subsequently inactivated by the addition of its DNA blocker strand (Add 3). (**c**) Kinetic fluorescence data of genelet unblocking, activation, and subsequent blocking. The blocked genelet was incubated with its DNA activator (Add 1) and activated by the addition of its DNA coactivator (Add 2). Activation was reversed with the subsequent addition of the DNA blocker strand (Add 3). (**d**) Kinetic fluorescence data of genelet unblocking, activation, and subsequent blocking via RNA degradation. The blocked genelet was incubated with its DNA activator (Add 1) and activated by the addition of its RNA coactivator (Add 2). Activation was reversed by degradation of the RNA coactivator with RNase H (Add 3). At the end of each reaction an excess of the genelet's DNA repressor strand was added (Add 4) to obtain a maximum fluorescence signal. Reactions were conducted as described in the Methods of the main text in the absence of enzymes unless otherwise noted with the concentrations of the reaction components shown in the table in (**a**). The blocked genelet complexes were annealed as described in the Methods of the main text with 50% excess of the DNA blocker strand. Sequences are in Supplementary Table 2.

3.3 Design of genelet output domains for efficient downstream regulation

With the HPC5 scheme working when tested with DNA coactivators, we next sought to ensure that transcription of RNA coactivators could efficiently regulate HPC5 nodes. We used a constitutively active upstream transcription template that expressed the RNA coactivator rC1 of a blocked genelet as a test sequence (Supplementary Fig. 10a). The KWW genelets typically use the sequence 5'GGGAGA starting at the +1 position of the T7 RNAP promoter as this sequence has been shown to lead high transcription efficiency[10]. However, we initially designed the transcription template to possess a single guanine base at the +1 position of the T7 RNAP promoter (5' end of rC1) as this is the minimum required sequence for initiation of transcription[10] (Supplementary Figure 10b, left). We made this change because the 5'GGGAGA sequence can make RNA transcripts more prone to unwanted secondary structure or off target interactions with other nucleic acids. However, we found that rC1 transcribed from a template with only a single G at its 5' end coactivated G1S1 much more slowly than a control where a DNA coactivator was added to coactivate this same genelet (Supplementary Figure 10c).

We theorized that having only a single guanine base at the +1 position of the T7 RNAP promoter may lead to low transcription efficiency. Thus, we designed a transcription template that encoded for a hairpin structure at the 5' end of the RNA transcript. The RNA transcript was designed to begin with the 5'GGGAGA preferred transcription initiation sequence and fold up into a hairpin at the 5' end so that the additional 5'GGGAGA tag would be sequestered from any other interactions (Supplementary Figure 10b, right). We found that this transcription template significantly sped up coactivation (Supplementary Figure 10c). Based on these results, we included the modular 5' preferred transcription initiation sequence hairpin (5PSHP) at the beginning of all of the transcribed RNA coactivators, RNA repressors, and inducer RNAs to ensure efficient transcription.

The addition of the 5PSHP sequence to transcripts might not only enhance transcription because it contains T7 RNAP's preferred transcription initiation sequence, the addition of this sequence might also help prevent the formation of unwanted secondary structure that arises when additional bases are added to the 5' end of the transcript[1]. For example, if T7 RNAP added additional guanine bases at the 5' end of a transcript[1,11], these additional bases can cause the transcript to adopt undesired secondary structure. Indeed, NUPACK analysis of the rC1 transcript with two 5' guanines predicted that significant secondary structure would form whereas comparatively little secondary structure would form from a rC1 transcript with only one 5' guanine. In contrast, the rC1-5PSHP RNA is not predicted to have any secondary structure even when two additional guanines are appended to its 5' end (Supplementary Figure 10d).

We also found that the sequence of the 8-base toehold that facilitates the coactivation reaction influences the kinetics of the coactivation. The coactivation of a second blocked genelet node (G2C1 node design) had slow coactivation kinetics even when the coactivator was transcribed containing the 5PSHP motif. We theorized that the slow coactivation was due to the low GC content of the 8-base coactivation toehold of the blocker (dB2-1) for this node (Supplementary Figure 11a). To test this hypothesis, we created a new variant for this node's blocker (dB2-2) that used the same coactivation toehold as dB1 (which had 50% GC content). Coactivation with dB2-2 was much faster than coactivation with dB2-1 (Supplementary Figure 11b). We then designed two more blocker variants with >50% GC content in the coactivation toehold and observed that coactivation was fast for both of them (Supplementary Figure 11c,d). These results suggest that when the toeholds for transcriptional

coactivation (and likely repression) have at least 50% GC content, transcriptional coactivation tends to be fast. We used the dB2 variant as the blocker for all subsequent G2 nodes.

We also found that transcription rates could depend on the sequence and structure of the transcription template[3]. For example, we initially truncated the 3' end of the non-template strands for many of our transcription templates and genelets. This allowed us to order sequences that were less than 90 or 100 bases and the non-template strand is typically not necessary for transcription downstream of the promoter sequence[2,12,13]. However, we found for a specific node (G9S2), using a transcription template that had been truncated by 13 bases at the 3' end of its non-template strand resulted in much slower coactivation kinetics than an untruncated template (Supplementary Figure 12a,b, respectively). The importance of maintaining the full length of the non-template strand might be related to the particular sequence at the 3' end of the RNA coactivator for this particular node, which contains a 5-base tract of GCs. Tracts of GCs at the end of a run-off transcription template have been shown to cause T7 RNAP to stall[3] and so the presence of this tract might result in very slow or very little transcription of the full-length transcript. Additionally, a polymerase stalled on the GC tract might have an increased rate of template strand switching[3] when stalled near the free 3' end of the non-template strand, which would produce a self-complementary inactive transcript. The polymerase should not stall at a GC tract if the tract is not at the 3' end of the transcript[3]. We found that adding 15 bases to the 3' of the transcript increased the rate of coactivation (Supplementary Figure 12c). It is not entirely clear why truncating the non-template strand results in slower coactivation than the untruncated template as both templates could cause T7 RNAP to stall, but these results suggest that excessive non-template strand truncation should be avoided to circumvent sequence specific variations in transcription rates.

In summary the results discussed above suggest three design heuristics for genelet node, coactivator, and blocker sequences: (1) all RNA transcripts should include the 5PSHP motif to promote efficient downstream regulation (Supplementary Figure 10), (2) the toehold for the coactivation and repression reactions should have at least 50% GC content to promote fast reaction kinetics (Supplementary Figure 11), and (3) truncating the non-template strand of the genelets should be kept to a minimum (Supplementary Figure 12).

A final observation that is important for assembling transcriptional coactivation cascades is we found that the blocked genelets can have a transcription leak when incubated with their DNA activators. The G1S1:dB1 and G1S1 complexes do not show any significant transcription when incubated with T7 RNAP in the absence of dA1. However, if G1S1:dB1 is incubated with T7 RNAP and dA1, appreciable transcription is observed (Supplementary Figure 13a). This undesired transcription occurs at <10% of the rate of G1S1 in an ON state – the rate of 25 nM G1S1:dB1 with dA1 transcribes at a rate somewhere between the rate of 5 nM and 1 nM of a G1S1:dA1 complex (Supplementary Figure 13b). Leak transcription was also observed for the sequestered activator designs tested in Supplementary Section 3.1 so leak transcription is not inherent to the blocked genelet design but rather seems inherent to any design that attempts to block the interaction between a genelet and its activator.

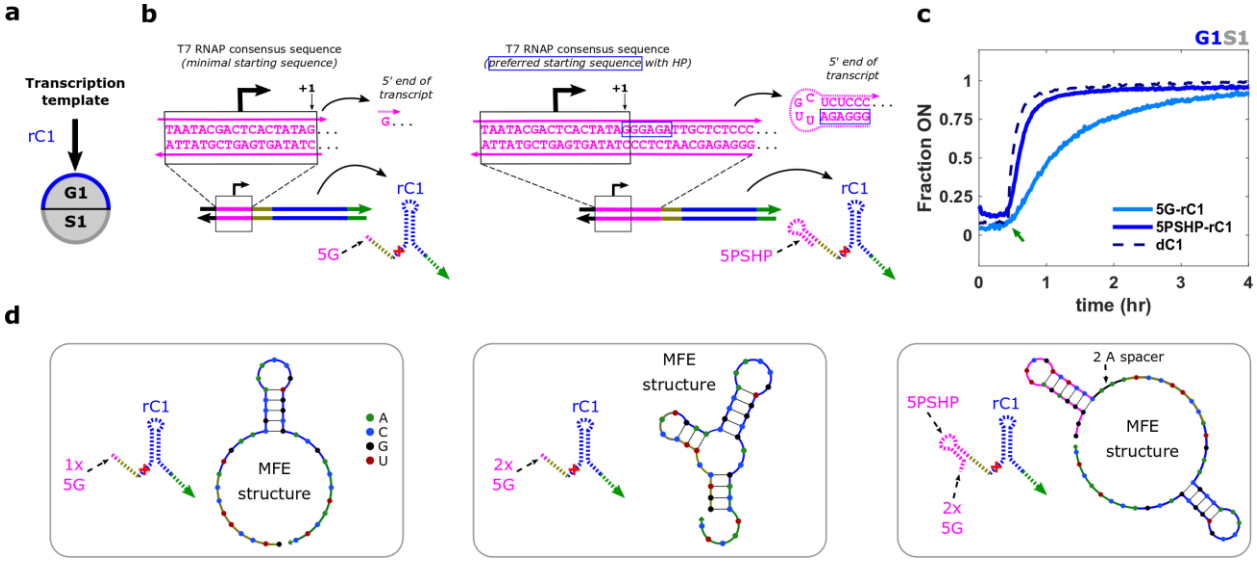

Supplementary Figure 10 | The 5' motif that initiates transcription of the RNA coactivator for G1S1 influences coactivation kinetics. (**a**) Overview of the experiment conducted in (**c**); the rate of functional transcript produced is measured by the rate of coactivation of the G1S1 node. An experiment where 500 nM DNA coactivator (dC1) was added was also conducted serve as a reference. (**b**) Diagram of the transcription templates for rC1 with either a single guanine base at the +1 position of the T7 promoter (left) or a 5' hairpin containing the preferred initiation sequence for T7 RNAP at the +1 position of the T7 promoter (right). (**c**) Normalized genelet activation levels for G1S1 during the transcription of rC1 from the two transcription templates depicted in (**b**). (**d**) Minimum free energy (MFE) structures as predicted by NUPACK[14] for rC1 with a single 5'G (left), two 5'G's (middle), or two additional 5'G's in addition to the 5PSHP (right). The 5PSHP motif also disfavors any 5' heterogeneity that might be introduced during transcription[1] from introducing undesired secondary structure in the transcript (a two-adenine spacer after the 5PSHP motif was introduced to further ensure no other secondary structure). For example, if an additional 5'G were introduced on 5G-rC1, the RNA is predicted to fold into an alternative structure which could explain the slower kinetics of coactivation by this RNA compared to the 5PSHP-rC1 RNA and the dC1 control. Transcription reactions conducted as described in the Methods of the main text with [G1S1] = 25 nM, [dA1] = 125 nM, [transcription templates] = 10 nM, [T7 RNAP] = 3.57 U/µL. Sequences are in Supplementary Table 2.

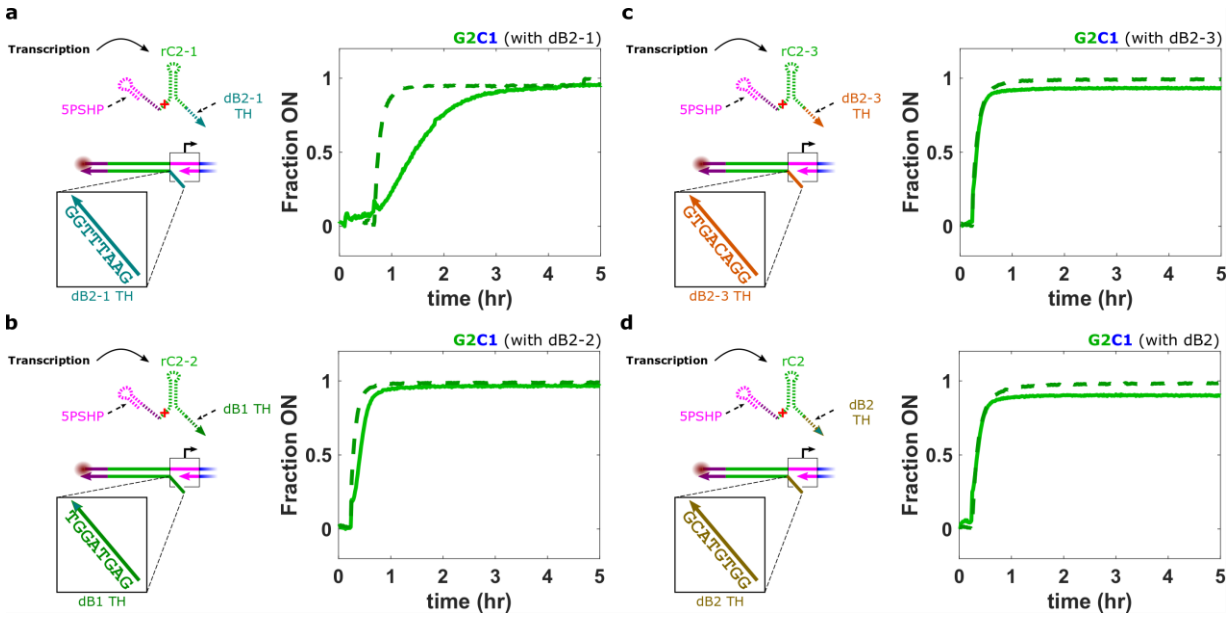

Supplementary Figure 11 | Transcriptional coactivation proceeds more quickly when the coactivation toehold has high GC content. (**a-d**) Coactivation kinetics of G2C1 with dB variants in response to the addition of a DNA coactivator (dashed) or in response to transcription of different coactivators where the coactivator and corresponding blocker strands each had different coactivation toehold sequences. The sequences of the coactivation toeholds are shown to the left of the plots. dB2-1 has 37.5% GC content (**a**), dB2-2, which has the coactivation toehold of dB1, has 50% GC content (**b**), and dB2-3 and dB2 have 62.5% GC content (**c**,**d**, respectively). Transcription reactions were conducted as described in the Methods of the main text with [G2C1] = 25 nM, [dA2] = 250 nM, [transcription templates] = 15 nM, [RNase H] = 4.46 x 10^{-3} U/µL, [YIPP] = 1.35 x 10^{-3} U/µL, [T7 RNAP] = 3.57 U/µL. Control experiments with DNA coactivators were conducted in the absence of enzymes with DNA coactivators added to a final concentration of 500 nM (dashed lines). Sequences are in Supplementary Table 2.

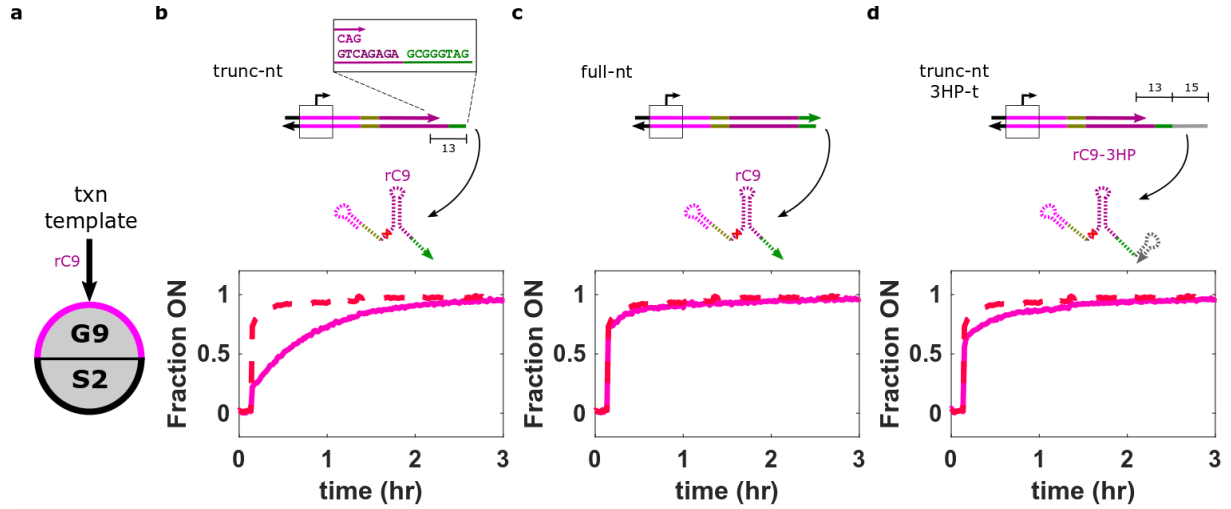

Supplementary Figure 12 | Transcription efficiency depends on the structure of the transcription template. (**a**) Depiction of the experiment conducted in (**b**-**d**). (**b-d**) Coactivation kinetics of the G9S2 node *via* the addition of a DNA coactivator (dashed) or *via* transcription of rC9 from the different transcription templates depicted. The structure of the transcription templates and RNA coactivators are shown above the plots. The 3' hairpin for rC9-3HP was introduced to prevent the additional bases added to this RNA from introducing any undesired secondary structure. Transcription reactions were conducted as described in the Methods of the main text with [G9S2] = 25 nM, [dA9] = 250 nM, [transcription templates] = 25 nM, [RNase H] = 8.93 x 10^{-3} U/µL, [YIPP] = 1.35 x 10^{-3} U/µL, [T7 RNAP] = 3.57 U/µL. Control experiments with DNA coactivators were conducted in the absence of enzymes with dC9 added to a final concentration of 500 nM (dashed lines). Sequences are in Supplementary Table 2.

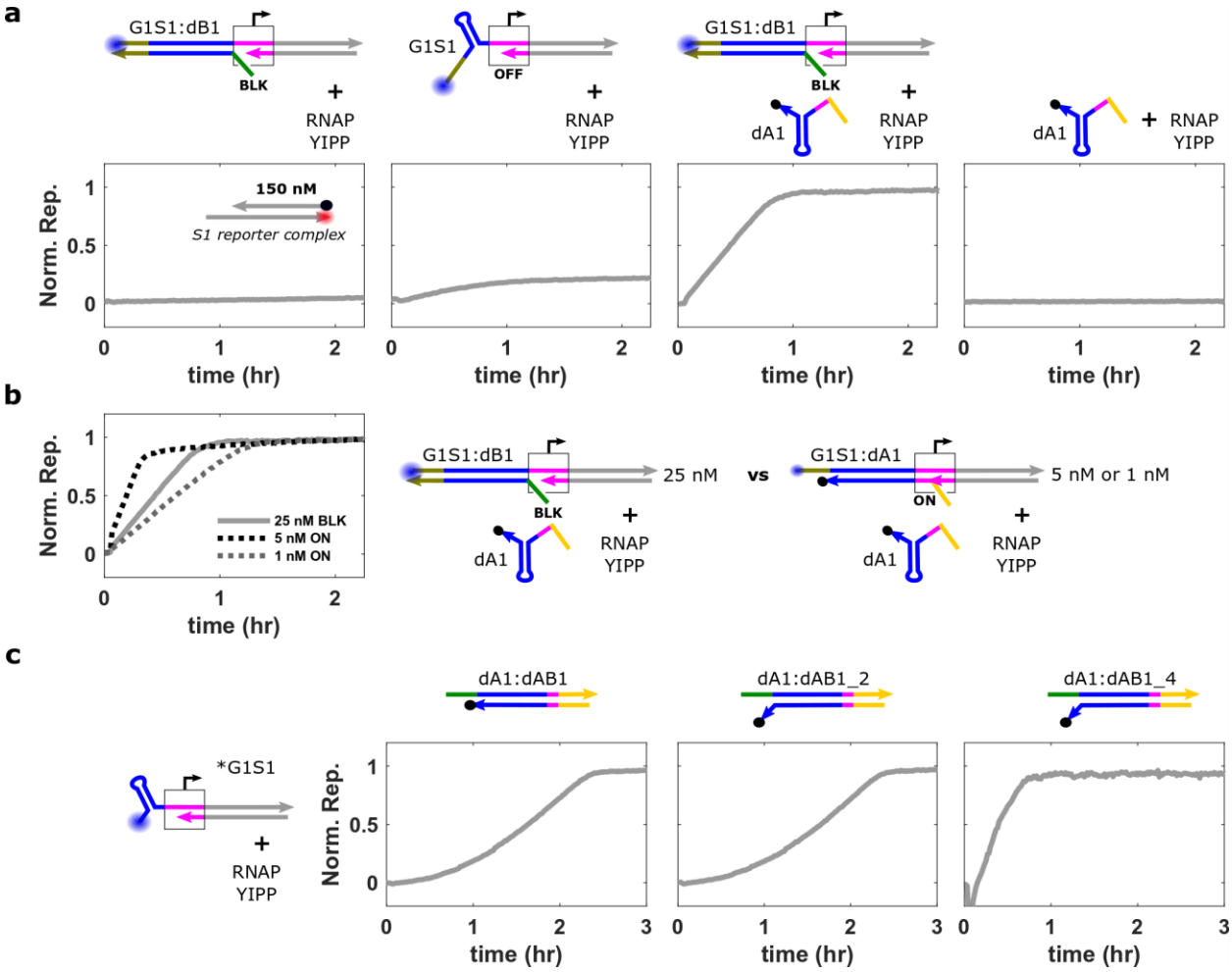

Supplementary Figure 13 | Blocked genelets with their activators and unblocked genelets with blocked activators both exhibit leak transcription. (**a**) Normalized S1 reporter complex fluorescence during incubation with the genelet species and enzymes shown above the plots. When present, G1S1 was at 25 nM and dA1 was at 125 nM. The blocked G1S1 genelet exhibits leak transcription only when incubated with its corresponding DNA activator. (**b**) Normalized S1 reporter complex fluorescence during incubation of the reporter with the genelet species and enzymes shown to the right of the plot. The rates of increase of fluorescence in these experiments can be used to estimate the leak transcription rate of blocked G1S1 with its activator. Since the leak transcription rate is roughly halfway between the transcription rates of 5 nM or 1 nM ON G1S1, the leak rate is on order 10% of the ON transcription rate. (**c**) Normalized S1 reporter complex fluorescence during incubation with Gv1-m4n8, enzymes and the blocked activator species shown above the plots. These results demonstrate that genelets also exhibit leak transcription in the presence of blocked activators. S1 reporter complex was present at 150 nM in all experiments. [T7 RNAP] = 3.57 U/µL and [YIPP] = 1.35×10^{-3} U/µL. Reactions were otherwise conducted as described in the methods. Blocked genelets were annealed with 50% excess of the blocker strand and the blocked activators were annealed with 25% excess of the dAB strands. Sequences are in Supplementary Table 2.

Supplementary Table 2 | Sequences from experiments in Supplementary Sections 2 and 3. All strands were ordered from IDT. S1-t was the template strand for *G1S1, G1S1-HPC5_75, and G1S1 genelets. Sequences with the same names as those in Supplementary Table 1 are repeated here for clarity.

GENELETS	
KWW1-nt	5'ATTGAGGTAAGAAAGGTAAGGATAATACGACTCACTATAGACATACAGATTAACCAGA CAGTGACAAAGTCACAAA
KWW1-t	5'TTTGTGACTTTGTCACTGTCTGGTTAATCTGTATGTCTATAGTGAGTCG
G1-HPC3-nt	/56FAM/CGCCAGCAACCGGCTGGCGACGTAATACGACTCACTATAGTTACCTCAATCTT CGCCT
G1-HPC3 -t	5'AGGCGAAGATTGAGGTAACTATAGTGAGTCG
*G1S1-nt (HPC5o)	/56FAM/TGCACGCCAAACCGTGGCGACGTAATACGACTCACTATAGACATACAGATTAA CCAGACAGTGAC
G1S1-HPC5_75-nt	/56FAM/ACGTCGTCGCCAAACCGTGGCGTAATACGACTCACTATAGACATACAGATTAA CCAGACAGTGAC
G1S1-nt	/56FAM/TCCTTCCATGCACGCCAAACCGTGGCGACGTAATACGACTCACTATA GACATACAGATTAACCAGACAGTGAC
S1-t	5'GTCACTGTCTGGTTAATCTGTATGTCTATAGTGAGTCG
G2C1-nt	/5TYE665/AGCCAAGATTCAGGTCAATAAGTGACCAAGTAATACGACTCACTATA GGGAGATTCGTCTCCCAAATCCTTCCATGAACGCCAAACCGTGGCGACGACCTACTC
C1-t	5'GAGTAGGTCGTCGCCACGGTTTGGCGTTCATGGAAGGATTTGGGAGACGAATCTCCCTATAG TGAGTCG
G9S2-nt	/TYE665/CCAACTACCTATGACTGTAACCCAGTCTCTTAATACGACTCACTATA GGGAGACGGTCGGGTCCAGATATTCGTATCTGTCGAGTAGAG
S2 -t	5'GGGAGCCCACACTCTACTCGACAGATACGAATATCTGGACCCGACCGTCTCCCTATAGTGAG TCG
ACTIVATORS	
KWW dA 3'TH	5'TATTATCCTTACCTTTCTTACCTCAATCTTCGCCT/3BHQ_2/
KWW dA 5'TH	5'CTTCGCCTTATTATCCTTACCTTTCTTACCTCAAT
dA1 HPC3	5'TATTACGTCGCCAGCCGGTTGCTGGCGTCCAGCTC/3BHQ_1/
dA1 HPC5_08	5'TCCAGCTCTATTACGTCGCCAGCCGGTTGCTGGCG/3BHQ_1/
dA1	5'TCCAGCTCTATTACGTCGCCACGGTTTGGCGTGCA/3IABkFQ/
dA1 HPC5_75	5'TCCAGCTCTATTACGCCACGGTTTGGCGACGACGT/3IABkFQ/
dA2	5'CATCCCACTATTACTTGGTCACTTATTGACCTGAA/3IAbRQSp/
dA9	5'AGCAGAAGTATTAAGAGACTGGGTTACAGTCATAG/3IAbRQSp/
ACTIVATOR BINDERS	
dAB1	5'TGGAAAGGTGCACGCCAAACCGTGGCGACGTAATAGAGCTGGA
dAB1_2	5'TGGAAGGACACGCCAAACCGTGGCGACGTAATAGAGCTGGA
dAB1_4	5'TGGAAAGGCGCCAAACCGTGGCGACGTAATAGAGCTGGA
ACTIVATOR RELEASERS	
dARm	5'TCCAGCTCTATTACTTCGCCACGGTTTGGCGTGCACCTTTCCA
dARm2	5'TCCAGCTCTATTACTTCGCCACGGTTTGGCGTGTCCTTCCA
dARm4	5'TCCAGCTCTATTACTTCGCCACGGTTTGGCGCCTTTCCA
BLOCKER	
dB1	5'GAGTAGGT CGTCGCCACGGTTTGGCGTGCATGGAAGGA
dB2-1	5'GAATTTGG CTTGGTCACTTATTGACCTGAATCTTGGCT
dB2-2	5'GAGTAGGT CTTGGTCACTTATTGACCTGAATCTTGGCT
dB2-3	5'GGACAGTG CTTGGTCACTTATTGACCTGAATCTTGGCT
dB2	5'GGTGTACG CTTGGTCACTTATTGACCTGAATCTTGGCT
dB9	5'GATGGGCG AGAGACTGGGTTACAGTCATAGGTAGTTGG
COACTIVATORS	
dC1	5'TCCTTCCATGAACGCCAAACCGTGGCGACGACCTACTC
dC1 FC	5'TCCTTCCATGCACGCCAAACCGTGGCGACGACCTACTC
rC1	5'rUrCrCrUrUrCrCrArUrGrArArCrGrCrCrArArA rCrCrGrUrGrGrCrGrArCrGrArCrCrUrArCrUrC
dC2-1	5'AGCCAAGATTAAGGTCAATAAGTGACCAAGCCAAATTC
dC2-2	5'AGCCAAGATTAAGGTCAATAAGTGACCAAGACCTACTC
dC2-3	5'AGCCAAGATTAAGGTCAATAAGTGACCAAGCACTGTCC

dC2	5′AGCCAAGATTAAGGTCAATAAGTGACCAAGCGTACACC
dC9	5′CCAACTACCTCTGACTGTAACCCAGTCTCTCGCCCATC
REPRESSORS	
dR1 HPC3	5′GAGCTGGACGCCAGCAACCGGCTGGCGACGTAATA
dR1 HPC5_08	5′CGCCAGCAACCGGCTGGCGACGTAATAGAGCTGGA
dR1	5′TGCACGCCAAACCGTGGCGACGTAATAGAGCTGGA
dR1 HPC5_75	5′ACGTCGTCGCCAAACCGTGGCGTAATAGAGCTGGA
REPORTER COMPLEXES	
S1_HP_reporter	/5TEX615/TGTCTGGTTAATCTGTTTAACC/3IAbRQSp/
dS1	5′GACATACAGATTAACCAGACAGTGAC
S1_reporter_F	5′GTCACTGTCTGGTTAATCTGTATGTC/3TEX615/
S1_reporter_Q	/5IAbRQ/GACATACAGATTAACCAGACA
TRANSCRIPTION TEMPLATES	
C-G1-5G-nt	5′TTCTAATACGACTCACTATAGTCCTTCCATGAACGCCAAACCGTGGCGACACCTAC
C-G1-5G-t	5′GAGTAGGTGTCGCCACGGTTTGGCGTTCATGGAAGGACTATAGTGAGTCGTATTAGAA
C-G1-5PSHP-nt	5′TCCTAATACGACTCACTATAGGGAGATTCGTCTCCCAAATCCTTCCATGAACGCCAAACCGT GGCGACGACC
C-G1-5PSHP-t	5′GAGTAGGTCGTCGCCACGGTTTGGCGTTCATGGAAGGATTTGGGAGACGAATCTCCCTATAG TGAGTCGTATTAGGA
C-G2-1-nt	5′TCCTAATACGACTCACTATAGGGAGATTCGTCTCCCAAAGCCAAGATTAAGGTCAATAAGTG ACCAAGCCAAATTC
C-G2-1-t	5′GAATTTGGCTTGGTCACTTATTGACCTTAATCTTGGCTTTGGGAGACGAATCTCCCTATAGT GAGTCGTATTAGGA
C-G2-2-nt	5′TCCTAATACGACTCACTATAGGGAGATTCGTCTCCCAAAGCCAAGATTAAGGTCAATAAGTG ACCAAGACC
C-G2-2-t	5′GAGTAGGTCTTGGTCACTTATTGACCTTAATCTTGGCTTTGGGAGACGAATCTCCCTATAGT GAGTCGTATTAGGA
C-G2-3-nt	5′TTCTAATACGACTCACTATAGGGAGATTCGTCTCCCAAAGCCAAGATTAAGGTCAATAAGTG ACCAAGCACTGTCC
C-G2-3-t	5′GGACAGTGCTTGGTCACTTATTGACCTTAATCTTGGCTTTGGGAGACGAATCTCCCTATAGT GAGTCGTATTAGAA
C-G2-nt	5′TTCTAATACGACTCACTATAGGGAGATTCGTCTCCCAAAGCCAAGATTAAGGTCAATAAGTG ACCAAGCGTACACC
C-G2-t	5′GGTGTACGCTTGGTCACTTATTGACCTTAATCTTGGCTTTGGGAGACGAATCTCCCTATAGT GAGTCGTATTAGAA
C-G9-trunc-nt	5′CCTAATACGACTCACTATAGGGAGATTCGTCTCCCAACCAACTACCTCTGACTGTAACCCAG
C-G9-full-nt	5′CCTAATACGACTCACTATAGGGAGATTCGTCTCCCAACCAACTACCTCTGACTGTAACCCAG TCTCTCGCCCATC
C-G9-t	5′GATGGGCGAGAGACTGGGTTACAGTCAGAGGTAGTTGGTTGGGAGACGAATCTCCCTATAGT GAGTCGTATTAGG
C-G9-3HP-t	5′CCTAATACGACTCACTATAGGGAGATTCGTCTCCCAACCAACTACCTCTGACTGTAACCCAG TCTCTCGCCCATCACTGACTTCGGTCAG

4. Scaling up the number of standardized genelet nodes

This section describes the methods used to generate sequences for the library of standardized genelet nodes developed in this work. To create a library of standardized genelet nodes that could be assembled into *in vitro* transcriptional regulatory networks, we first used NUPACK to design a large set of genelet node sequences (genelet input domains, activators, blockers, coactivators, and repressors) that NUPACK predicts only rarely hybridize with one another other than through designed interactions (Supplementary Section 4.1). We found that the kinetics of activation *via* addition of a DNA activator for some designs are very slow so before moving forward with building genelet networks we measured the activation rates of 34 different genelets using their DNA activators. Of these 34 screened nodes we identified 16 genelet and activator pairs with reasonably fast kinetics of DNA activation (Supplementary Section 4.2). We then measured the rates at which these 16 genelet nodes were coactivated and repressed by transcription of their RNA coactivators and repressors (Supplementary Section 4.3). Of these 16 nodes we identified 6 that could be both rapidly coactivated and rapidly repressed and 5 additional nodes that could be either coactivated or repressed *via* transcription of their coactivators and repressors (Supplementary Section 4.4). These nodes served as the building blocks of the *in vitro* transcriptional regulatory networks we constructed. We also followed this same protocol to identify five more standardized nodes as described in Supplementary Section 11.

4.1 NUPACK design of orthogonal genelet nodes

To design orthogonal genelet nodes for use in regulatory network assembly we used NUPACK 3.2.2[14] with a temperature of 37^{o}C and default salt conditions (1 M Na^{+}, 0 M Mg^{2+}). The default salt conditions were used because the NTP concentration is very high during a transcription reaction, and NTPs bind magnesium, so the effective magnesium concentration is not the actual concentration of magnesium initially added. NUPACK does not model DNA-RNA interactions so we modeled all the species as RNA molecules since RNA-RNA/RNA-DNA interactions tend to be stronger than DNA-RNA interactions. Thus, these simulations served as a worst-case prediction of spurious hybridization interactions between components. Because NUPACK models only secondary structure interactions and only interactions that do not involve pseudoknotted species, this design process eliminates some, but likely not all, spurious interactions of the designed sequences.

Below is a sample script for designing three orthogonal genelet nodes and will design the sequences of three genelets' input domains, activators, blockers, coactivators, and repressors. The script designs each of the coactivators to have the one mismatch between each coactivator and its corresponding blocker that was introduced by design (Supplementary Section 3.2). The script seeks to minimize the extent of interaction between all of the strands that are not supposed to interact as well as make the known spurious interactions as weak as possible. For example, the coactivator and activator of a given genelet node have some unavoidable complementarity and the NUPACK script designs against the introduction of any additional complementarity between these strands. This is achieved by defining r*C*d*A*i structures that represent the secondary structure of the complementary regions of RNA coactivators and their corresponding DNA activators. This script can be extended to design as many genelet nodes as desired. Further, the script can be constrained to design new nodes against existing node sequences by simply defining the appropriate structures and threading the existing sequences onto these structures.

```
material = rna
temperature[C] = 37.0
trials = 10

# component structures using DU+ notation
# activators:
structure dA1 = U16 D5 (U5) U4
structure dA2 = U16 D5 (U5) U4
structure dA3 = U16 D5 (U5) U4
# genelet activator binding domains
structure G1 = U12 D5 (U5) U8
structure G2 = U12 D5 (U5) U8
structure G3 = U12 D5 (U5) U8
# blockers
structure dB1 = U11 D5 (U5) U12
structure dB2 = U11 D5 (U5) U12
structure dB3 = U11 D5 (U5) U12
# coactivators
structure rC1 = U12 D5 (U5) U11
structure rC2 = U12 D5 (U5) U11
structure rC3 = U12 D5 (U5) U11
# repressors
structure rR1 = U4 D5 (U5) U16
structure rR2 = U4 D5 (U5) U16
structure rR3 = U4 D5 (U5) U16

# Designed mismatches between RNA coactivators and blocker/activators
# coactivator:blocker complex
structure rC1dB1 = D10 (U1 D27+ U1)
structure rC2dB2 = D10 (U1 D27+ U1)
structure rC3dB3 = D10 (U1 D27+ U1)
# coactivator:activator complex
structure rC1dA1 = U8 D2 (U1 D19 (U8 + U13) U1)
structure rC2dA2 = U8 D2 (U1 D19 (U8 + U13) U1)
structure rC3dA3 = U8 D2 (U1 D19 (U8 + U13) U1)

# sequence domains
domain ta = TAATA
# repression toehold
domain thA1 = N8
domain thA2 = N8
domain thA3 = N8
# coactivation toehold
domain thB1 = N8
domain thB2 = N8
domain thB3 = N8
# blocking toehold
domain thG1 = N8
domain thG2 = N8
domain thG3 = N8
# genelet activator binding domains
domain G1_5 = N2
domain G1_b = N1
domain G1_3 = N19
domain C1_b = N1

domain G2_5 = N2
domain G2_b = N1
```

```
domain G2_3 = N19
domain C2_b = N1

domain G3_5 = N2
domain G3_b = N1
domain G3_3 = N19
domain C3_b = N1

# thread sequence domains onto target structures
# genelet activator binding domains
G1.seq = thG1 G1_5 G1_b G1_3 ta
G2.seq = thG2 G2_5 G2_b G2_3 ta
G3.seq = thG3 G3_5 G3_b G3_3 ta
# activators
dA1.seq = thA1 ta* G1_3* G1_b* G1_5*
dA2.seq = thA2 ta* G2_3* G2_b* G2_5*
dA3.seq = thA3 ta* G3_3* G3_b* G3_5*
# blockers
dB1.seq = thB1 G1_3* G1_b* G1_5* thG1*
dB2.seq = thB2 G2_3* G2_b* G2_5* thG2*
dB3.seq = thB3 G3_3* G3_b* G3_5* thG3*
# coactivators
rC1.seq = thG1 G1_5 C1_b G1_3 thB1*
rC2.seq = thG2 G2_5 C2_b G2_3 thB2*
rC3.seq = thG3 G3_5 C3_b G3_3 thB3*
# repressors
rR1.seq = G1_5 G1_b G1_3 ta thA1*
rR2.seq = G2_5 G2_b G2_3 ta thA2*
rR3.seq = G3_5 G3_b G3_3 ta thA3*
# coactivator:blocker complexes
rC1dB1.seq = thG1 G1_5 C1_b G1_3 thB1* thB1 G1_3* G1_b* G1_5* thG1*
rC2dB2.seq = thG2 G2_5 C2_b G2_3 thB2* thB2 G2_3* G2_b* G2_5* thG2*
rC3dB3.seq = thG3 G3_5 C3_b G3_3 thB3* thB3 G3_3* G3_b* G3_5* thG3*
# coactivator:activator complexes
rC1dA1.seq = thG1 G1_5 C1_b G1_3 thB1* thA1 ta* G1_3* G1_b* G1_5*
rC2dA2.seq = thG2 G2_5 C2_b G2_3 thB2* thA2 ta* G2_3* G2_b* G2_5*
rC3dA3.seq = thG3 G3_5 C3_b G3_3 thB3* thA3 ta* G3_3* G3_b* G3_5*

tube As = dA1 dA2 dA3
tube C_Rs = rC1 rC2 rC3 rR1 rR2 rR3

As.maxsize = 2
C_Rs.maxsize = 2

prevent = AAAA, CCCC, GGGG, UUUU, KKKKKK, MMMMMM, RRRRRR, SSSSSS, WWWWWW, YYYYYY
```

4.2 Screening genelet and DNA activator pairs for fast activation kinetics

After developing the blocked genelet design for the G1S1 node in Supplementary Section 3.2, we used NUPACK (Supplementary Section 4.1) to design the sequences of the two additional genelet nodes (G2 and Gv3). The script used to design these sequences chose sequences that minimized the spurious interaction between the two new nodes and the existing G1S1 node.

After designing the G2 and Gv3 input domain and DNA activator sequences and testing DNA activation kinetics with prototype genelets, we found that the Gv3 genelet took considerably longer the than G1 and G2 genelets to turn ON after its DNA activator was added (Supplementary Figure 14). Inspection of the DNA activator sequences of the G1, G2, and Gv3 nodes did not reveal any obvious reason why Gv3 would activate slower than the other two nodes.

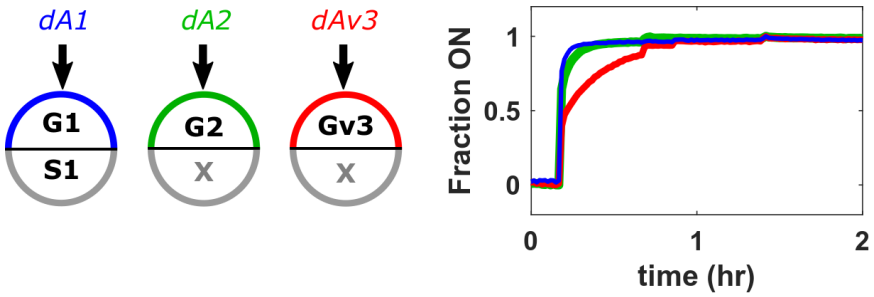

Supplementary Figure 14 | Rates of DNA activation of three genelet nodes by their respective DNA activators. The G2 and Gv3 nodes were prototypes and their output domains are shown as Xs because they have no downstream use. Reactions were conducted as described in the Methods of the main text in the absence of enzymes. Genelets were initially incubated in their OFF state in isolation at 25 nM. After 10 minutes of incubation, the corresponding DNA activators were added to each genelet sample to a final concentration of 125 nM. Sequences are presented in Supplementary Table 3.

We thus were not able to use these designs to develop specific design criteria for sequences that would ensure fast genelet DNA activation. We instead designed a large set of potential genelet sequences and then screened them all to identify sequences for nodes that could be activated quickly with their DNA activators. We designed an additional 34 genelet node sequences using a NUPACK design script (Supplementary Section 4.1) that included the regulatory sequences of both the G1 and G2 nodes to minimize spurious interactions between these nodes and the 34 new nodes. The script also minimizes interaction between all of the 34 new node sequences.

To make it economical to test the rate of DNA activation of each of these designs, we developed a new assay to measure them that used low-cost DNA strands. In previous experiments, the extent of a genelet's activation was measured using fluorescence spectroscopy in an assay where the genelet input domain possessed a fluorophore modification at its 5' end and a DNA activator with a corresponding quencher at its 3' end (Figure 1 of the main text). We calculated that adding the modifications to each of the two strands for these 34 potential nodes would have cost over $5,000 from IDT, with the required purification costing even more. To reduce the cost of screening experiments, we developed an assay that allows a node to be screened using universal fluorophore/quencher modified sequences. We designed a single fluorophore-modified strand that could hybridize to all of the genelet input sequences and a single quencher-modified strand that could hybridize to all of the DNA activator sequences on a 5' extension of the activator (Supplementary Figure 15a). In this modified assay, the estimated cost for

ordering the strands to measure the activation rates of all 34 nodes was roughly $700 (at $0.19/base for unpurified strands ordered in a 96 well plate from IDT as of this writing). Below, this assay is referred to as the high-throughput testing (HTT) assay. Before ordering all of the sequences, we first characterized the accuracy of the HTT assay using the G1 input domain and corresponding activator. The rate of DNA activation measured in the HTT assay for these sequences (Supplementary Figure 15b, HTT G) was similar to the kinetics of DNA activation of the G1S1 node measured using a specifically modified input domain and DNA activator (Supplementary Figure 14).

Using the HTT assay, we then screened the 34 potential nodes for DNA activation kinetics and identified 12 nodes that activated to 90% in less than an hour, 7 nodes that activated to 90% in less than 2 hours, and 15 nodes that took over 2 hours to activate to 90%. The roughly 35% success rate suggested that screening was a practical way to identify genelet nodes that could be efficiently activated.

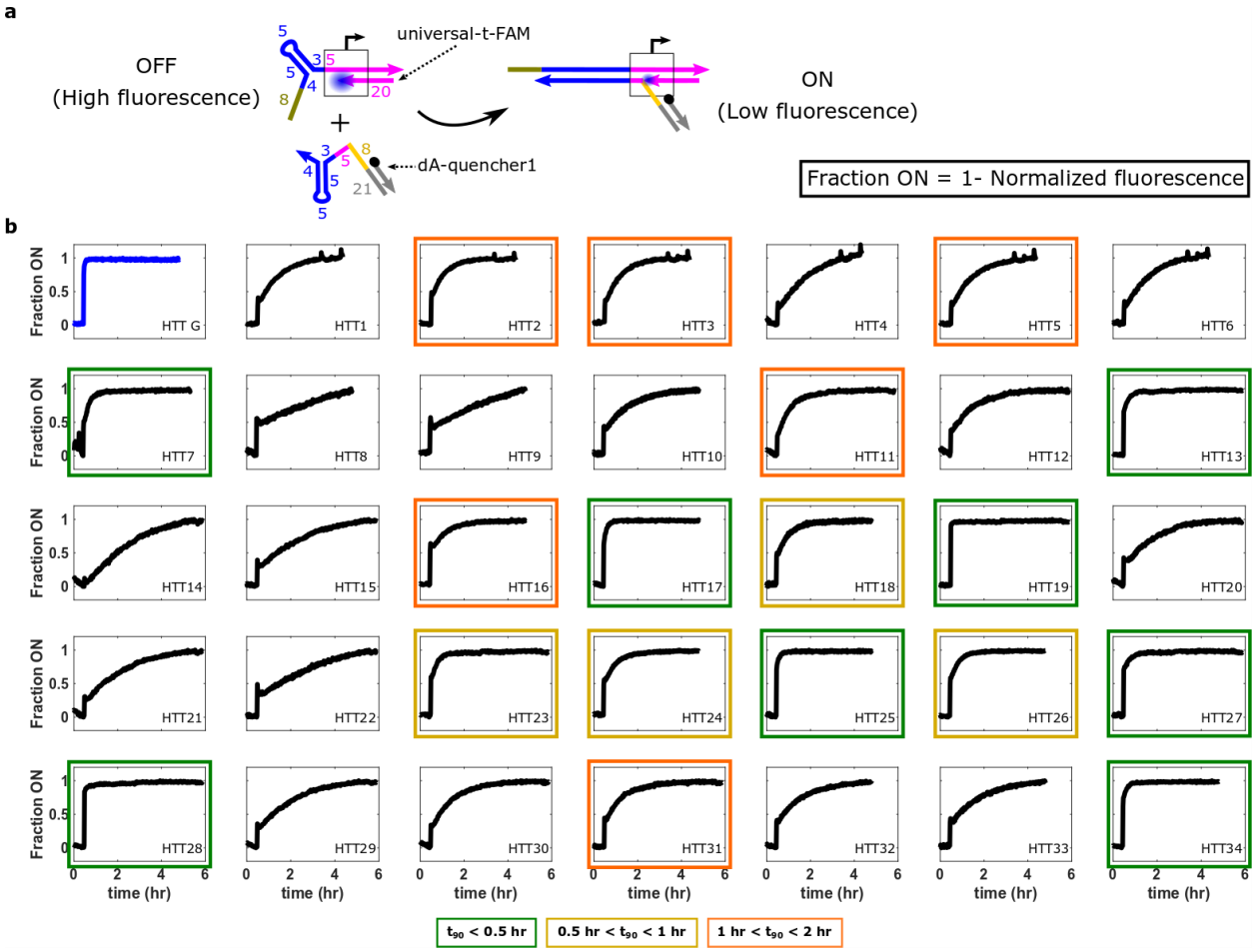

Supplementary Figure 15 | The kinetics of DNA activation of a library of 34 HTT genelet variants. (**a**) Schematic of the DNA activation assay. The assay allowed different HTT variants to be screened using a single fluorophore labeled strand and a single quencher labeled strand (universal-t-FAM and dA-quencher1 in Supplementary Table 4). Numbers indicate domain lengths in nucleotides. The kinetics of activation were measured by initially incubating an HTT genelet in the absence of its activator (OFF state) to obtain a maximum fluorescence value. The corresponding DNA activator was then added to turn the genelet on. The raw fluorescence values were normalized to be between 0 and 1 based on the max and min fluorescence values over the course of the 8-hour experiment. (**b**) Normalized HTT genelet activation levels during the experiment described in (a). DNA activators were added roughly 15 minutes into the experiment. The colors of the boxes surrounding each graph indicate the amount of time required to reach 90% activation as described by the legend at the bottom. Variants without colored boxes around them were took more than 2 hours to reach 90% activation, which was deemed too slow for use of these nodes in genelet networks. Reactions were conducted as described in the Methods of the main text in the absence of enzymes. The DNA activator strands were annealed 90°C to 20°C (-1°C/min) with an equimolar concentration of the dA-quencher1 strand prior to use in experiments. Genelets were present at 30 nM and annealed DNA activators were added to a final concentration of 150 nM. All sequences are in Supplementary Table 4.

After the screening the genelets in Supplementary Figure 15, we tried to further investigate whether specific sequence regions of the genelets and their activators might be more important for determining the rate of DNA activation than others. We created a small library of chimeric genelet:activator pairs in which the sequence of different sub-domains from a slow activating genelet (HTT2) was replaced by the sequence of the corresponding sub-domain from the G1 input domain (HTT-G in Supplementary Figure 16a). These experiments indicated that of the domains of the activator sequence, the sequence of the stem of the DNA activator hairpin had the strongest influence on the kinetics of activation: HTT2 chimeras containing the G1 hairpin stem activated almost as fast as G1 whereas other chimeras activated much more slowly (Supplementary Figure 16b).

To look at features of stem sequences that might explain the differences in DNA activation kinetics we prepared sequence logos[15] of both the fast activator sequences and the slow activator sequences. We did not observe any differences between the two logos except possibly that the stem sequences of HTT genelets that activated slowly had slightly higher GC content on average than the stem sequences of HTT genelets that activated more quickly (Supplementary Figure 17). The stem of G1 also has high GC content, yet G1 still activates quickly so it doesn't appear that GC content alone determines how quickly a genelet activates.

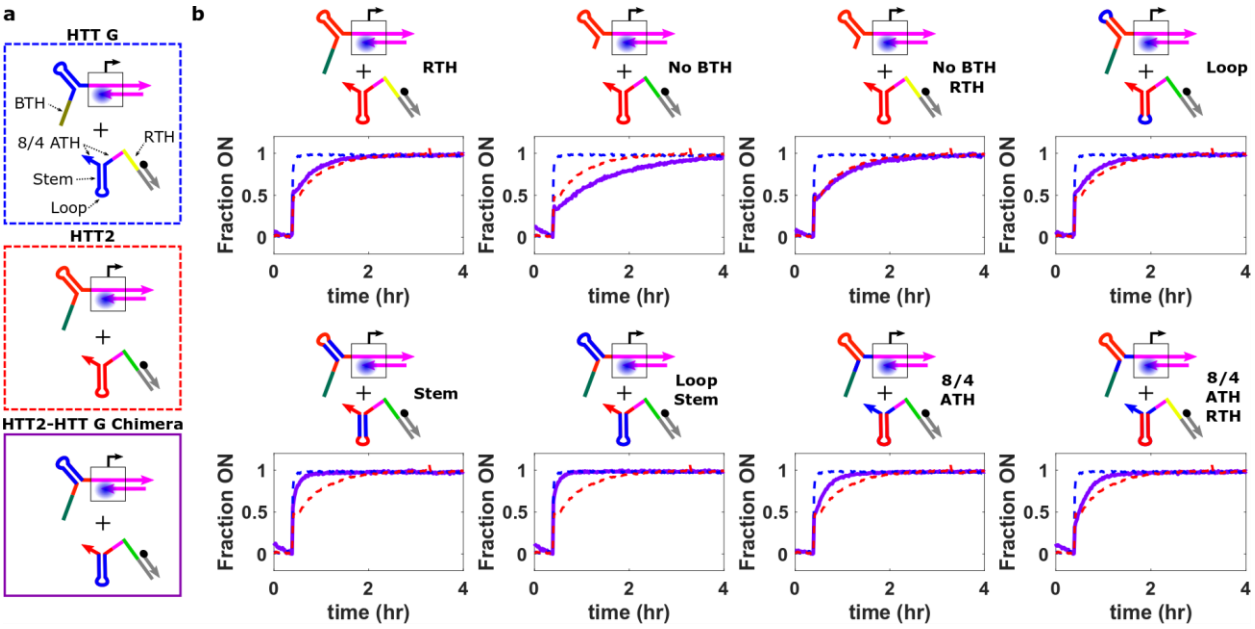

Supplementary Figure 16 | The kinetics of DNA activation of a library of chimeric HTT2-HTT G variants. (**a**) Diagram of HTT G, HTT2, and HTT2-HTT G chimeric genelet:activator pairs. The names given to the sub-domains of HTT G that were used to create the chimeras are in the top panel. The colors and line styles of the boxes surrounding the genelet:activator pairs indicate the color and line style of the kinetic plots for each in (b). (*e.g.,* the kinetics of HTT2 are plotted as a red dashed line in (b)). (**b**) Normalized activation levels of each of the HTT2-HTT G chimeras (purple solid lines) after the addition of DNA activators at 15 minutes. All chimeras have a base HTT2 sequence. The sequences of the sub-domains indicated by labels and colors of the domains in each plot have been replaced by sequences of the corresponding subdomains of HTT G. The blue and red dashed lines are the kinetics of DNA activation of the HTT G and HTT2 genelets, respectively. Reactions were conducted as described for the HTT assay in Supplementary Figure 15. Genelets were present at 30 nM and activators were added to a final concentration of 150 nM. Sequences are in Supplementary Table 4.

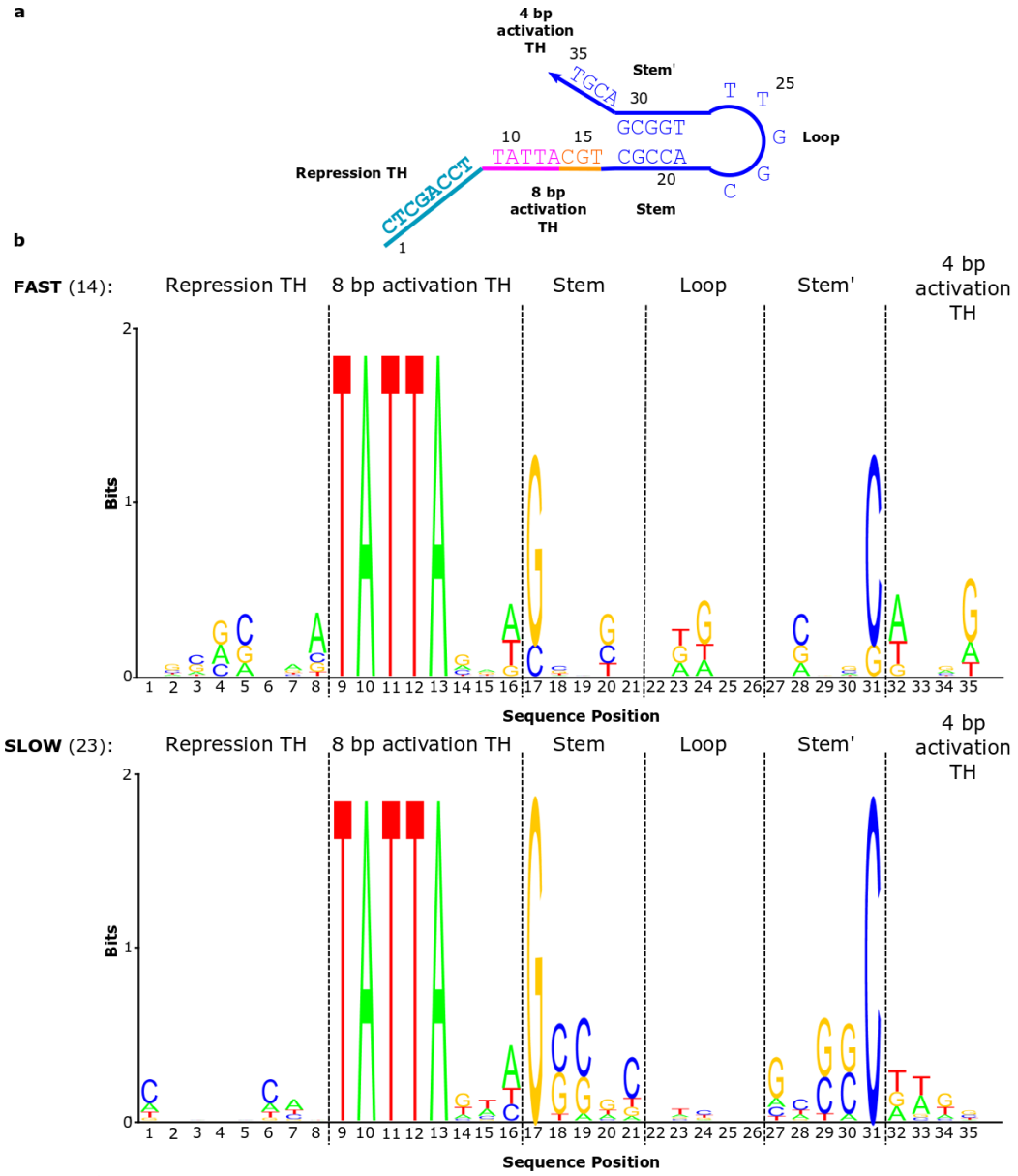

Supplementary Figure 17 | Sequence logo analysis of the DNA activators screened in Supplementary Figures 14 and 15. (**a**) Annotated schematic of dA1. The sub-domains of dA1 are labeled and correspond to the dashed partitions in (**b**). Numbers correspond to the sequence positions in (**b**). (**b**) Sequence logos of 14 fast activator sequences: G1, G2, and the HTT nodes highlighted in green and yellow in Supplementary Figure 14 (top logo), and 23 slow activator sequences: Gv3 and the rest of the HTT nodes in Supplementary Figure 14 (bottom logo). Sequence logos were generated using the *seqlogo( )* function in MATLAB.

Supplementary Table 3 | Sequences of G2 and Gv3 genelets and their DNA activators (Supplementary Figure 14). All strands were ordered HPLC purified from IDT.

GENELETS	
G1S1-nt	See Supplementary Table 2
S1-t	See Supplementary Table 2
G2X-nt	/5TYE665/AGCCAAGATTCAGGTCAATAAGTGACCAAGTAATACGACTCACTATA GTCCTTCCATGAACGCCAAACCGTGGCGACGACCTACTC
G2X-t	5'GAGTAGGTCGTCGCCACGGTTTGGCGTTCATGGAAGGACTATAGTGAGTCG
Gv3X-nt	/5HEX/TCACCCTCACACGTCGCCTGCTGCGACTACTAATACGACTCACTATA GTGCACGCCAAACCGTGGCGACGTAATAGAGCTGGA
Gv3X-t	5'TCCAGCTCTATTACGTCGCCACGGTTTGGCGTGCACTATAGTGAGTCG
ACTIVATORS	
dA2	See Supplementary Table 2
dAv3	TTCCCAAGTATTAGTAGTCGCAGCAGGCGACGTGT/3IABkFQ/

Supplementary Table 4 | The sequences of genelet and DNA activator pairs screened in Supplementary Figures 15 and 16. The quencher strand was ordered HPLC purified from IDT. All other strands were ordered unpurified from IDT.

LABELING STRANDS	
universal-t-FAM	5'CGTCTCCCTATAGTGAGTCG/36-FAM/
dA-quencher1	/5IABkFQ/CATAACACATCTCACAATCCA
GENELETS	
G HTTG	5'TCCTTCCATGCACGCCAAACCGTGGCGACGTAATA CGACTCACTATA GGGAGACG
G HTT1	5'AGATAAACGGAAGCGACATGAGGTCGCAGGTAATA CGACTCACTATA GGGAGACG
G HTT2	5'ACCTCCACCTTTGCGTCCGCTTGACGCTTCTAATA CGACTCACTATA GGGAGACG
G HTT3	5'CCCTCATCCATTGCGGTTCTACACCGCTTCTAATA CGACTCACTATA GGGAGACG
G HTT4	5'CCTACCCTGCTAGGCTCTGCTCGAGCCGTCTAATA CGACTCACTATA GGGAGACG
G HTT5	5'CCCACTCTACACGCGCTCACATAGCGCTACTAATA CGACTCACTATA GGGAGACG
G HTT6	5'GAGAATAGAGGTGTACCGTATAGGTACTAGTAATA CGACTCACTATA GGGAGACG
G HTT7	5'GAAGATGAAGGTGTACCGTATAGGTACTAGTAATA CGACTCACTATA GGGAGACG
G HTT8	5'TCACCACTCCTAGGCGCCTATTGCGCCATTTAATA CGACTCACTATA GGGAGACG
G HTT9	5'CCACTCTCCAACGCCAGGCAAACTGGCTAATAATA CGACTCACTATA GGGAGACG
G HTT10	5'CACTATCTTCCAGGCTAAGGAGTAGCCGTTTAATA CGACTCACTATA GGGAGACG
G HTT11	5'GAAATCTAGAAAGCAGGATGGGCCTGCGAATAATA CGACTCACTATA GGGAGACG
G HTT12	5'CAATATAACCACGGGACCAAATGTCCCTAATAATA CGACTCACTATA GGGAGACG
G HTT13	5'CCAACTACCTATGACTGTAACCCAGTCTCTTAATA CGACTCACTATA GGGAGACG
G HTT14	5'CCTCACTACCTTGGCGCACGAAGCGCCTACTAATA CGACTCACTATA GGGAGACG
G HTT15	5'GCCCTCTAATTTGGCGCGAGCAGCGCCTCCTAATA CGACTCACTATA GGGAGACG
G HTT16	5'GATAAATAGAGAGCCGCACAGAGCGGCAGATAATA CGACTCACTATA GGGAGACG
G HTT17	5'GAATAGAACAGAGGGTTAGCAGAACCCAGATAATA CGACTCACTATA GGGAGACG
G HTT18	5'CCATCCCTACCTGCCGTGCTCAACGGCTTCTAATA CGACTCACTATA GGGAGACG
G HTT19	5'GCTCTCCATCTTCCAGGTACACCCTGGCTCTAATA CGACTCACTATA GGGAGACG
G HTT20	5'GCAATAAAGAACGTGGCGAATGGCCACTAATAATA CGACTCACTATA GGGAGACG
G HTT21	5'CCACCATAACAAGGGTCGTGAAGACCCGAATAATA CGACTCACTATA GGGAGACG
G HTT22	5'CCTTAACATCTTGCCGCACCAAGCGGCTTCTAATA CGACTCACTATA GGGAGACG
G HTT23	5'CCACTTCACCTTGTCGGCATTTCCGACTCCTAATA CGACTCACTATA GGGAGACG
G HTT24	5'GAAGTCTGCGTAGTGGCGTCTGGCCACATTTAATA CGACTCACTATA GGGAGACG
G HTT25	5'TCTCTTACCCTCGCTCGTCCTCCGAGCCTCTAATA CGACTCACTATA GGGAGACG
G HTT26	5'CCCTTCAACTCTGCGGACGCCCTCCGCTTCTAATA CGACTCACTATA GGGAGACG
G HTT27	5'CCAACCTACTCTGCCGTTCCATACGGCTCCTAATA CGACTCACTATA GGGAGACG
G HTT28	5'CCTATCCACCGTGCGGAAATCATCCGCTATTAATA CGACTCACTATA GGGAGACG
G HTT29	5'CCTCTTACCTACGGCTGATGAGCAGCCTACTAATA CGACTCACTATA GGGAGACG
G HTT30	5'CCTACTTACCGAGGCGCGTTAAGCGCCAAATAATA CGACTCACTATA GGGAGACG
G HTT31	5'ACTCTCCACCGTGCGGCTGACTGCCGCTATTAATA CGACTCACTATA GGGAGACG
G HTT32	5'CATCCTCACCACGCTCCAACCGGGAGCTTATAATA CGACTCACTATA GGGAGACG
G HTT33	5'CAATTCAACAGCGGCTGTAGACCAGCCTTATAATA CGACTCACTATA GGGAGACG
G HTT34	5'GTCCAATTCCACGGCTCGTCAAGAGCCACCTAATA CGACTCACTATA GGGAGACG
G HTT2_G_Loop	5'AGATAAACGGAAGCGACAACCGGTCGCAGGTAATA CGACTCACTATA GGGAGACG
G HTT2_G_Stem	5'AGATAAACGGAACGCCAATGAGTGGCGAGGTAATA CGACTCACTATA GGGAGACG

G HTT2_G_Stem_Loop	5’AGATAAACGGAACGCCAAACCGTGGCGAGGTAATA CGACTCACTATA GGGAGACG
G HTT2_G_8_4_ATH	5’AGATAAACTGCAGCGACATGAGGTCGCACGTAATA CGACTCACTATA GGGAGACG
G HTT2_-BTH	5’ GGAAGCGACATGAGGTCGCAGGTAATA CGACTCACTATA GGGAGACG
ACTIVATORS	
A HTTG	5’TGGATTGTGAGATGTGTTATG TCCAGCTCTATTACGTCGCCACGGTTTGGCGTGCA
A HTT1	5’TGGATTGTGAGATGTGTTATG AACACTGCTATTACCTGCGACCTCATGTCGCTTCC
A HTT2	5’TGGATTGTGAGATGTGTTATG AGCACCAGTATTAGAAGCGTCAAGCGGACGCAAAG
A HTT3	5’TGGATTGTGAGATGTGTTATG CACGACCCTATTAGAAGCGGTGTAGAACCGCAATG
A HTT4	5’TGGATTGTGAGATGTGTTATG ACACGCACTATTAGACGGCTCGAGCAGAGCCTAGC
A HTT5	5’TGGATTGTGAGATGTGTTATG CGTCCATCTATTAGTAGCGCTATGTGAGCGCGTGT
A HTT6	5’TGGATTGTGAGATGTGTTATG TTCCGCACTATTACTAGTACCTATACGGTACACCT
A HTT7	5’TGGATTGTGAGATGTGTTATG CCGACAAATATTACTAGTACCTATACGGTACACCT
A HTT8	5’TGGATTGTGAGATGTGTTATG CTCGTGCATATTAAATGGCGCAATAGGCGCCTAGG
A HTT9	5’TGGATTGTGAGATGTGTTATG CCGATCTTTATTATTAGCCAGTTTGCCTGGCGTTG
A HTT10	5’TGGATTGTGAGATGTGTTATG CGACACAATATTAAACGGCTACTCCTTAGCCTGGA
A HTT11	5’TGGATTGTGAGATGTGTTATG CCCTCCATTATTATTCGCAGGCCCATCCTGCTTTC
A HTT12	5’TGGATTGTGAGATGTGTTATG CCGATCTTTATTATTAGGGACATTTGGTCCCGTGG
A HTT13	5’TGGATTGTGAGATGTGTTATG AGCAGAAGTATTAAGAGACTGGGTTACAGTCATAG
A HTT14	5’TGGATTGTGAGATGTGTTATG CCGTTTCTTATTAGTAGGCGCTTCGTGCGCCAAGG
A HTT15	5’TGGATTGTGAGATGTGTTATG GTGTGCATTATTAGGAGGCGCTGCTCGCGCCAAAT
A HTT16	5’TGGATTGTGAGATGTGTTATG TGTGCAATTATTATCTGCCGCTCTGTGCGGCTCTC
A HTT17	5’TGGATTGTGAGATGTGTTATG GTCGCGTGTATTATCTGGGTTCTGCTAACCCTCTG
A HTT18	5’TGGATTGTGAGATGTGTTATG AGCGCGAATATTAGAAGCCGTTGAGCACGGCAGGT
A HTT19	5’TGGATTGTGAGATGTGTTATG TGCGACGATATTAGAGCCAGGGTGTACCTGGAAGA
A HTT20	5’TGGATTGTGAGATGTGTTATG CTTCGTTATATTATTAGTGGCCATTCGCCACGTTC
A HTT21	5’TGGATTGTGAGATGTGTTATG GCGTCCTTTATTATTCGGGTCTTCACGACCCTTGT
A HTT22	5’TGGATTGTGAGATGTGTTATG AGCGACAATATTAGAAGCCGCTTGGTGCGGCAAGA
A HTT23	5’TGGATTGTGAGATGTGTTATG AGCGCAGATATTAGGAGTCGGAAATGCCGACAAGG
A HTT24	5’TGGATTGTGAGATGTGTTATG AGGAGGCATATTAAATGTGGCCAGACGCCACTACG
A HTT25	5’TGGATTGTGAGATGTGTTATG GGGACGAATATTAGAGGCTCGGAGGACGAGCGAGG
A HTT26	5’TGGATTGTGAGATGTGTTATG GCAGCGAATATTAGAAGCGGAGGGCGTCCGCAGAG
A HTT27	5’TGGATTGTGAGATGTGTTATG GGAGATAATATTAGGAGCCGTATGGAACGGCAGAG
A HTT28	5’TGGATTGTGAGATGTGTTATG CAGCAGCATATTAATAGCGGATGATTTCCGCACGG
A HTT29	5’TGGATTGTGAGATGTGTTATG TCGGGTCATATTAGTAGGCTGCTCATCAGCCGTAG
A HTT30	5’TGGATTGTGAGATGTGTTATG GCCGCTGTTATTATTTGGCGCTTAACGCGCCTCGG
A HTT31	5’TGGATTGTGAGATGTGTTATG GGCGCAGTTATTAATAGCGGCAGTCAGCCGCACGG
A HTT32	5’TGGATTGTGAGATGTGTTATG CCTCTCAATATTATAAGCTCCCGGTTGGAGCGTGG
A HTT33	5’TGGATTGTGAGATGTGTTATG TCCCGTTCTATTATAAGGCTGGTCTACAGCCGCTG
A HTT34	5’TGGATTGTGAGATGTGTTATG GTGCGTGTTATTAGGTGGCTCTTGACGAGCCGTGG
A HTT2_G_Loop	5’TGGATTGTGAGATGTGTTATG AACACTGCTATTACCTGCGACCGGTTGTCGCTTCC
A HTT2_G_Stem	5’TGGATTGTGAGATGTGTTATG AACACTGCTATTACCTCGCCACTCATTGGCGTTCC
A HTT2_G_Stem_Loop	5’TGGATTGTGAGATGTGTTATG AACACTGCTATTACCTCGCCACGGTTTGGCGTTCC
A HTT2_G_RTH	5’TGGATTGTGAGATGTGTTATG TCCAGCTCTATTACCTGCGACCTCATGTCGCTTCC
A HTT2_G_8_4_ATH	5’TGGATTGTGAGATGTGTTATG AACACTGCTATTACGTGCGACCTCATGTCGCTGCA
A HTT2_G_8_4_ATH_RTH	5’TGGATTGTGAGATGTGTTATG TCCAGCTCTATTACGTGCGACCTCATGTCGCTGCA

4.3 Screening for domains efficiently regulated by coactivator and repressor transcription

We next tested whether the genelet nodes we identified in Supplementary Section 4.2 could be efficiently coactivated and/or repressed *via* transcription of their RNA coactivators and repressors. We started by characterizing the coactivation and repression rates of the G1S1 node both using DNA versions of the coactivators and repressors and using constitutively active transcription templates that produced RNA coactivators and repressors. These transcription templates were designed according to the RNA transcription design criteria discussed in Supplementary Section 3.3.

To measure rates of coactivation, we incubated the genelets in a BLK state alongside their DNA activators and, after obtaining an initial baseline fluorescence signal, either added the appropriate DNA coactivator or the appropriate RNA coactivator transcription template and the enzymes (T7 RNAP, RNase H, and YIPP). The same procedure was followed to measure the repression rates, except the genelets were initially incubated in their OFF state without DNA blockers present. Their DNA activators were then added and allowed to react fully to turn the genelets on prior to the addition of either the appropriate DNA repressor or RNA repressor transcription template and enzymes. Transcription of rC1 and rR1 resulted in fast coactivation and repression rates for the G1S1 node, comparable to the rate of coactivation and repression obtained with DNA coactivators and repressors (Supplementary Figure 18). Likewise, using the Gv2 input domain we had previously identified, we tested a G2C1 node which exhibited similar coactivation and repression behavior using the dB2 strand identified in Supplementary Figure 11d.

We then ordered three more genelet nodes that could be potentially used in networks using input domains that we observed were activated quickly in the HTT DNA activation assay. These nodes were modified for fluorescence measurements as depicted in Figure 1 of the main text as we intended to use them in networks. We then tested the rates of coactivation and repression of these three nodes with both DNA coactivators and repressors and transcription templates encoding RNA coactivators and repressors. One node (G3R1 (HTT7 input domain)) could be both rapidly (>90% regulation in less than an hour) coactivated and repressed *via* transcription of rC3 and rR3. Another node (G9S2 (HTT13 input domain)) could be coactivated quickly via transcription of rC9 but repression via transcription of rR9 took nearly 2 hours to reach >90% regulation. Both coactivation and repression via transcription of the appropriate RNA coactivator and repressors of the last node tested (G HTT28 S3) took nearly 2 hours to reach 90% regulation (Supplementary Figure 18). Coactivation and repression was fast for all nodes when DNA coactivators or DNA repressors were used. Given these five nodes exhibited variable performance for coactivation and repression when their coactivators or repressors were transcribed, we decided to screen the coactivation and repression rates of all of the potential nodes identified in Supplementary Section 4.2 to identify domains with standardized behavior for assembly into networks. We specifically defined standardized behavior as nodes that could be up- or downregulated by >90% in less than an hour *via* transcription of RNA coactivators or repressors, respectively.

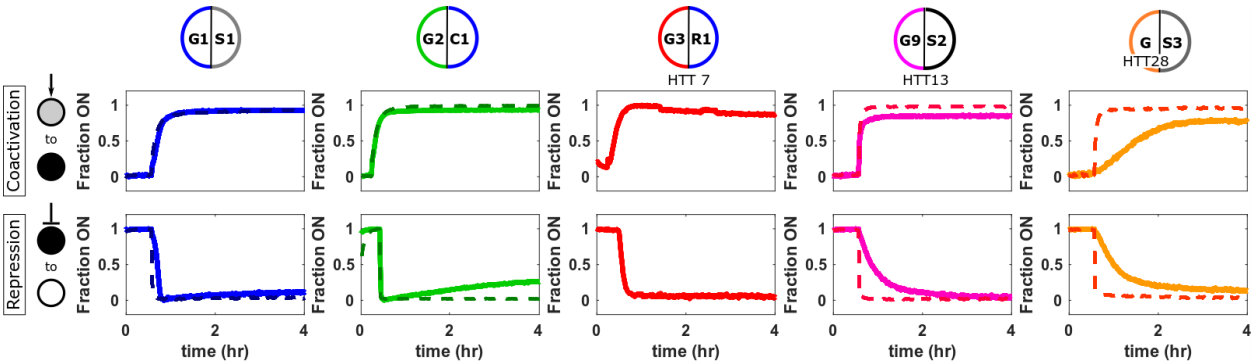

Supplementary Figure 18 | Normalized node activation levels over time during coactivation or repression via transcription of RNA coactivators and repressors (solid lines) and during control experiments in which DNA coactivators or DNA repressors were added to samples in the absence of enzymes (dashed lines). The G1S1 node and G2C1 nodes were designed in before the HTT DNA activation screening was conducted. The remaining three nodes possess input domains identified in the HTT screening assay and their names from that assay are shown below the nodes. DNA coactivators and repressors were added to a final concentration of 500 nM and 1000 nM, respectively. Reactions were otherwise conducted as described in the Methods of the main text with [YIPP] = 1.35 x 10^{-3} U/μL, [T7 RNAP] = 3.57 U/μL, [RNase H] = 8.93 x 10^{-3} U/μL, [genelets] = 25 nM, and [activators] = 250 nM unless otherwise stated. Some of the concentrations for transcriptional regulation were slightly different across the experiments for these five nodes but the main comparison is between each node's transcriptional regulation rate and its regulation rate with a corresponding DNA regulator. G1S1, G9S2, G HTT28 coactivation and repression reactions were conducted 15 nM of each coactivation and repression transcription template. G2 coactivation and repression reactions were conducted with 15 nM coactivation transcription template, 25 nM repression transcription template, and [RNase H] = 4.46 x 10^{-3} U/μL. G3R1 coactivation and repression reactions were conducted with 125 nM activator for coactivation, and 25 nM repression transcription template. The transcriptional coactivation of G3R1 was conducted using 25 nM of an upstream genelet with 250 nM of this upstream genelet's activator (G2C3 and dA2) rather than a constitutively active transcription template. Sequences are in Supplementary Table 5.

The genelets tested in Supplementary Figure 18 were labeled with a fluorophore and quencher in the same way as the genelet shown in Figure 1 of the main text: each genelet input domain strand was modified with a fluorophore at its 5' end and each DNA activator was modified with a quencher at its 3' end. To reduce the cost of measuring the rates of coactivation and repression for the remaining library members, we created a modified design for these nodes that could be used for screening but required the purchase of fewer modified strands per screened node. In this design, we extended the 3' ends of the activators by adding a common sequence that was complementary to a quencher-modified tag strand (Supplementary Figure 19). In this way, the same quencher labeled strand could be used for each screened node. We did not simply reuse the design shown in Supplementary Figure 15a for measuring the rates of coactivation and repression because we were concerned that non-specific transcription initiated on the single-stranded regions of the DNA activators[4,16] might displace the quencher strand, confounding interpretation of the fluorescence measurements. In our modified assay design, the quencher strand being bound to the 3' end of the DNA activator is expected to prevent such a reaction[4]. We also used an unpurified genelet input domain strand with a 5' FAM modification. This strand was also truncated, possessing only 6 bases after the T7 RNAP promoter sequence, which allowed the same universal template strand to be used for each genelet input domain.

To test that this design would allow for accurate measurements of the rates of coactivation and repression, we first ordered a version of this screening node for G1. The rates of coactivation and repression both with DNA coactivators/repressors and with transcription of RNA coactivators/repressors

were indistinguishable from those measured using the G1S1 node (Supplementary Figure 18 for G1S1 and Supplementary Figure 20 for the screening design (HTT G)).

After this test, we ordered the screening design for the 11 remaining nodes that we observed were efficiently activated by their DNA activators in the HTT activation assay (Supplementary Section 4.2) and measured their rates of coactivation and repression with our new assay both with DNA coactivators/ repressors and with transcription of RNA coactivators/repressors. Three of these nodes were both rapidly coactivated and rapidly repressed *via* transcription of their RNA coactivators and RNA repressors, exhibiting kinetics similar to those observed *via* addition of their DNA coactivators and repressors (Supplementary Figure 20, green) and four of them could be either rapidly coactivated or rapidly repressed *via* transcription of their RNA coactivators or repressors, respectively (Supplementary Figure 20, yellow). Addition of DNA coactivators and DNA repressors resulted in >90% regulation in less than an hour for all of the 11 nodes tested.

By screening the 11 nodes shown in Supplementary Figure 20 and the 5 nodes in Supplementary Figure 18, we measured the kinetics of both coactivation and repression *via* transcription of 16 nodes, a total of 32 possible reactions. Six of these nodes were coactivated and repressed to >90% in less than an hour by transcription of RNA coactivators/repressors (12 successful reactions) and five additional nodes could be either coactivated or repressed to >90% in less than an hour *via* transcription of RNA coactivation/repressors (5 successful reactions). Thus, in total 53% (17/32) of the coactivation and repression reactions we tested were deemed fast enough for use. The 11 standardized nodes identified in these two screening processes were then used interchangeably for *in vitro* transcriptional regulatory network assembly in the remainder of this work. The measured kinetics of coactivation and repression for these 11 nodes are compiled in Supplementary Section 4.4 for reference.

We were not able to specifically identify reasons for the variations in the rates of coactivation and repression *via* transcription between the nodes that were screened. Given that all of the 16 screened nodes were coactivated or repressed rapidly by DNA coactivators or repressors (dashed lines in Supplementary Figures 18 and 20), the slow rates of coactivation or repression observed when RNA coactivators or RNA repressors were transcribed likely arises from either: (1) differences in the rates of the coactivation and repression reactions when an RNA coactivator/repressor *vs.* a DNA coactivator/repressor is used, (2) sequence specific differences in the rates of transcription of RNA coactivators and repressors, (3) the presence of unpredicted structure or the dimerization of RNA coactivators or repressors during transcription, given the challenges of accurately predicting RNA structure and interaction[17] or (4) sequence-specific differences in the rates of premature termination of transcription. We did find that increasing the concentration of the regulating node did not increase the rate of regulation for the G10 node, which exhibited much slower transcriptional coactivation than when dC10 was used to trigger coactivation (Supplementary Figure 21). These results suggest that slow transcription (mechanism 2 above) is likely not the cause of poor transcriptional regulation.

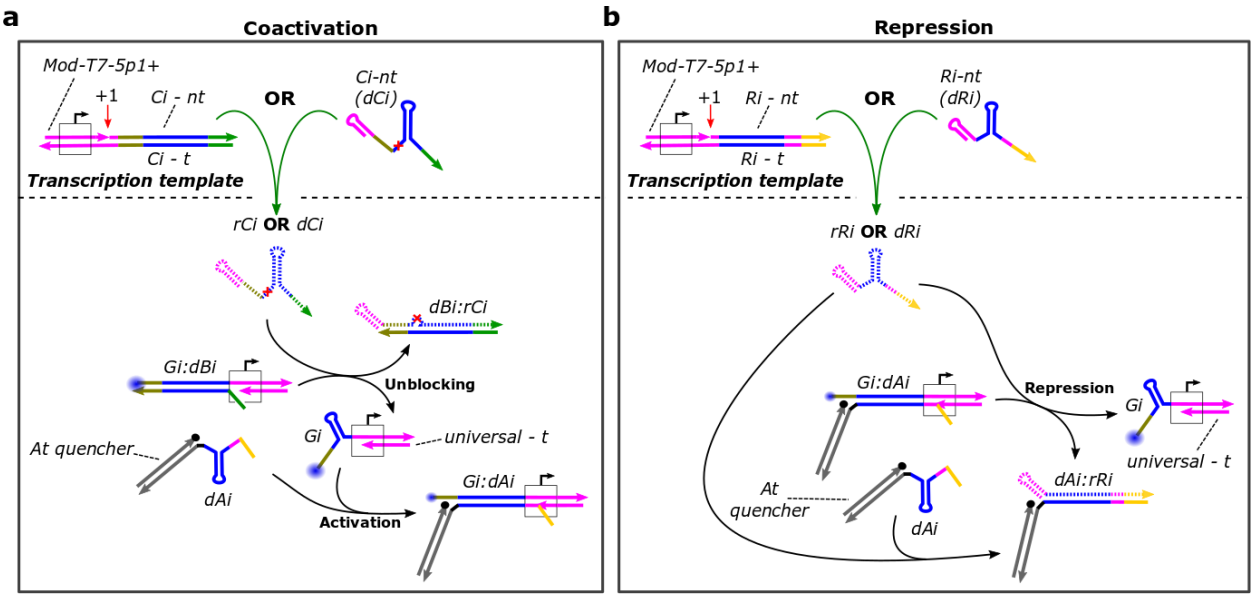

Supplementary Figure 19 | Measurement of the rates of coactivation and repression of 11 library nodes by DNA coactivators/repressors and by transcription of RNA coactivators/repressors. (**a**,**b**) Schematic of the reactions involved in and the fluorescence labeling scheme used to measure coactivation (a) and repression (b). The transcription templates were composed of 3 strands. The nick between the top two strands is at the +1 T7 RNAP promoter site so that each non-template strand could double as a DNA coactivator or DNA repressor for control experiments in the absence of enzymes. The sequences are in Supplementary Table 6.

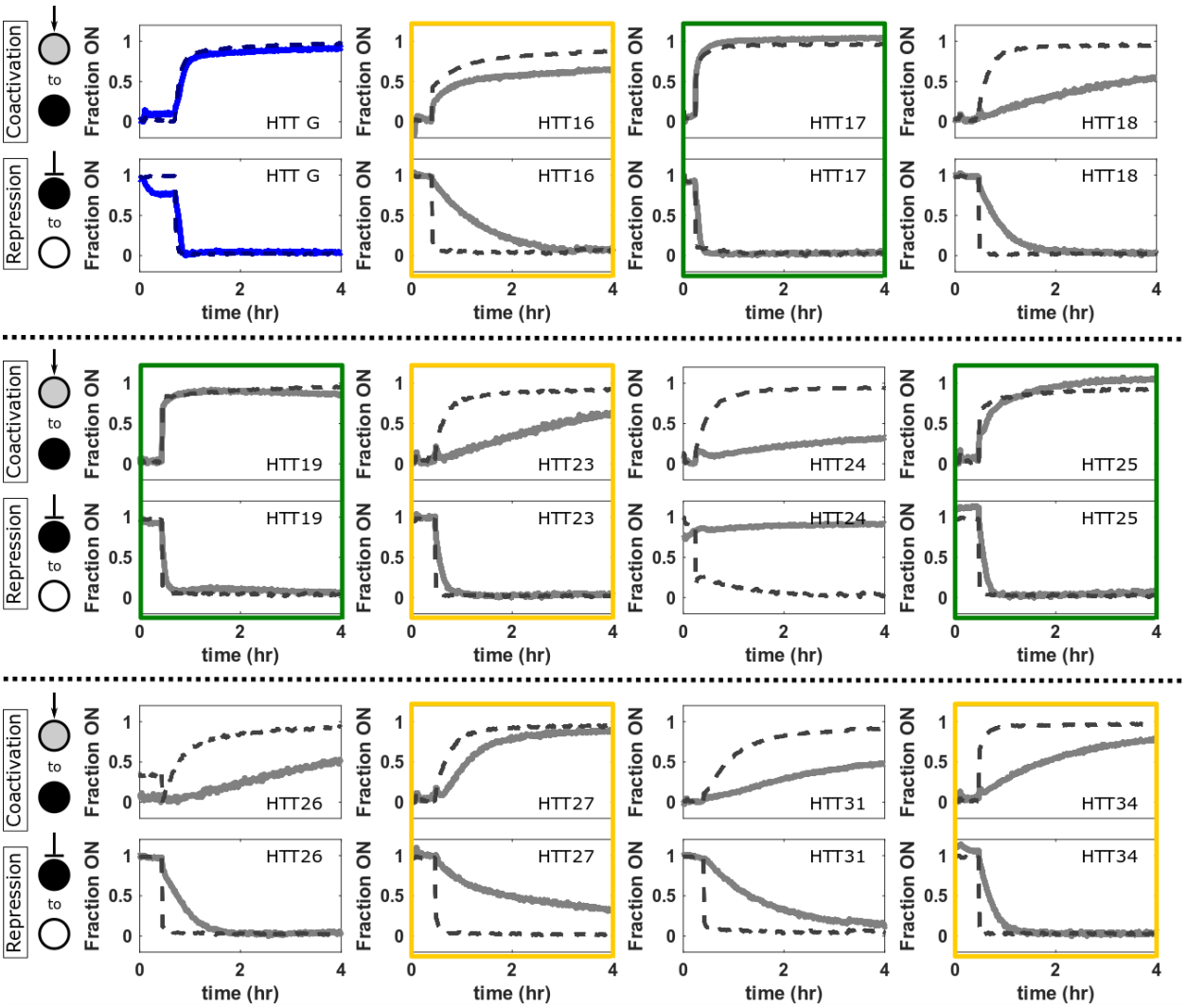

Supplementary Figure 20 | Normalized node activation levels when nodes are coactivated and repressed by RNA transcribed from transcription templates (solid lines) and by DNA coactivators or repressors (dashed lines) using the assay depicted in Supplementary Figure 19. These DNA coactivators and DNA repressors (the -nt strands of the transcription templates) were added to a final concentration of 500 nM and 1000 nM, respectively. Reactions were conducted under the conditions described in the Methods of the main text with DNA activator complexes at 250 nM, genelet complexes at 25 nM, and transcription templates at 25 nM, and [RNase H] = 4.46 x 10^{-3} U/µL, [YIPP] = 1.35 x 10^{-3} U/µL, [T7 RNAP] = 3.57 U/µL. DNA activator strands were annealed with equimolar concentrations of the At quencher stand. Transcription templates were annealed with equimolar concentrations of the Mod_T7_+1p, -nt, and -t strands (90°C to 20°C @ -1°C/min). In these experiments genelets were initially incubated in either a BLK (for coactivation experiments) or OFF (for repression experiments) state in the absence of activators, enzymes, and transcription templates. During this incubation, fluorescence measurements were taken to obtain a maximum fluorescence value for the BLK genelets. After roughly 15 minutes of incubation, the corresponding DNA activators were added to the samples. After a 30-minute incubation the enzyme mix was added to the samples. This 30-minute incubation was conducted for both coactivation and repression reactions and ensured the genelets in repression samples had time to bind with their DNA activators. The addition of the enzyme mix marks the beginning of the experiments in (**b**) and after another 30-minute incubation, the transcriptional templates were added to a final concentration of 25 nM to begin the coactivation and repression reactions. The fluorescence data was normalized as described in Supplementary Section 13: at the end of the experiments measuring the rates of node repression, an excess of the appropriate DNA repressor was added to obtain the fluorescence value corresponding to the node being fully repressed. The fluorescence data was then normalized starting at the time of enzyme addition (where the node was presumed fully ON). For the coactivation data the minimum fluorescence value for the transcriptional coactivation samples was taken from their corresponding DNA coactivator controls.

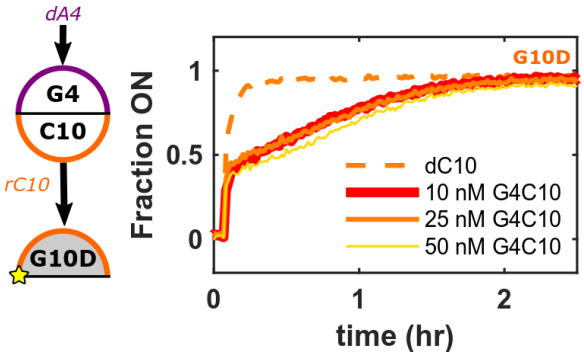

Supplementary Figure 21 | The kinetics of G10D coactivation via transcription of rC10 does not change when the concentration of G4C10 is increased. This suggests the slower coactivation via transcription compared to the addition of the DNA coactivator (dC10) is not due to slow transcription of the rC10 sequence. Reactions were conducted as described in the Methods of the main text In all experiments G10D was at 25 nM, the G4C10 was at the concentrations presented in the legend. dA4 was added to 250 nM and no additional blocker was added. Non-template strands for G4C10 are in Supplementary Table 7, all other sequences are in Supplementary Table 1.

Supplementary Table 5 | Sequences from coactivation and repression tests of five different genelet nodes (Supplementary Figure 18). All strands were ordered HPLC purified from IDT.

GENELETS	
G1S1-nt	See Supplementary Table 2
S1-t	See Supplementary Table 2
G2C1-nt	See Supplementary Table 2
C1-t	See Supplementary Table 1
G3R1-nt	/5TEX615/GAAGATGAAGGTGTACCGTATAGGTACTAGTAATACGACTCACTATA GGGAGATTCGTCTCCCATGCACGCCAAACCGTGGCGACGTAAT
R1-t	See Supplementary Table 1
G2C3-nt	See Supplementary Table 12
C3-t	See Supplementary Table 1
G9S2-nt	See Supplementary Table 2
S2-t	See Supplementary Table 2
G HTT28-nt	/5TYE563/CCTATCCACCGTGCGGAAATCATCCGCTATTAATACGACTCACTATA GGGATCCCGACTGGCGAGAGCCAGGTAACGAATGGATCC
G HTT28-t	5'GGATCCATTCGTTACCTGGCTCTCGCCAGTCGGGATCCCTATAGTGAGTCG
ACTIVATORS	
dA1	See Supplementary Table 1
dA2	See Supplementary Table 1
dA3	See Supplementary Table 1
dA9	See Supplementary Table 1
dA HTT28	5'CAGCAGCATATTAATAGCGGATGATTTCCGCACGG/3IABkFQ/
BLOCKERS	
dB1	See Supplementary Table 1
dB2	See Supplementary Table 1
dB3	See Supplementary Table 1
dB9	See Supplementary Table 1
dB HTT28	5'GGTAAGGGATAGCGGATGATTTCCGCACGGTGGATAGG

TRANSCRIPTION TEMPLATES	
C-G1-5PSHP-nt	See Supplementary Table 2
C-G1-5PSHP-t	See Supplementary Table 2
R-G1-nt	5′TAGTAATACGACTCACTATAGGGAGATTCGTCTCCCATGCACGCCAAACCGTGGCGACG
R-G1-t	5′TCCAGCTCTATTACGTCGCCACGGTTTGGCGTGCATGGGAGACGAATCTCCCTATAGTG AGTCGTATTACTA
C-G2-nt	See Supplementary Table 2
C-G2-t	See Supplementary Table 2
R-G2-nt	5′TTCTAATACGACTCACTATAGGGAGATTCGTCTCCCATTCAGGTCAATAAGTGACCAAG TAATAGTGGGATG
R-G2-t	5′CATCCCACTATTACTTGGTCACTTATTGACCTGAATGGGAGACGAATCTCCCTATAGTG AGTCGTATTAGAA
C-G3-nt	G2C3 / dA2 were used
C-G3-t	G2C3 / dA2 were used
R-G3-nt	5′TTCTAATACGACTCACTATAGGGAGATTCGTCTCCCAAGGTGTACCGTATAGGTACTAG TAATATTTGTCGG
R-G3-t	5′CCGACAAATATTACTAGTACCTATACGGTACACCTTGGGAGACGAATCTCCCTATAGTG AGTCGTATTAGAA
C-G9-full-nt	See Supplementary Table 2
C-G9-t	See Supplementary Table 2
R-G9-nt	5′TTCTAATACGACTCACTATAGGGAGATTCGTCTCCCACTATGACTGTAACCCAGTCTCT TAATACTTCTGCT
R-G9-t	5′AGCAGAAGTATTAAGAGACTGGGTTACAGTCATAGTGGGAGACGAATCTCCCTATAGTG AGTCGTATTAGAA
C-HTT28-nt	5′TTCTAATACGACTCACTATAGGGAGATTCGTCTCCCAACCTATCCACCCTGCGGAAATC ATCCGCTATCCCTTACC
C-HTT28-t	5′GGTAAGGGATAGCGGATGATTTCCGCAGGGTGGATAGGTTGGGAGACGAATCTCCCTAT AGTGAGTCGTATTAGAA
R-HTT28-nt	5′TTCTAATACGACTCACTATAGGGAGATTCGTCTCCCAACCGTGCGGAAATCATCCGCTA TTAATATGCTGCTG
R-HTT28-t	5′CAGCAGCATATTAATAGCGGATGATTTCCGCACGGTTGGGAGACGAATCTCCCTATAGT GAGTCGTATTAGAA

Supplementary Table 6 | Sequences used to measure the rates of coactivation and repression of HTT nodes (Supplementary Figure 20). The At quencher strand was ordered HPLC purified and all other strands were ordered unpurified from IDT.

GENELETS	
Gt HTT G	/56-FAM/ TCCTTCCATGCACGCCAAACCGTGGCGACGTAATACGACTCACTATAGGGAGA
Gt HTT16	/56-FAM/TGATAAATAGAGAGCCGCACAGAGCGGCAGATAATACGACTCACTATAGGGAGA
Gt HTT17	/56-FAM/TGAATAGAACAGAGGGTTAGCAGAACCCAGATAATACGACTCACTATAGGGAGA
Gt HTT18	/56-FAM/CCATCCCTACCTGCCGTGCTCAACGGCTTCTAATACGACTCACTATAGGGAGA
Gt HTT19	/56-FAM/TGCTCTCCATCTTCCAGGTACACCCTGGCTCTAATACGACTCACTATAGGGAGA
Gt HTT23	/56-FAM/CCACTTCACCTTGTCGGCATTTCCGACTCCTAATACGACTCACTATAGGGAGA
Gt HTT24	/56-FAM/TGAAGTCTGCGTAGTGGCGTCTGGCCACATTTAATACGACTCACTATAGGGAGA
Gt HTT25	/56-FAM/TCTCTTACCCTCGCTCGTCCTCCGAGCCTCTAATACGACTCACTATAGGGAGA
Gt HTT26	/56-FAM/CCCTTCAACTCTGCGGACGCCCTCCGCTTCTAATACGACTCACTATAGGGAGA
Gt HTT27	/56-FAM/CCAACCTACTCTGCCGTTCCATACGGCTCCTAATACGACTCACTATAGGGAGA
Gt HTT31	/56-FAM/ACTCTCCACCGTGCGGCTGACTGCCGCTATTAATACGACTCACTATAGGGAGA
Gt HTT34	/56-FAM/TGTCCAATTCCACGGCTCGTCAAGAGCCACCTAATACGACTCACTATAGGGAGA
universal-t	5'TCTCCCTATAGTGAGTCG
ACTIVATORS	
At HTT G	5'TCCAGCTCTATTACGTCGCCACGGTTTGGCGTGCA ACACCACCAAACTTCATCTCA
At HTT16	5'TGTGCAATTATTATCTGCCGCTCTGTGCGGCTCTC ACACCACCAAACTTCATCTCA
At HTT17	5'GTCGCGTGTATTATCTGGGTTCTGCTAACCCTCTG ACACCACCAAACTTCATCTCA
At HTT18	5'AGCGCGAATATTAGAAGCCGTTGAGCACGGCAGGT ACACCACCAAACTTCATCTCA
At HTT19	5'TGCGACGATATTAGAGCCAGGGTGTACCTGGAAGA ACACCACCAAACTTCATCTCA
At HTT23	5'AGCGCAGATATTAGGAGTCGGAAATGCCGACAAGG ACACCACCAAACTTCATCTCA
At HTT24	5'AGGAGGCATATTAAATGTGGCCAGACGCCACTACG ACACCACCAAACTTCATCTCA
At HTT25	5'GGGACGAATATTAGAGGCTCGGAGGACGAGCGAGG ACACCACCAAACTTCATCTCA
At HTT26	5'GCAGCGAATATTAGAAGCGGAGGGCGTCCGCAGAG ACACCACCAAACTTCATCTCA
At HTT27	5'GGAGATAATATTAGGAGCCGTATGGAACGGCAGAG ACACCACCAAACTTCATCTCA
At HTT31	5'GGCGCAGTTATTAATAGCGGCAGTCAGCCGCACGG ACACCACCAAACTTCATCTCA
At HTT34	5'GTGCGTGTTATTAGGTGGCTCTTGACGAGCCGTGG ACACCACCAAACTTCATCTCA
At quencher	TGAGATGAAGTTTGGTGGTG/3IAbRQSp/
BLOCKERS	
Bt HTT16	5'CCTCCCGCTCTGCCGCTCTGTGCGGCTCTCTATTTATC
Bt HTT17	5'CCTCGTCCTCTGGGTTCTGCTAACCCTCTGTTCTATTC
Bt HTT18	5'GTAGTTGGGAAGCCGTTGAGCACGGCAGGTAGGGATGG
Bt HTT19	5'GGTAGGGTGAGCCAGGGTGTACCTGGAGGATGGAGAGC
Bt HTT23	5'GAATGAGTGGAGTCGGAAATGCCGACAAGGTGAAGTGG
Bt HTT24	5'CCAATAATAATGTGGCCAGACGCCACTACGCAGACTTC
Bt HTT25	5'GTAGTGTGGAGGCTCGGAGGACGAGCGAGGGTAAGAGA
Bt HTT26	5'GAGAGTGTGAAGCGGAGGGCGTCCGCATAGTTGAAGGG
Bt HTT27	5'GGTAGTGTGGAGCCGTATGGAACGGCAGAGTAGGTTGG
Bt HTT31	5'GAGGATGGATAGCGGCAGTCAGCCGCACGGTGGAGAGT
Bt HTT34	5'GATGGGATGGTGGCTCTTGACGAGCCGTGGAATTGGAC
TRANSCRIPTION TEMPLATES	
C-HTT G-nt	5'GGAGATTCGTCTCCCAAATCCTTCCATGAACGCCAAACCGTGGCGACGACCTACTC
C-HTT G-t	5'GAGTAGGTCGTCGCCACGGTTTGGCGTTCATGGAAGGATTTGGGAGACGAATCTCCCTATAGTGAGTC GTATTAGAA
R-HTT G-nt	5'GGAGATTCGTCTCCCATGCACGCCAAACCGTGGCGACGTAATAGAGCTGGA
R-HTT G-t	5'TCCAGCTCTATTACGTCGCCACGGTTTGGCGTGCATGGGAGACGAATCTCCCTATAGTGAGTC GTATTAGAA
C-HTT16-nt	5'GGAGATTCGTCTCCCAGATAAATAGAAAGCCGCACAGAGCGGCAGAGCGGGAGG
C-HTT16-t	5'CCTCCCGCTCTGCCGCTCTGTGCGGCTTTCTATTTATCTGGGAGACGAATCTCCCTATAGTGAGTC GTATTAGAA
R-HTT16-nt	5'GGAGATTCGTCTCCCAGAGAGCCGCACAGAGCGGCAGATAATAATTGCACA
R-HTT16-t	5'TGTGCAATTATTATCTGCCGCTCTGTGCGGCTCTCTGGGAGACGAATCTCCCTATAGTGAGTCG TATTAGAA

C-HTT17-nt	5′GGAGATTCGTCTCCCAGAATAGAACAAAGGGTTAGCAGAACCCAGAGGACGAGG
C-HTT17-t	5′CCTCGTCCTCTGGGTTCTGCTAACCCTTTGTTCTATTCTGGGAGACGAATCTCCCTATAGTGAGTC GTATTAGAA
R-HTT17-nt	5′GGAGATTCGTCTCCCAAACAGAGGGTTAGCAGAACCCAGATAATACACGCGAC
R-HTT17-t	5′GTCGCGTGTATTATCTGGGTTCTGCTAACCCTCTGTTTGGGAGACGAATCTCCCTATAGTGAGTCG TATTAGAA
C-HTT18-nt	5′GGAGATTCGTCTCCCAAACCATCCCTACATGCCGTGCTCAACGGCTTCCCAACTAC
C-HTT18-t	5′GTAGTTGGGAAGCCGTTGAGCACGGCATGTAGGGATGGTTTGGGAGACGAATCTCCCTATAGTGAGTC GTATTAGAA
R-HTT18-nt	5′GGAGATTCGTCTCCCAAAACCTGCCGTGCTCAACGGCTTCTAATATTCGCGCT
R-HTT18-t	5′AGCGCGAATATTAGAAGCCGTTGAGCACGGCAGGTTTTGGGAGACGAATCTCCCTATAGTGAGTCG TATTAGAA
C-HTT19-nt	5′GGAGATTCGTCTCCCAGCTCTCCATCCTCCAGGTACACCCTGGCTCACCCTACC
C-HTT19-t	5′GGTAGGGTGAGCCAGGGTGTACCTGGAGGATGGAGAGCTGGGAGACGAATCTCCCTATAGTGAGTCG TATTAGAA
R-HTT19-nt	5′GGAGATTCGTCTCCCATCTTCCAGGTACACCCTGGCTCTAATATCGTCGCA
R-HTT19-t	5′TGCGACGATATTAGAGCCAGGGTGTACCTGGAAGATGGGAGACGAATCTCCCTATAGTGAGTCG TATTAGAA
C-HTT23-nt	5′GGAGATTCGTCTCCCAAACCACTTCACCATGTCGGCATTTCCGACTCCACTCATTC
C-HTT23-t	5′GAATGAGTGGAGTCGGAAATGCCGACATGGTGAAGTGGTTTGGGAGACGAATCTCCCTATAGTGAGTC GTATTAGAA
R-HTT23-nt	5′GGAGATTCGTCTCCCAAACCTTGTCGGCATTTCCGACTCCTAATATCTGCGCT
R-HTT23-t	5′AGCGCAGATATTAGGAGTCGGAAATGCCGACAAGGTTTGGGAGACGAATCTCCCTATAGTGAGTCG TATTAGAA
C-HTT24-nt	5′GGAGATTCGTCTCCCAGAAGTCTGCGGAGTGGCGTCTGGCCACATTATTATTGG
C-HTT24-t	5′CCAATAATAATGTGGCCAGACGCCACTCCGCAGACTTCTGGGAGACGAATCTCCCTATAGTGAGTC GTATTAGAA
R-HTT24-nt	5′GGAGATTCGTCTCCCAAACGTAGTGGCGTCTGGCCACATTTAATATGCCTCCT
R-HTT24-t	5′AGGAGGCATATTAAATGTGGCCAGACGCCACTACGTTTGGGAGACGAATCTCCCTATAGTGAGTCG TATTAGAA
C-HTT25-nt	5′GGAGATTCGTCTCCCATCTCTTACCCACGCTCGTCCTCCGAGCCTCCACACTAC
C-HTT25-t	5′GTAGTGTGGAGGCTCGGAGGACGAGCGTGGGTAAGAGATGGGAGACGAATCTCCCTATAGTGAGTCG TATTAGAA
R-HTT25-nt	5′GGAGATTCGTCTCCCAAACCTCGCTCGTCCTCCGAGCCTCTAATATTCGTCCC
R-HTT25-t	5′GGGACGAATATTAGAGGCTCGGAGGACGAGCGAGGTTTGGGAGACGAATCTCCCTATAGTGAGTCG TATTAGAA
C-HTT26-nt	5′GGAGATTCGTCTCCCAAACCCTTCAACTATGCGGACGCCCTCCGCTTCACACTCTC
C-HTT26-t	5′GAGAGTGTGAAGCGGAGGGCGTCCGCATAGTTGAAGGGTTTGGGAGACGAATCTCCCTATAGTGAGTC GTATTAGAA
R-HTT26-nt	5′GGAGATTCGTCTCCCACTCTGCGGACGCCCTCCGCTTCTAATATTCGCTGC
R-HTT26-t	5′GCAGCGAATATTAGAAGCGGAGGGCGTCCGCAGAGTGGGAGACGAATCTCCCTATAGTGAGTCG TATTAGAA
C-HTT27-nt	5′GGAGATTCGTCTCCCAAACCAACCTACTATGCCGTTCCATACGGCTCCACACTACC
C-HTT27-t	5′GGTAGTGTGGAGCCGTATGGAACGGCATAGTAGGTTGGTTTGGGAGACGAATCTCCCTATAGTGAGTC GTATTAGAA
R-HTT27-nt	5′GGAGATTCGTCTCCCACTCTGCCGTTCCATACGGCTCCTAATATTATCTCC
R-HTT27-t	5′GGAGATAATATTAGGAGCCGTATGGAACGGCAGAGTGGGAGACGAATCTCCCTATAGTGAGTCG TATTAGAA
C-HTT31-nt	5′GGAGATTCGTCTCCCAAACTCTCCACCCTGCGGCTGACTGCCGCTATCCATCCTC
C-HTT31-t	5′GAGGATGGATAGCGGCAGTCAGCCGCAGGGTGGAGAGTTTGGGAGACGAATCTCCCTATAGTGAGTC GTATTAGAA
R-HTT31-nt	5′GGAGATTCGTCTCCCAAACCGTGCGGCTGACTGCCGCTATTAATAACTGCGCC
R-HTT31-t	5′GGCGCAGTTATTAATAGCGGCAGTCAGCCGCACGGTTTGGGAGACGAATCTCCCTATAGTGAGTCG TATTAGAA
C-HTT34-nt	5′GGAGATTCGTCTCCCAAAGTCCAATTCCTCGGCTCGTCAAGAGCCACCATCCCATC
C-HTT34-t	5′GATGGGATGGTGGCTCTTGACGAGCCGAGGAATTGGACTTTGGGAGACGAATCTCCCTATAGTGAGTC GTATTAGAA
R-HTT34-nt	5′GGAGATTCGTCTCCCAAACCACGGCTCGTCAAGAGCCACCTAATAACACGCAC
R-HTT34-t	5′GTGCGTGTTATTAGGTGGCTCTTGACGAGCCGTGGTTTGGGAGACGAATCTCCCTATAGTGAGTCG TATTAGAA
Mod-T7-5p1+	5′TTCTAATACGACTCACTATAG

4.4 The rates of coactivation and repression of library nodes

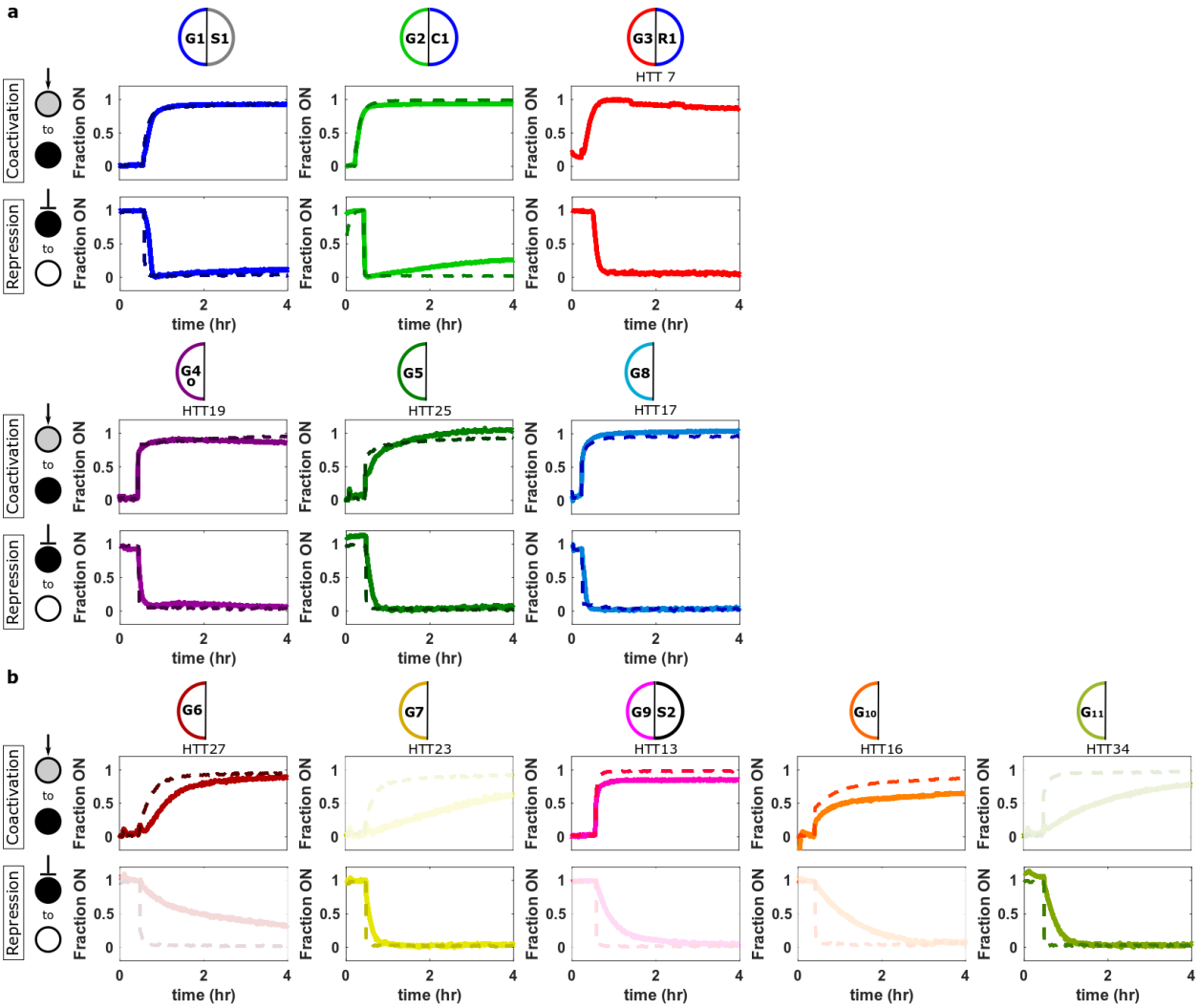

Supplementary Figure 22 | The rates of coactivation and repression of each of the final library of standardized genelet nodes used to assemble in vitro transcription networks. The numbering of the nodes' input domains (G1-G11) is somewhat arbitrary, based on order of discovery and/or order of use in different regulatory networks. Each node's alternative name given during HTT testing is shown under its final library name (G1-11). (**a-b**) Normalized level of activation for each node as it is coactivated (top) or repressed (bottom) by RNAs transcribed from templates *in situ* (solid lines). Dashed lines are the rates of coactivation and repression in response to DNA coactivators or DNA repressors in the absence of enzymes. These controls were never performed for the G3R1 node. Rates for nodes that can be both efficiently coactivated and repressed are shown in (a). Rate for nodes that could be either the rapidly coactivated or rapidly repressed (but not both) are shown in (b). For reference, the rates of the slow regulation in the opposite direction are shown for these nodes behind a transparency. All of the data presented here is from the experiments described in Supplementary Section 4.3. The data for G1S1, G2C1, G3R1, and G9S2 is also shown in Supplementary Figure 18. The data for G4o, G5, G8, G6, G7, G10, and G11 is also shown Supplementary Figure 20.

4.5 The input and output domains of standardized nodes are interchangeable

A key criterion for building a plethora of different regulatory networks with standardized nodes is the interchangeability of their input and output domains. That is, the same genelet input domain should be able to regulate the expression of many different RNA coactivator and repressor outputs and conversely, it should be possible to regulate the expression of the same RNA coactivator or repressor using many different input domains each regulated by their own distinct inputs. The 6 bidirectionally regulated nodes, the 3 nodes that can be coactivated, and the 2 nodes that can be repressed together can be inputs and outputs on 187 possible genelet templates.

To assess the interchangeability of the library's input and output domains, we first tested whether 28 different genelets that combined seven different input domains and 10 different output domains could rapidly switch the activation levels of their respective downstream nodes. In these experiments, each individual node designed to transcribe a specific RNA repressor was incubated with a fluorescently labeled reporting genelet comprised of the target input domain and activator of the RNA repressor. The repression kinetics of this corresponding reporting genelet were measured to evaluate the rate of repressor transcription and repression for each input and output combination. All the combinations tested exhibited the desired regulatory behavior, specifically reducing the reporting nodes fraction ON to <0.9 in less than an hour (Supplementary Figure 23).

We next tested whether an input domain could be combined with different output domains to control the expression of different RNA coactivators. We designed three nodes that each had a G3 input domain but that expressed three different coactivators. We found that coactivation of each node could, in turn, coactivate the corresponding downstream reporting node. We also observed that the kinetics of coactivation could be controlled by changing the concentration of either the reporting node's blocker or the concentration of the genelet expressing the coactivator (Supplementary Figure 24a-c). Further, these three coactivating nodes could be operated together to create a fan-out module (Supplementary Figure 24d).

We also tested six other input and coactivator output combinations with three different input domains that could transcribe at least two different RNA coactivators and found that all but one coactivation process was rapid (Supplementary Figure 25) – G4C10 was able to coactivate G10 to >0.9 fraction ON but it took 1.5 hours to do so. We also found that nodes could self-activate through expression of their own coactivator (Supplementary Figure 25, plot 1).

Across all of these experiments, four of the input domains were designed to express at least one repressor and one coactivator molecule and the G1, G3, and G4 domains were tested with at least five different output domains comprised of multiple different coactivators and repressors. The fact that all 28 input and output combinations that we tested (nearly 15% of the total) were able to perform their designed regulatory function provides compelling evidence for the general interchangeability of these standardized domains. All the tested nodes exhibited regulation of their target nodes, but we did find that the input domain could influence the rate of output transcription. For example, *G3R8 repressed *G8D slower than *G1R8 or *G4R8 suggesting there can be some context dependence on regulatory function.

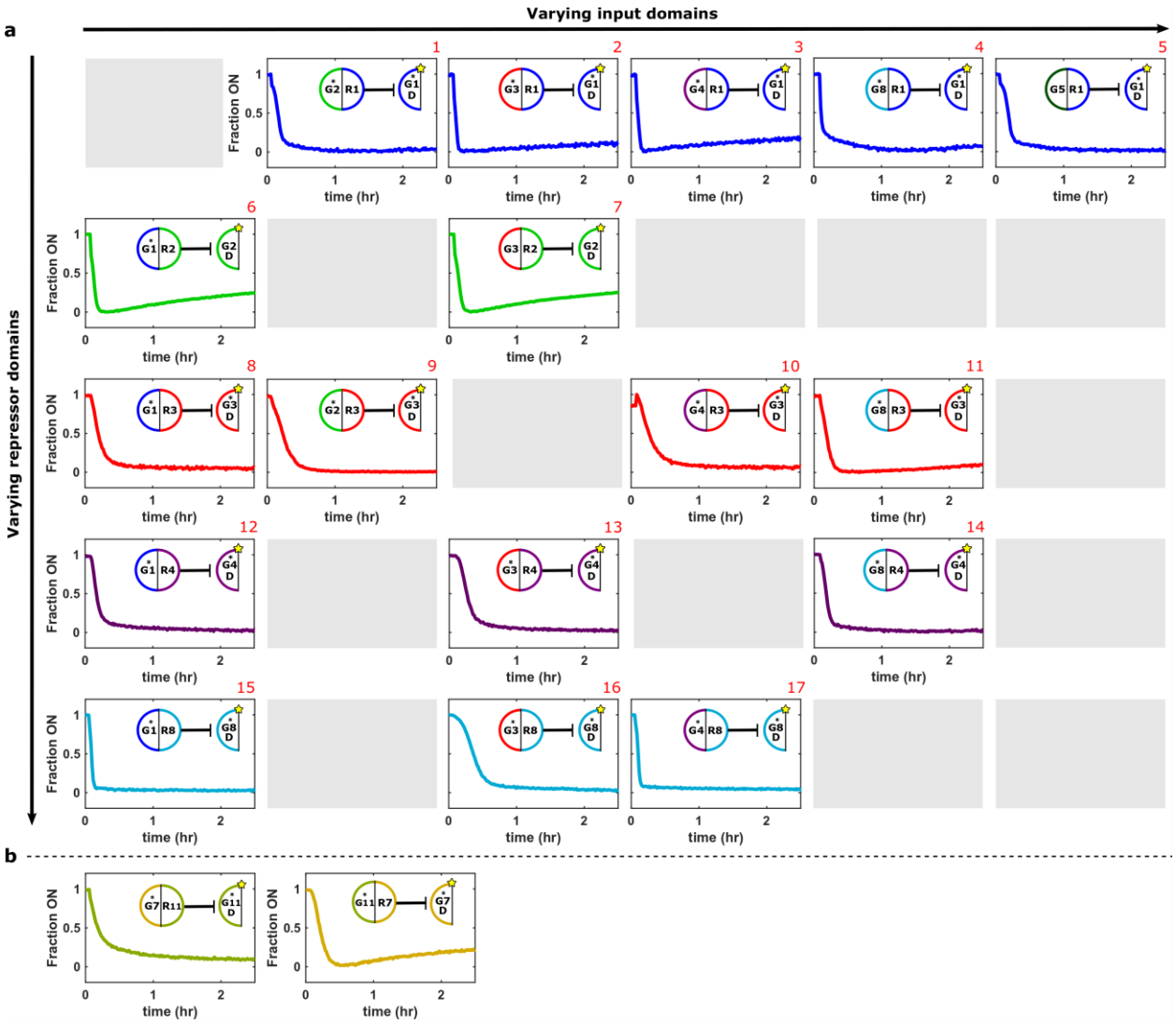

Supplementary Figure 23 | Input domains and repressor sequences are interchangeable. The insets in each plot represent the repression reaction in each experiment. A * on the input domain of a node indicates that the blocker toehold (BTH in Fig. 1c of the main text and Supplementary Figure 1) was not present on the genelets. (**a**) Normalized activation levels during repression of five different reporting genelets by upstream genelets with different input domains. Gray boxes are combinations that were never tested. For the results in plots 1-5, 8-15, 17, the repressor producing nodes were at 50 nM and the reporting genelets were at 25 nM. For the results in plots 6 and 7, the repressor producing genelets were at 25 nM and the reporting genelets were at 50 nM. For the results in plots 15 and 17, the repressor producing genelets were at 25 nM and the reporting genelets were at 25 nM. (**b**) Normalized activation levels of other input/repressor output combinations tested. The repressor producing nodes were at 50 nM and the reporting genelets were at 25 nM. The activators were present at 250 nM in all experiments. Reactions otherwise conducted as described in the Methods of the main text. Non-template strands for all coactivator producing genelets are in Supplementary Table 7, all other sequences are in Supplementary Table 1.

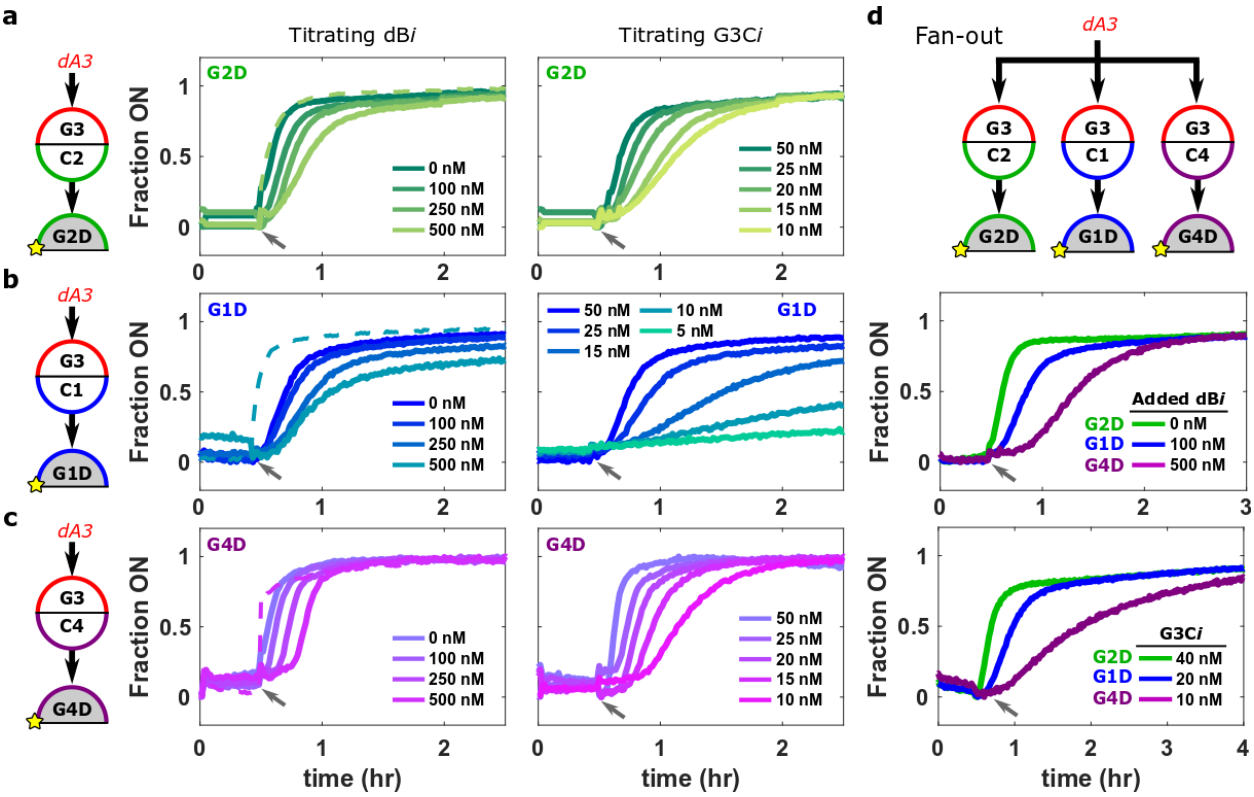

Supplementary Figure 24 | Different coactivator sequences can be regulated by the same input domains for fan-out downstream signal expression. (**a-c**) Normalized activation levels of network nodes during coactivation with different concentrations of DNA blocker strands (dBi, left) or upstream nodes (G3Ci, right) where i is 2, 1, or 4 for three unique genelet nodes (G2D, G1D, and G4D). Each downstream node is activated with an upstream template that is activated by the same input (dA3). [T7 RNAP] = 3.57 U/μL and [RNase H] = 0.0089 U/μL. (**d**) Normalized activation levels of network nodes for a fan-out circuit where G2D, G1D, and G4D are all coactivated in the same reaction *via* the addition of dA3. [T7 RNAP] = 3.57 U/μL and [RNase H] = 0.027 U/μL. Top: by changing the concentration of the DNA blocker strands for each downstream node the timing of G2D, G1D, and G4D activation can be tuned, with the node possessing the lowest blocker concentration activating first and the node possessing the highest blocker concentration activating last. In this experiment, G3C*i* genelets were present at 25 nM. Bottom: by changing the concentration of the upstream genelet G3C*i* for each downstream node the timing of G2D, G1D, and G4D activation can be tuned, with the node possessing the highest G3C*i* concentration activating first and the node possessing the lowest G3C*i* concentration activating last. In this experiment, dB*i* strands were present at 250 nM. In all experiments, reporting genelets (G2D, G1D, and G4D) were present at 25 nM and all activators were present at 250 nM. Experiments were otherwise conducted as described in the methods of the main text. Gray arrows indicate when dA3 was added to start the coactivation reaction. Non-template strands for all coactivator-producing genelets are in Supplementary Table 7, all other sequences are in Supplementary Table 1.

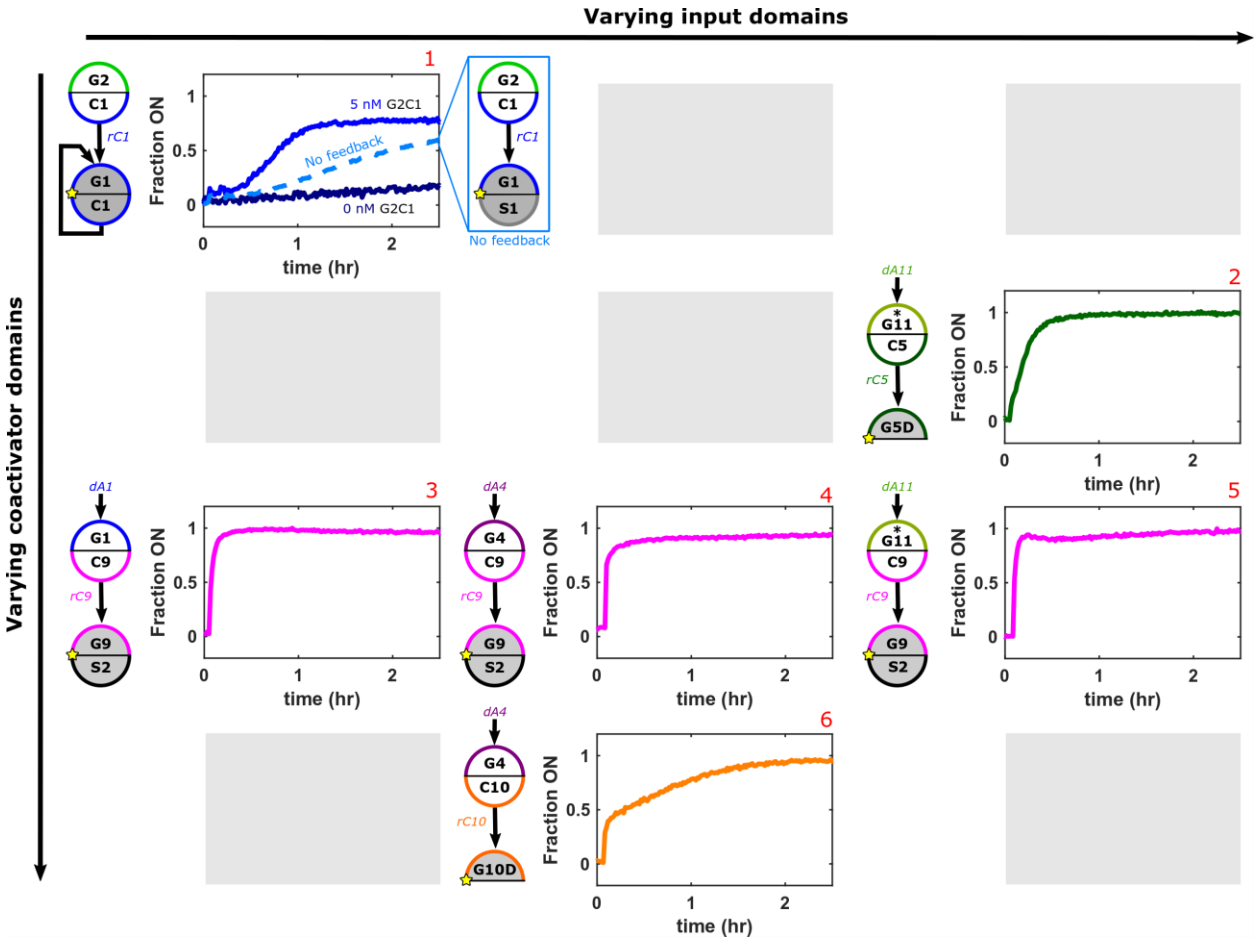

Supplementary Figure 25 | Input domains and coactivator sequences are interchangeable. A * on the input domain of a node indicates that the blocker toehold (BTH in Fig. 1c of the main text and Supplementary Figure 1) was not present on the genelets. Plot 1 shows how genelet nodes can regulate themselves: In this experiment the G2C1 node was used as an input to turn G1C1 on slightly at which point G1C1 could enhance its own activation. 5 nM of G2C1 without feedback turns on G1 much more slowly. [G1C1] = [G1S1] = 25 nM, [dA1] = 250 nM, and [dB1] = 500 nM. Reactions were otherwise conducted as described in the Methods of the main text. Plots 2-6 show normalized activation levels during coactivation of different nodes. In all experiments the reporting genelets were at 25 nM, the coactivator producing nodes were at 25 nM, all activators were at 250 nM, and no additional blocker was added. Non-template strands for all coactivator-producing genelets are in Supplementary Table 7, all other sequences are in Supplementary Table 1.

Supplementary Table 7 | Sequences of non-template (-nt) strands used for the experiments in Supplementary Section 4.5. Corresponding template (-t) strands, activators, blockers, and dummy reporting genelet strands are in Supplementary Table 1. A * on the non-template strand indicates the HPC5o design (Supplementary Figure 1) in which the blocker toehold (BTH in Fig. 1c of the main text) was removed and no blockers were present for this node.

GENELETS	
G3C1-nt	5'GAAGATGAAGGTGTACCGTATAGGTACTAGTAATACGACTCACTATA GGGAGATTCGTCTCCCAAATCCTTCCATGAACGCCAAACCGTGGCGACGACCT
G3C2-nt	5'GAAGATGAAGGTGTACCGTATAGGTACTAGTAATACGACTCACTATA GGGAGATTCGTCTCCCAAAGCCAAGATTAAGGTCAATAAGTGACCAAGCGTAC
G3C4-nt	5'GAAGATGAAGGTGTACCGTATAGGTACTAGTAATACGACTCACTATA GGGAGATTCGTCTCCCAGCTCTCCATCCTCCAGGTACACCCTGGCTCACCCT
G1C1-nt	/56-FAM/TCCTTCCATGCACGCCAAACCGTGGCGACGTAATACGACTCACTATA GGGAGATTCGTCTCCCAAATCCTTCCATGAACGCCAAACCGTGGCGACGACC
*G11C5-nt	5'CCACGGCTCGTCAAGAGCCACCTAATACGACTCACTATA GGGAGATTCGTCTCCCATCTCTTACCCACGCTCGTCCTCCGAGCCTCCACA
*G11C9-nt	5'CCACGGCTCGTCAAGAGCCACCTAATACGACTCACTATA GGGAGATTCGTCTCCCAACCAACTACCTCTGACTGTAACCCAGTCTCTCGC
G1C9-nt	5'TCCTTCCATGCACGCCAAACCGTGGCGACGTAATACGACTCACTATA GGGAGATTCGTCTCCCAACCAACTACCTCTGACTGTAACCCAGTCTCTCGCCC
G4C10-nt	5'GCTCTCCATCTTCCAGGTACACCCTGGCTCTAATACGACTCACTATA GGGAGATTCGTCTCCCAGATAAATAGAAAGCCGCACAGAGCGGCAGAGCGGGA
*G2R1-nt	/5HEX/TTCAGGTCAATAAGTGACCAAGTAATACGACTCACTATA GGGAGATTCGTCTCCCATGCACGCCAAACCGTGGCGACGTAA
*G2R3-nt	5'TTCAGGTCAATAAGTGACCAAGTAATACGACTCACTATA GGGAGATTCGTCTCCCAAGGTGTACCGTATAGGTACTAGTAA
G5R1-nt	/5HEX/TCTCTTACCCTCGCTCGTCCTCCGAGCCTCTAATACGACTCACTATA GGGAGATTCGTCTCCCATGCACGCCAAACCGTGGCGACGTAATA
*G8R1-nt	5'CAGAGGGTTAGCAGAACCCAGATAATACGACTCACTATA GGGAGATTCGTCTCCCATGCACGCCAAACCGTGGCGACGTAATAGAGCTGG
*G8R3-nt	5'CAGAGGGTTAGCAGAACCCAGATAATACGACTCACTATA GGGAGATTCGTCTCCCAAGGTGTACCGTATAGGTACTAGTAATATTTGTCG
*G8R4-nt	5'CAGAGGGTTAGCAGAACCCAGATAATACGACTCACTATA GGGAGATTCGTCTCCCATCTTCCAGGTACACCCTGGCTCTAATATCCTCGC
*G1R8-nt	5'TGCACGCCAAACCGTGGCGACGTAATACGACTCACTATA GGGAGATTCGTCTCCCAAACAGAGGGTTAGCAGAACCCAGATAATACACGC
*G3R8-nt	5'AGGTGTACCGTATAGGTACTAGTAATACGACTCACTATA GGGAGATTCGTCTCCCAAACAGAGGGTTAGCAGAACCCAGATAATACACGC
*G4R8-nt	5'TCTTCCAGGTACACCCTGGCTCTAATACGACTCACTATA GGGAGATTCGTCTCCCAAACAGAGGGTTAGCAGAACCCAGATAATACACGC
*G7R11-nt	5'CCTTGTCGGCATTTCCGACTCCTAATACGACTCACTATA GGGAGATTCGTCTCCCAAACCACGGCTCGTCAAGAGCCACCTAATAACACG
*G11R7-nt	5'CCACGGCTCGTCAAGAGCCACCTAATACGACTCACTATA GGGAGATTCGTCTCCCAAACCTTGTCGGCATTTCCGACTCCTAATATCTGC
G9S2-nt	See Supplementary Table 2
S2-t	See Supplementary Table 2

5. General genelet model

5.1 Model assumptions and reactions

To guide the experimental implementation of *in vitro* transcriptional regulatory networks, we utilized a simple mass action kinetic model of genelet reactions. The model is composed of all the designed transcription, degradation, and nucleic strand displacement or hybridization reactions for each network node (Supplementary Figure 26). T7 RNAP and RNase H drive RNA transcription and degradation, respectively, and we modeled these reactions using a first order approximation for enzyme kinetics as in previously developed models of genelet networks[18–20]. The rate of production of a transcribed RNA is given by: $\mathrm{k_{P,ji}[Gj{:}\,dAi]}$, where $\mathrm{k_{P,ji}}$ is the apparent first order rate constant for the production of the RNA transcript from the $\mathrm{[Gj{:}\,dAi]}$ template. The rate of degradation of an RNA is given by: $\mathrm{k_{DR(C),i}[rR(C)i{:}\,dA(B)i]}$, where $\mathrm{k_{DR,i}}$ is the apparent first order rate constant for the degradation of an RNA repressor (rRi) bound to a DNA activator (dAi). $\mathrm{k_{DC,i}}$ is, analogously, the apparent first order rate constant for the degradation of an RNA coactivator (rCi) bound to a DNA blocker (dBi).

We observed in experiments that the sequence of a node's input domain could influence the transcription rate of its RNA output (*i.e.,* G1R8:dA1 and G3R8:dA3 produced rR8 at different rates, Supplementary Section 4.5). Thus, our model assumes that each individual genelet can have its own $\mathrm{k_{P,ji}}$ value.

We assumed that the rates of transcription of genelet templates in their OFF states were low enough to be neglected, as observed in previous experiment (Supplementary Figure 13). In experiments we found that G:dB complexes exhibited roughly 5-10% leak transcription when their DNA activators were present (Supplementary Figure 13). In most of our simulations we ignored leak transcription from these G:dB complexes. However, we did find that this leak could influence network behavior in larger coactivation cascades (Supplementary Section 8.4). Thus, we also included an optional leak transcription term in our model. We modeled leak transcription as occurring from Gj:dBi complexes at a fraction of the transcription rate used for a given RNA output: $\mathrm{leak_{ji} * k_{P,ji}[Gj{:}\,dBi]}$, where $\mathrm{leak_{ji}}$ is a fraction between 0 and 1 of leak for the Gj:dBi complex, $\mathrm{k_{P,ji}}$ is the apparent first order rate constant for the production of the RNA transcript of the $\mathrm{[Gj{:}\,dAi]}$ template. As with $\mathrm{k_{P,ji}}$, we assume that each individual genelet could have its own $\mathrm{leak_{ji}}$ value. A significant amount of transcription from a G:dB complex was only observed when the corresponding DNA activator was also present (Supplementary Figure 13), suggesting that transient binding of the activator to the G:dB complex drove transcription. If this is the true cause of the leak transcription, the leak transcription rate should, in practice, depend on the activator concentration. However, given that in most of our experiments the activator concentrations were similar, we found that a simple model of leak transcription that depends only on the concentration of the G:dB complexes was sufficient to recapitulate the consequences of leak observed in experiments (Supplementary Fig. 13).

While our model can accommodate distinct rate constants for each reaction in given network, in practice that means there are over 450 unique reaction rate constants when considering all the input and output combinations for the 11 nodes in our genelet library. We did not explicitly measure all of these unique rate constants nor do we have enough experimental data to reliably fit all of them. We instead assessed how well a general model of genelet behavior could predict the behavior of larger genelet networks in experiments. Our approach to this question was to set all the rate constants for a

given reaction type to the same value (*i.e* $k_{P,11} = k_{P,21} = \cdots k_{P,ji}$ and $k_{GAR,1} = k_{GAR,2} = \cdots k_{GAR,i}$, etc). This simplified model was used to predict the qualitative behavior of a network and to understand qualitatively how changing the concentrations of network components would alter network behavior.

To determine reasonable rate constant values to use, we manually adjusted these constants to fit the experimental pulse heights and widths observed for the IFFL1 (Fig. 3b of the main text). These rate constants were similar to values fit for rate constants of analogous reactions within genelet networks[4,6,9] and are tabulated in Supplementary Table 8. These particular rate constants were used in all the simulations of networks presented in this paper.

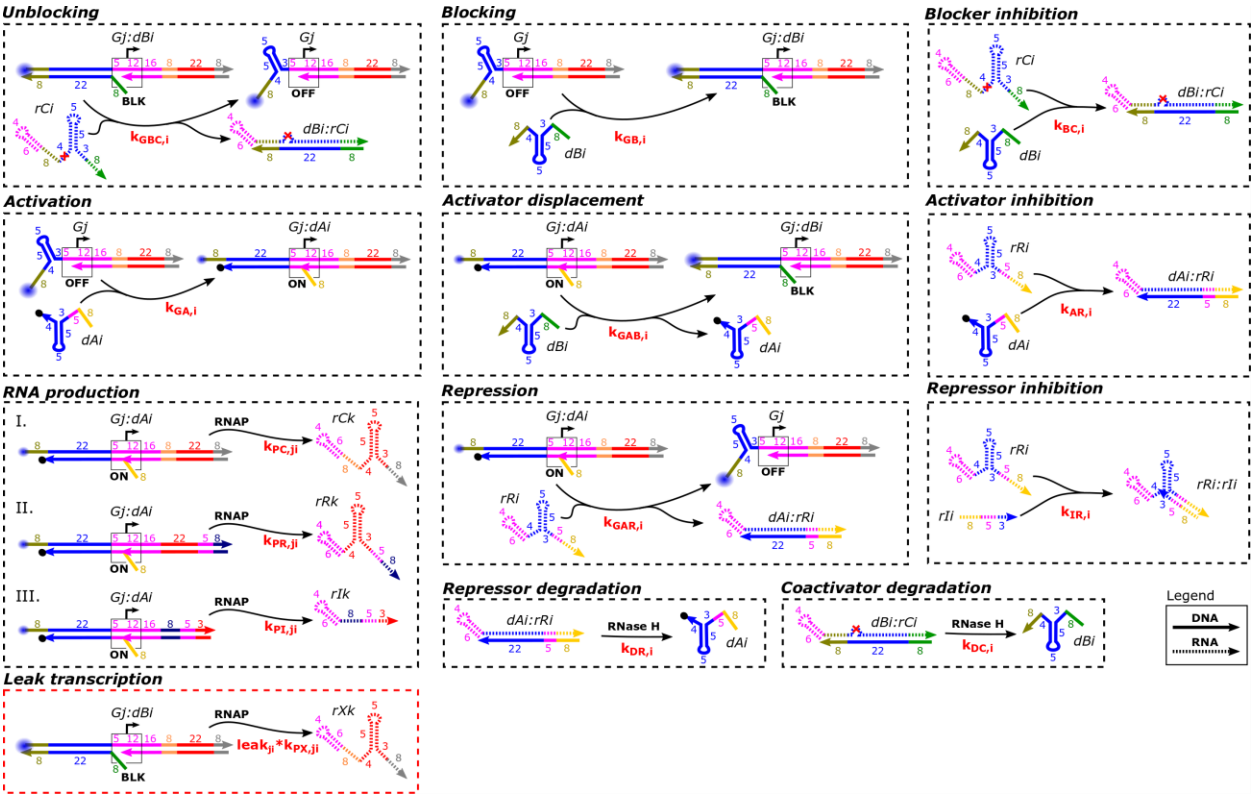

Supplementary Figure 26 | Genelet reactions considered in genelet network models. The subscript i ranges from 1 to n (the total number of orthogonal input domains in a network) and the subscript j ranges from 1 to m (the number of individual nodes in a network). An ON node produces either the coactivator of another node (I.), the RNA repressor of another node (II.), or the RNA inducer of another node's repressor (III.); for each genelet template no more than one of these reactions is included in the model. The leak transcription reaction was modeled as transcription from BLK nodes at a rate a fraction of that of the corresponding Gj:dAi complex. The product of the leak reaction rX can be rC, rR, or rI and is the same as the product of the corresponding ON node. Unless otherwise stated, the leak transcription reaction was not included in simulations. The term given to the rate constant for each reaction is shown in red.

5.2 Model equations and simulation

All kinetic simulations were either conducted with MATLAB 2018b using the *ode45( )* function or with Python's SciPy package (version 1.2.1) using the *solve_ivp( )* function. All the kinetic equations are presented in a general vector format such that the same general set of equations can represent any network topology. In this implementation the exact species and reactions that represent a given genelet network are determined by the network connectivity (*i.e.,* which activators, repressors, blockers,

coactivators, and inducers regulate which nodes in the network), and which nodes produce which RNA repressors, coactivators, or inducers. We defined network connectivity in connectivity matrices ($\mathbf{M}_{\mathbf{A(B)_C}}$) and which nodes produce which RNAs in production matrices ($\mathbf{M}_{\mathbf{R(C)_P}}$), both of which are described below. Each unique network simulated for this study starts with the same underlying vector equations but has its own unique set of connectivity and production matrices which determine the final reaction terms necessary for simulation. A specific example of these matrices' definitions is presented in Supplementary Figure 27. All simulations used the same set of kinetic rate constants presented in Supplementary Table 8.

In Equations (1) – (10) below, arrows ($\overrightarrow{[\ ]}$) indicate vectors of species concentrations and bolded **M's** indicate connectivity and production matrices ($\mathbf{M}_{\mathbf{A(B)_C}}$ and $\mathbf{M}_{\mathbf{R(C)_P}}$), respectively – explicitly defined below the equations. A * indicates matrix multiplication, $\overrightarrow{[\ ]}.\overrightarrow{[\ ]}$ indicates element by element-wise multiplication. Operations in parentheses must be conducted first. **M'** indicates the transpose of a given matrix. The red terms are associated with leak transcription which can be included (0<leak<1) or not (leak=0) for each element.

(1) $$\frac{d[\overrightarrow{rR}]}{dt} = -\vec{k}_{GAR}.(\mathbf{M_{A_C}}*[\overrightarrow{G{:}dA}]).[\overrightarrow{rR}] - \vec{k}_{AR}.[\overrightarrow{dA}].[\overrightarrow{rR}] + \mathbf{M_{R_P}}*(\vec{k}_{PR}.[\overrightarrow{G{:}dA}]) - \vec{k}_{IR}.[\overrightarrow{rR}].[\overrightarrow{rI}] + \mathbf{M_{R_P}}*(\overrightarrow{leak}.\vec{k}_{PR}.[\overrightarrow{G{:}dB}])$$

(2) $$\frac{d[\overrightarrow{dA}]}{dt} = \vec{k}_{DR}.[\overrightarrow{dA{:}rR}] - \vec{k}_{GA}.(\mathbf{M_{A_C}}*[\vec{G}]).[\overrightarrow{dA}] - \vec{k}_{AR}.[\overrightarrow{dA}].[\overrightarrow{rR}] + \vec{k}_{GAB}.(\mathbf{M_{B_C}}*[\overrightarrow{G{:}dA}]).[\overrightarrow{dB}]$$

(3) $$\frac{d[\overrightarrow{rC}]}{dt} = -\vec{k}_{GBC}.(\mathbf{M_{B_C}}*[\overrightarrow{G{:}dB}]).[\overrightarrow{rC}] - \vec{k}_{BC}.[\overrightarrow{dB}].[\overrightarrow{rC}] + \mathbf{M_{C_P}}*(\vec{k}_{PC}.[\overrightarrow{G{:}dA}]) + \mathbf{M_{C_P}}*(\overrightarrow{leak}.\vec{k}_{PC}.[\overrightarrow{G{:}dB}])$$

(4) $$\frac{d[\overrightarrow{dB}]}{dt} = \vec{k}_{DC}.[\overrightarrow{dB{:}rC}] - \vec{k}_{GB}.(\mathbf{M_{B_C}}*[\vec{G}]).[\overrightarrow{dB}] - \vec{k}_{BC}.[\overrightarrow{dB}].[\overrightarrow{rC}] - \vec{k}_{GAB}.(\mathbf{M_{B_C}}*[\overrightarrow{G{:}dA}]).[\overrightarrow{dB}]$$

(5) $$\frac{d[\overrightarrow{G{:}dA}]}{dt} = (\mathbf{M'_{A_C}}*(\vec{k}_{GA}.[\overrightarrow{dA}])).[\vec{G}] - (\mathbf{M'_{A_C}}*(\vec{k}_{GAR}.[\overrightarrow{rR}])).[\overrightarrow{G{:}dA}] - (\mathbf{M'_{B_C}}*(\vec{k}_{GAB}.[\overrightarrow{dB}])).[\overrightarrow{G{:}dA}]$$

(6) $$\frac{d[\overrightarrow{G{:}dB}]}{dt} = (\mathbf{M'_{B_C}}*(\vec{k}_{GB}.[\overrightarrow{dB}])).[\vec{G}] + (\mathbf{M'_{B_C}}*(\vec{k}_{GAB}[\overrightarrow{dB}]))[\overrightarrow{G{:}dA}] - (\mathbf{M'_{B_C}}*(\vec{k}_{GBC}.[\overrightarrow{rC}])).[\overrightarrow{G{:}dB}]$$

(7) $$\frac{d[\overrightarrow{rI}]}{dt} = -\vec{k}_{IR}.[\overrightarrow{rR}].[\overrightarrow{rI}] + \mathbf{M_{I_P}}*(\vec{k}_{PI}.[\overrightarrow{G{:}dA}]) + \mathbf{M_{I_P}}*(\overrightarrow{leak}.\vec{k}_{PI}.[\overrightarrow{G{:}dB}])$$

Mass balances:

(8) $$[\overrightarrow{dA{:}rR}] = [\overrightarrow{dA}]_{TOT} - [\overrightarrow{dA}] - \mathbf{M_{A_C}}*[\overrightarrow{G{:}dA}]$$

(9) $$[\overrightarrow{dB{:}rC}] = [\overrightarrow{dB}]_{TOT} - [\overrightarrow{dB}] - \mathbf{M_{B_C}}*[\overrightarrow{G{:}dB}]$$

(10) $$[\vec{G}] = [\vec{G}]_{TOT} - [\overrightarrow{G{:}dA}] - [\overrightarrow{G{:}dB}]$$

Vector and matrix definitions:

Below n *= the number of orthogonal input domains* in the network and *m = the total number of nodes* in the network.

Rate constant vectors:

$$\vec{k}_{GAR} = \begin{bmatrix} k_{GAR,1} \\ k_{GAR,i} \\ \vdots \\ k_{GAR,n} \end{bmatrix}, \ \vec{k}_{AR} = \begin{bmatrix} k_{AR,1} \\ k_{AR,i} \\ \vdots \\ k_{AR,n} \end{bmatrix}, \ \vec{k}_{PR} = \begin{bmatrix} k_{PR,1} \\ k_{PR,j} \\ \vdots \\ k_{PR,m} \end{bmatrix}, \vec{k}_{IR} = \begin{bmatrix} k_{IR,1} \\ k_{IR,i} \\ \vdots \\ k_{IR,n} \end{bmatrix}, \ \vec{k}_{DR} = \begin{bmatrix} k_{DR,1} \\ k_{DR,i} \\ \vdots \\ k_{DR,n} \end{bmatrix}, \vec{k}_{GA} = \begin{bmatrix} k_{GA,1} \\ k_{GA,i} \\ \vdots \\ k_{GA,n} \end{bmatrix},$$

$$\vec{k}_{GAB} = \begin{bmatrix} k_{GAB,1} \\ k_{GAB,i} \\ \vdots \\ k_{GAB,n} \end{bmatrix}, \vec{k}_{GBC} = \begin{bmatrix} k_{GBC,1} \\ k_{GBC,i} \\ \vdots \\ k_{GBC,n} \end{bmatrix}, \vec{k}_{BC} = \begin{bmatrix} k_{BC,1} \\ k_{BC,i} \\ \vdots \\ k_{BC,n} \end{bmatrix}, \vec{k}_{PC} = \begin{bmatrix} k_{PC,1} \\ k_{PC,j} \\ \vdots \\ k_{PC,m} \end{bmatrix}, \vec{k}_{DC} = \begin{bmatrix} k_{DC,1} \\ k_{DC,i} \\ \vdots \\ k_{DC,n} \end{bmatrix}, \ \vec{k}_{PI} = \begin{bmatrix} k_{PI,1} \\ k_{PI,j} \\ \vdots \\ k_{PI,m} \end{bmatrix}$$

Supplementary Table 8 | Rate constants used for the general genelet model. Unless otherwise stated, these parameters were used to simulate all genelet networks.

Rate constant vector	Rate constant value
$\vec{k}_{GAR}$ (repression)	$5x10^{3}$ $M^{-1}s^{-1}$
$\vec{k}_{AR}$ (activator inhibition)	$1x10^{4}$ $M^{-1}s^{-1}$
$\vec{k}_{PR}$ (repressor production)	0.02 s^{-1}
$\vec{k}_{IR}$ (repressor inhibition)	$1x10^{4}$ $M^{-1}s^{-1}$
$\vec{k}_{DR}$ (repressor degradation)	$3x10^{-4}$ s^{-1}
$\vec{k}_{GA}$ (activation)	$1x10^{4}$ $M^{-1}s^{-1}$
$\vec{k}_{GAB}$ (activator displacement)	$5x10^{3}$ $M^{-1}s^{-1}$
$\vec{k}_{GBC}$ (unblocking)	$5x10^{3}$ $M^{-1}s^{-1}$
$\vec{k}_{BC}$ (blocker inhibition)	$1x10^{4}$ $M^{-1}s^{-1}$
$\vec{k}_{PC}$ (coactivator production)	0.02 s^{-1}
$\vec{k}_{DC}$ (repressor degradation)	$3x10^{-4}$ s^{-1}
$\vec{k}_{PI}$ (inducer production)	0.02 s^{-1}

Non-genelet reaction species vectors:

$$[\overrightarrow{\mathrm{rR}}] = \begin{bmatrix} \mathrm{rR}_1 \\ \mathrm{rR}_\mathrm{i} \\ \vdots \\ \mathrm{rR}_\mathrm{n} \end{bmatrix}, [\overrightarrow{\mathrm{dA}}] = \begin{bmatrix} \mathrm{dA}_1 \\ \mathrm{dA}_\mathrm{i} \\ \vdots \\ \mathrm{dA}_\mathrm{n} \end{bmatrix}, [\overrightarrow{\mathrm{rC}}] = \begin{bmatrix} \mathrm{rC}_1 \\ \mathrm{rC}_\mathrm{i} \\ \vdots \\ \mathrm{rC}_\mathrm{n} \end{bmatrix}, [\overrightarrow{\mathrm{dB}}] = \begin{bmatrix} \mathrm{dB}_1 \\ \mathrm{dB}_\mathrm{i} \\ \vdots \\ \mathrm{dB}_\mathrm{n} \end{bmatrix}, [\overrightarrow{\mathrm{rI}}] = \begin{bmatrix} \mathrm{rI}_1 \\ \mathrm{rI}_\mathrm{i} \\ \vdots \\ \mathrm{rI}_\mathrm{n} \end{bmatrix},$$

$$[\overrightarrow{\mathrm{dA{:}\,rR}}] = \begin{bmatrix} \mathrm{dA}_1\mathrm{:rR}_1 \\ \mathrm{dA}_\mathrm{i}\mathrm{:rR}_\mathrm{i} \\ \vdots \\ \mathrm{dA}_\mathrm{n}\mathrm{:rR}_\mathrm{n} \end{bmatrix}, [\overrightarrow{\mathrm{dB{:}\,rC}}] = \begin{bmatrix} \mathrm{dB}_1\mathrm{:rC}_1 \\ \mathrm{dB}_\mathrm{i}\mathrm{:rC}_\mathrm{i} \\ \vdots \\ \mathrm{dB}_\mathrm{n}\mathrm{:rC}_\mathrm{n} \end{bmatrix}$$

Genelet reaction species vectors:

$$[\vec{\mathrm{G}}] = \begin{bmatrix} \mathrm{G}_1 \\ \mathrm{G}_\mathrm{j} \\ \vdots \\ \mathrm{G}_\mathrm{m} \end{bmatrix}, [\overrightarrow{\mathrm{G{:}\,dA}}] = \begin{bmatrix} \mathrm{G}_1\mathrm{:dA}_{(\,)} \\ \mathrm{G}_\mathrm{j}\mathrm{:dA}_{(\,)} \\ \vdots \\ \mathrm{G}_\mathrm{m}\mathrm{:dA}_{(\,)} \end{bmatrix}, [\overrightarrow{\mathrm{G{:}\,dB}}] = \begin{bmatrix} \mathrm{G}_1\mathrm{:dB}_{(\,)} \\ \mathrm{G}_\mathrm{j}\mathrm{:dB}_{(\,)} \\ \vdots \\ \mathrm{G}_\mathrm{m}\mathrm{:dB}_{(\,)} \end{bmatrix}$$

Where ( ) subscripts can be any number from 1:n. The activators and blockers associated with each genelet are defined by the connectivity matrices below.

Connectivity matrices definition:

The connectivity matrices define which activators ($\mathbf{M_{AC}}$) and blockers ($\mathbf{M_{BC}}$) bind to which genelets. An entry is 1 in the $\mathbf{M_{AC}}$ matrix if the ith activator binds to the jth genelet and 0 otherwise. Likewise, an entry is 1 in the $\mathbf{M_{BC}}$ matrix if the ith blocker binds to the jth genelet and 0 otherwise. The activator and blocker connectivity matrices also define which repressors and coactivators, respectively, are associated with each genelet.

$$\mathbf{M_{A_C}} = \begin{matrix} \\ \mathrm{dA}_1 \\ \vdots \\ \mathrm{dA}_\mathrm{n} \end{matrix} \begin{matrix} \mathrm{G}_1 & \mathrm{G}_\mathrm{j}\ldots & \mathrm{G}_\mathrm{m} \\ [0|1 & \ldots & 0|1] \\ [\ \vdots & \ddots & \vdots\ ] \\ [0|1 & \ldots & 0|1] \end{matrix}, \mathbf{M_{B_C}} = \begin{matrix} \\ \mathrm{dB}_1 \\ \vdots \\ \mathrm{dB}_\mathrm{n} \end{matrix} \begin{matrix} \mathrm{G}_1 & \mathrm{G}_\mathrm{j}\ldots & \mathrm{G}_\mathrm{m} \\ [0|1 & \ldots & 0|1] \\ [\ \vdots & \ddots & \vdots\ ] \\ [0|1 & \ldots & 0|1] \end{matrix}$$

Production matrices definition:

The production matrices define which genelets produce which RNA repressors, coactivators, or inducers. There are three such matrices that respectively specify which repressors, coactivators and inducers are produced by which genelet. An entry is 1 in the matrices if the ith RNA repressor ($\mathbf{M_{RP}}$), coactivator ($\mathbf{M_{CP}}$), or inducer ($\mathbf{M_{IP}}$) is produced by the jth genelet and 0 otherwise.

$$\mathbf{M_{R_P}} = \begin{matrix} \\ \mathrm{rR}_1 \\ \vdots \\ \mathrm{rR}_\mathrm{n} \end{matrix} \begin{matrix} \mathrm{G}_1 & \mathrm{G}_\mathrm{j}\ldots & \mathrm{G}_\mathrm{m} \\ [0|1 & \ldots & 0|1] \\ [\ \vdots & \ddots & \vdots\ ] \\ [0|1 & \ldots & 0|1] \end{matrix}, \mathbf{M_{C_P}} = \begin{matrix} \\ \mathrm{rC}_1 \\ \vdots \\ \mathrm{rC}_\mathrm{n} \end{matrix} \begin{matrix} \mathrm{G}_1 & \mathrm{G}_\mathrm{j}\ldots & \mathrm{G}_\mathrm{m} \\ [0|1 & \ldots & 0|1] \\ [\ \vdots & \ddots & \vdots\ ] \\ [0|1 & \ldots & 0|1] \end{matrix}, \mathbf{M_{I_P}} = \begin{matrix} \\ \mathrm{rI}_1 \\ \vdots \\ \mathrm{rI}_\mathrm{n} \end{matrix} \begin{matrix} \mathrm{G}_1 & \mathrm{G}_\mathrm{j}\ldots & \mathrm{G}_\mathrm{m} \\ [0|1 & \ldots & 0|1] \\ [\ \vdots & \ddots & \vdots\ ] \\ [0|1 & \ldots & 0|1] \end{matrix}$$

Example:

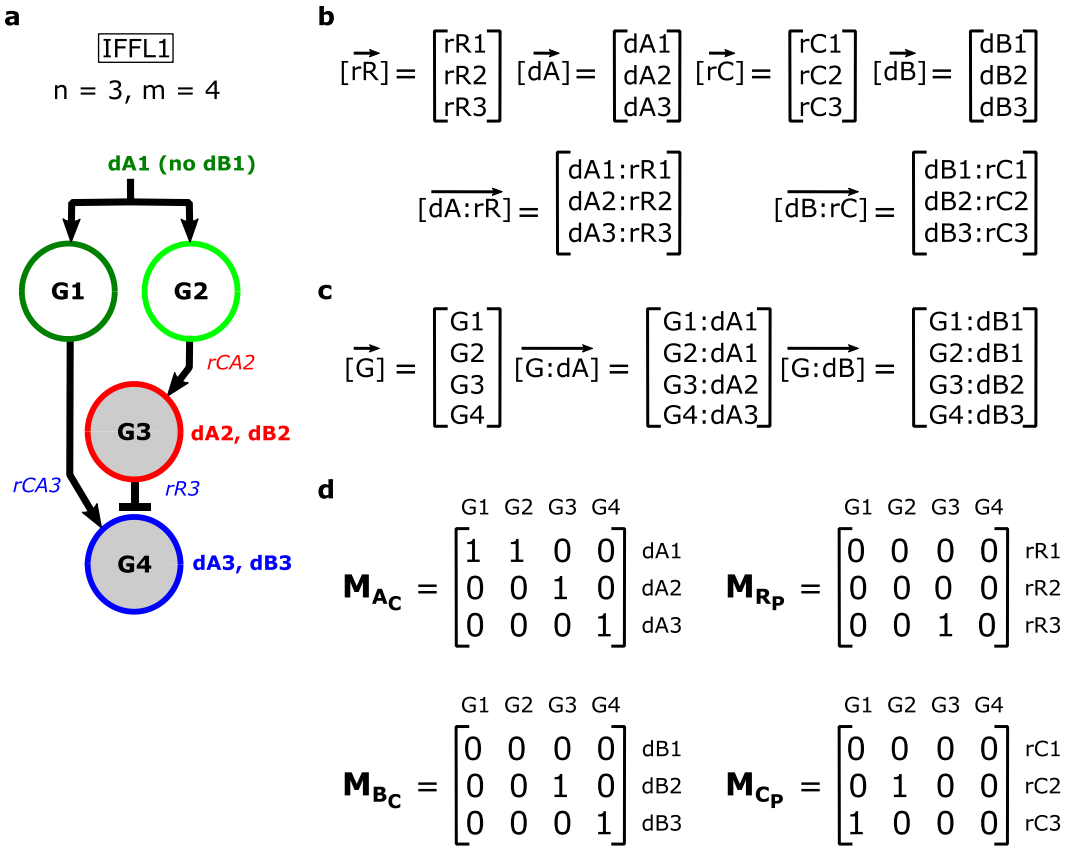

Supplementary Figure 27 | The vector and matrix definitions for the general genelet model for the IFFL1 network as an example of the notation the general genelet model as described in the Vector and Matrix definitions above. (**a**) The IFFL1 network with the nodes, activators and blockers labeled as they appear in the model. There are 4 total nodes in this network (m = 4) but only 3 orthogonal genelet input domains (n = 3) as G1 and G2 share the same activator. The numbers of the nodes refer to their numbers in the model and do not correspond to the specific nodes used to build the IFFL1 (main text Figure 4 and Supplementary Section 7). (**b**) Vector definitions of the repressors, activators, coactivators, blockers and their complexes with one another contained within the network. There are no inducers in this network, so an inducer vector was omitted. (**c**) Vector definitions of the genelet species. Note G1 and G2 share the same activator (dA1) and blocker (dB1) in this example. (**d**) The connectivity (left) and production (right) matrices for the network in (a). There are no inducer matrices for this network, so the inducer matrix has 0 rows and is not listed.

6. Design and characterization of the IFFL1, IFFL2, and IFFL3 modules

6.1 Simulations of the IFFL module

Simulations of the dynamics of an incoherent feedforward module were conducted as described in Supplementary Section 5. While Supplementary Figure 28a shows the IFFL1 and uses the names of the nodes in IFFL1 as the names of the nodes in the simulation, the predictions of the model are agnostic to the sequences of the domains used since the model assumes all nodes possess identical kinetic behavior. The simulations were used to understand how changing the concentrations of the genelet or their DNA activators would change the shape of the pulses that would result. They predict that changing the concentraiton of G2C1 primarily modulates pulse height, changing the concentrations of G3R1 or G2C3 primarily modulates pulse width, and changing the concentration of dA1 (the activator of G1S1) modulates both pulse height and pulse width.

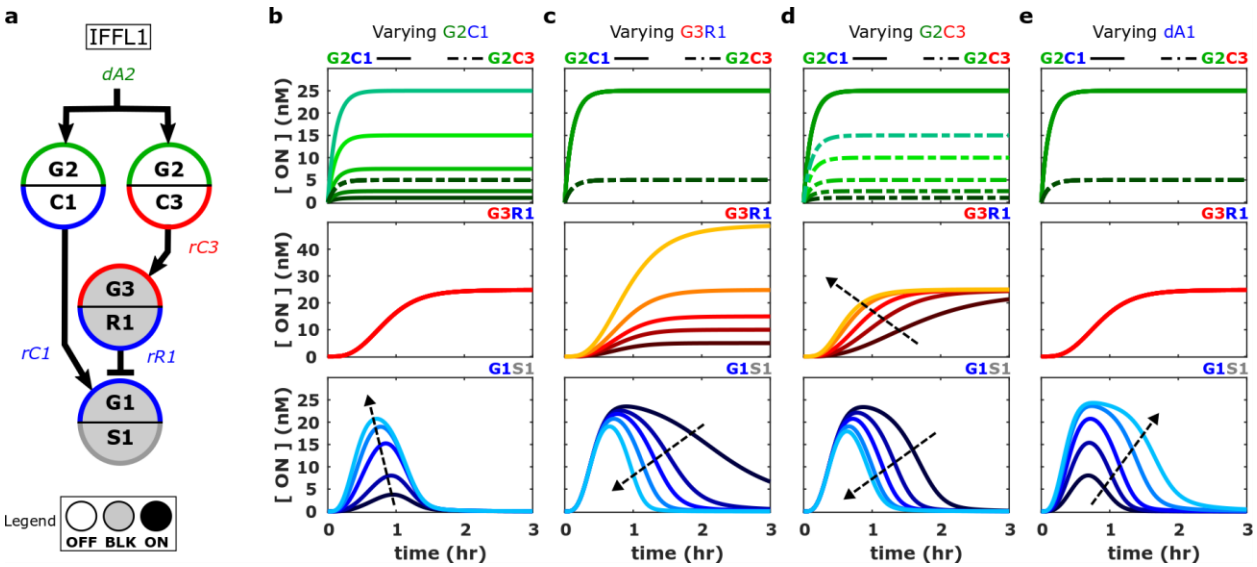

Supplementary Figure 28 | Simulations of the IFFL network predict a variety of G1S1 pulse dynamics depending on the concentrations of the different genelets and their DNA activators. (**a**) An IFFL architecture shown with nodes used for IFFL1. (**b-e**) The concentrations of the network nodes that are in an ON state over time during kinetic simulations of the IFFL network for different concentrations of genelets and DNA activators. Each column shows the predicted concentrations of the four types of nodes that are on for a set of simulations for networks with different total concentration of one genelet or DNA activator; the concentrations of the other nodes were kept constant. The node whose genelet or activator concentration is varied is indicated by the label in each column above the top plots. The dashed arrows in the plots point in the direction of increasing concentration of the species that was varied in each simulation. For (b), the concentration of G2C1 was either 1, 5, 7.5, 15, or 25 nM. For (c), the concentration of G3R1 was either 5, 10, 15, 25, or 50 nM. For (d), the concentration of G2C3 was either 1, 2.5, 5, 10, or 25 nM. For (e), the concentration of dA1 was either 50, 125, 250, 500, or 750 nM. In all simulations G1S1 was at 25 nM. Except where stated above, the concentrations of G2C1 and G3R1 were 25 nM and the concentration of G2C3 was 5 nM. Simulations were conducted as described in Supplementary Section 5.

6.2 Protocols for characterization of IFFL modules

In different experiments, the concentrations of some of the species' concentrations were varied compared to the values presented in Supplementary Tables 9 – 11. These different concentrations are described in the specific experiments, all concentrations of species that were not explicitly varied are as tabulated below. Added blocker strands refer to additional blocker that was added beyond the 50% excess blocker all blocked genelets were annealed with. All IFFL1 – 3 experiments in the main text use the blocker variants with 2' methylated RNA 3' ends.

For all IFFL experiments, all nucleic acid components other than the DNA activator that triggers the network were mixed together in transcription conditions. The fluorescence of each network was tracked in a qPCR machine for 10 – 15 minutes to obtain a maximum fluorescence value for the nodes being tracked in the experiment. The enzyme mix and the DNA activator that triggers the network to start was then added to each network mixture. For all IFFL experiments, a reference well was also included for each fluorescently labeled node that was being coactivated in the experiment. Each reference well contained an isolated node of interest initially in a blocked state without any enzymes and at the start of the experiment the DNA coactivator for the node of interest was added to the reference well to obtain the minimum fluorescence value. This minimum fluorescence value obtained in the reference wells was used as a minimum value for normalizing coactivated nodes (Supplementary Section 13.2).

Supplementary Table 9 | Concentrations of the components used in the IFFL1 experiments.

Component #	Component	Concentration
1	G2C1	25 nM
2	G2C3	5 nM
3	G3R1	25 nM
4	G1S1	25 nM
5	dA2	250 nM
6	dA3	125 nM
7	dA1	250 nM
8	Added dB1	0 nM
9	Added dB3 (or dB3-2omR)	0 nM
10	YIPP	1.35 x 10^{-3} U/µL
11	RNase H	8.92 x 10^{-3} U/µL
12	T7 RNAP	3.57 U/µL

Supplementary Table 10 | Concentrations of the components used in the IFFL2 experiments.

Component #	Component	Concentration
1	G5C4	25 nM
2	G5C6	5 nM
3	G6R4 (or G6R4o)	25 nM
4	G4S1	25 nM
5	dA5	250 nM
6	dA6	250 nM
7	dA4 (or dA4o)	250 nM
8	Added dB4	0 nM
9	Added dB6	0 nM
10	YIPP	1.35 x 10^{-3} U/µL
11	RNase H	8.92 x 10^{-3} U/µL
12	T7 RNAP	3.57 U/µL

Supplementary Table 11 | Concentrations of the components used in the IFFL3 experiments.

Component #	Component	Concentration
1	G9C8	25 nM
2	G9C10	5 nM
3	G10R8	25 nM
4	G8D	25 nM
5	dA9	250 nM
6	dA10	250 nM
7	dA8	250 nM
8	Added dB10 (or dB10-2omR)	0 nM
9	Added dB8 (or dB8-2omR)	50 nM
10	YIPP	1.35 x 10^{-3} U/µL
11	RNase H	8.92 x 10^{-3} U/µL
12	T7 RNAP	3.57 U/µL

6.3 Design of IFFL1 module

To assemble the IFFL1 module, we selected three orthogonal input domains (G1, G2, and G3) from the standardized domains we identified in Supplementary Section 4.3. All three of these input domains exhibited fast transcriptional coactivation and repression so they could be used for any of the components of the IFFL. The assignments of the nodes to positions in the network were thus arbitrary (Fig. 3a, main text).

Supplementary Table 12 | DNA and RNA oligonucleotides synthesized specifically for the IFFL1 network. The non-template and template strands of genelet are labeled with -nt and -t, respectively. All strands were ordered from Integrated DNA Technologies, Inc (IDT) and the modifications marked with / / are labeled as defined by IDT. All other activators, blockers, and template strands are presented in Supplementary Table 1.

GENELETS	
G2C1-nt	/5TYE665/AGCCAAGATTCAGGTCAATAAGTGACCAAGTAATACGACTCACTATA GGGAGATTCGTCTCCCAAATCCTTCCATGAACGCCAAACCGTGGCGACG
G2C3-nt	5'AGCCAAGATTCAGGTCAATAAGTGACCAAGTAATACGACTCACTATA GGGAGATTCGTCTCCCAGAAGATGAAGATGTACCGTATAGGTA
G3R1-nt	/5TEX615/GAAGATGAAGGTGTACCGTATAGGTACTAGTAATACGACTCACTATA GGGAGATTCGTCTCCCATGCACGCCAAACCGTGGCGACGTAAT
G1S1-nt	/56FAM/TCCTTCCATGCACGCCAAACCGTGGCGACGTAATACGACTCACTATAGACATAC AGATTAACCAGACAGTGAC
dB3	5'GCTCGTTCCTAGTACCTATACGGTACACCTTCATCTTC
S1-t	5'GTCACTGTCTGGTTAATCTGTATGTCTATAGTGAGTCG

6.4 Additional IFFL1 experiments

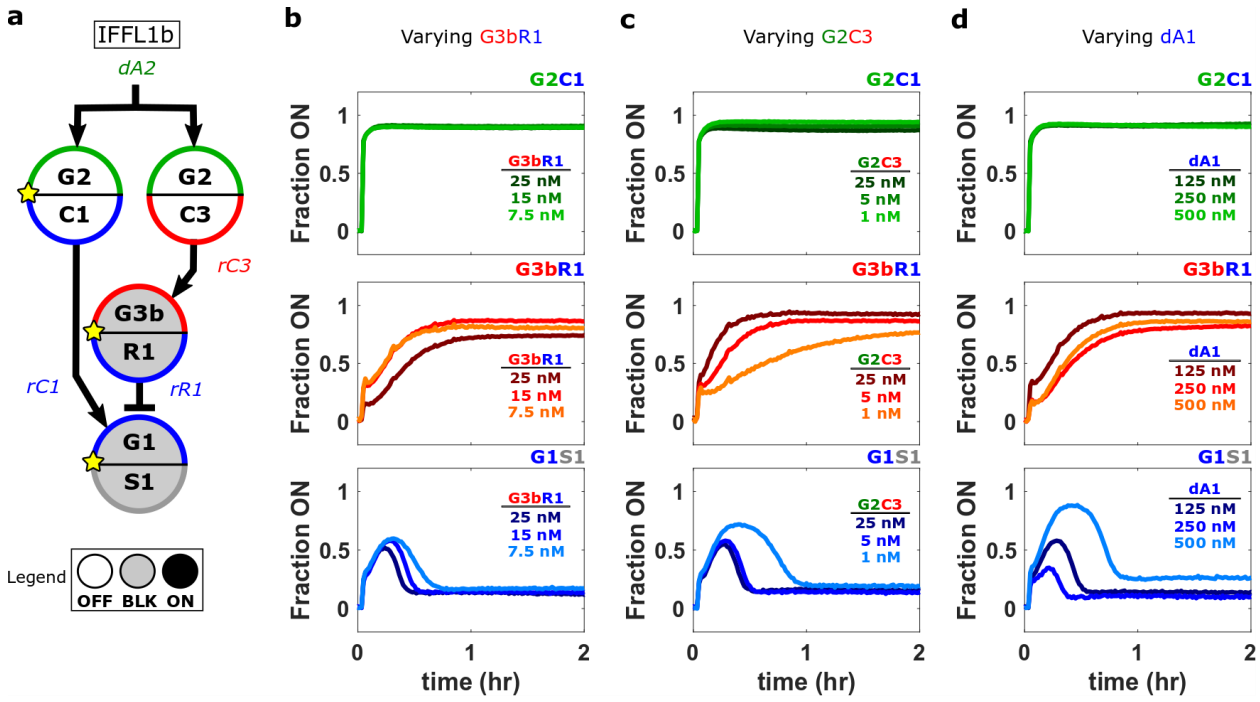

Supplementary Figure 29 | The IFFL1b can be tuned to produce a variety of pulse dynamics. (**a**) Schematic of the IFFL1b module. This module used an all-DNA version of dB3. Sequences are in Supplementary Table 12. (**b**-**c**) Normalized activation levels of network nodes during pulses with varying concentrations of the G3bR1 genelet (b), the G2C3 genelet (c), or the activator (dA1) of G1S1 (d). Varying the concentration of dA1 produces the most variation in pulse dynamics in the network. The concentrations of the species that were varied in each experiment are shown beside the plots. Reactions were otherwise conducted as described in Supplementary Section 6.2 using dB3.

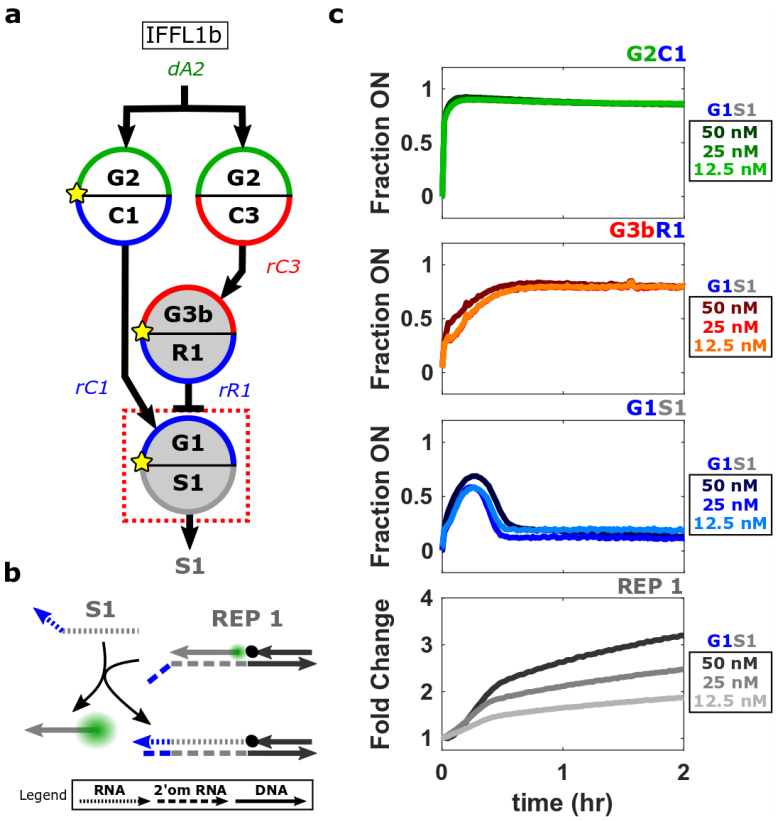

Supplementary Figure 30 | The amount of RNA output produced by an IFFL can be changed by changing the concentration of G1S1 genelet. (**a**) Schematic of the IFFL1b module. (**b**) Schematic of the fluorescence reporting scheme used to monitor the production of RNA from the G1S1 node. The S1 RNA transcript can displace a fluorescent strand from a quenched reporting complex (REP 1). The reporting complex was designed such that the domain where the S1 transcript binds was composed of 2' methylated RNA to prevent the bound transcript from being degraded by RNase H. The S1 reporting sequences were: S1_rep_bottom: 5'mGmUmCmAmCmUmGmUmCmUmGmGmUmUmAmAmUmCmUmGmUmAmUmGmUCTGGGTGGTGAGATGGATTGTG, S1_rep_F: /5HEX/ACATACAGATTAACCAGACA, S1_rep_Q: 5'CACAATCCATCTCACCACCCA/BHQ1/. (**c**) Normalized activation levels of IFFL1 network nodes and REP 1 signal during pulses with different concentrations of G1S1. The concentrations of G1S1 used in each experiment are shown beside the plots. Reactions were otherwise conducted as described in Supplementary Section 6.2 using dB3 with a total REP 1 concentration of 2 µM (150 nM REP 1 was fluorescently labeled and 1.85 µM was unlabeled to avoid saturating the fluorescence signal). Changing the concentration of G1S1 changes the total amount of S1 produced without changing the IFFL1 pulse kinetics.

6.5 Design of the IFFL2 module

To assemble the IFFL2 module, we selected three orthogonal input domains (G4o, G5, and G6) from the standardized domains we identified in Supplementary Section 4.3. The domains we selected for the IFFL2 were all different than the domains used to assemble the IFFL1 so that the two networks could be operated together. The G4o and G5 domains both demonstrated fast transcriptional coactivation and repression while the G6 domain only exhibited fast transcriptional coactivation. Thus, when assembling the IFFL2 network, we used the G6 domain in the node that represses the IFFL's output node when activated by an upstream node. Using this arrangement of nodes, the G6 domain never has to be repressed by another node in the network and it is present in the repression pathway of the IFFL which is designed to be slow (Figure 3c of the main text).

Supplementary Table 13 | DNA synthesized specifically for the IFFL2 network. Non-template and template strands of genelets are labeled with -nt and -t, respectively. All strands were ordered from Integrated DNA Technologies, Inc (IDT) and the modifications marked with / / are labeled as defined by IDT. All other activators, blockers, and template strands are presented in Supplementary Table 1.

GENELETS	
G5C4-nt	5'TCTCTTACCCTCGCTCGTCCTCCGAGCCTCTAATACGACTCACTATA GGGAGATTCGTCTCCCAGCTCTCCATCCTCCAGGTACACCCTGGCTCACCCTA
G5C6-nt	5'TCTCTTACCCTCGCTCGTCCTCCGAGCCTCTAATACGACTCACTATA GGGAGATTCGTCTCCCAAACCAACCTACTATGCCGTTCCATACGGCTCCACAC
G6R4o-nt	5'CCAACCTACTCTGCCGTTCCATACGGCTCCTAATACGACTCACTATA GGGAGATTCGTCTCCCATCTTCCAGGTACACCCTGGCTCTAATATCGTCG
R4o-t	5'TGCGACGATATTAGAGCCAGGGTGTACCTGGAAGATGGGAGACGAATCTCCCTATAGTGAGTCG
G6R4-nt	5'CCAACCTACTCTGCCGTTCCATACGGCTCCTAATACGACTCACTATA GGGAGATTCGTCTCCCATCTTCCAGGTACACCCTGGCTCTAATATCCTCG
G4S1-nt	/5HEX/TGCTCTCCATCTTCCAGGTACACCCTGGCTCTAATACGACTCACTATA GACATACAGATTAACCAGACAGTGAC
S1-t	5'GTCACTGTCTGGTTAATCTGTATGTCTATAGTGAGTCG
ACTIVATORS	
dA4o	5'TGCGACGATATTAGAGCCAGGGTGTACCTGGAAGA/3BHQ_1/

6.6 Design of the IFFL3 module

To design the IFFL3 module, we selected three input domains (G8, G9, and G10) from the standardized domains we identified in Supplementary Section 4.3 that were not used in the IFFL1 and IFFL2 modules. The G9 and G10 domains both demonstrated fast transcriptional coactivation but slow repression, while the G8 domain exhibited both fast transcriptional coactivation and repression (Supplementary Section 4.3). Thus, when assembling the IFFL3 network we used the G8 domain in the node that will pulse ON and OFF and the G9 and G10 domains in the nodes that only need to be turned on in the network. Given that the G10 domain exhibited slower transcriptional coactivation than the G9 domain (Supplementary Section 4.3), we put the G10 domain on the node that represses the IFFL's output node, as the repression pathway of the IFFL is designed to be slow to produce a pulse (Fig. 3d of the main text).

Supplementary Table 14 | DNA oligonucleotides synthesized for the IFFL3 network. Non-template and template strands of genelets are labeled with -nt and -t, respectively. All strands were ordered from Integrated DNA Technologies, Inc (IDT) and the modifications marked with / / are labeled as defined by IDT. All other activators, blockers, template and dummy node strands are presented in Supplementary Table 1.

GENELETS	
G9C8-nt	5'CCAACTACCTATGACTGTAACCCAGTCTCTTAATACGACTCACTATA GGGAGATTCGTCTCCCAGAATAGAACAAAGGGTTAGCAGAACCCAGAGGACGA
G9C10-nt	5'CCAACTACCTATGACTGTAACCCAGTCTCTTAATACGACTCACTATA GGGAGATTCGTCTCCCAGATAAATAGAAAGCCGCACAGAGCGGCAGAGCGGGA
G10R8-nt	5'GATAAATAGAGAGCCGCACAGAGCGGCAGATAATACGACTCACTATA GGGAGATTCGTCTCCCAAACAGAGGGTTAGCAGAACCCAGATAATACACGCG
dB8	5'CCTCGTCCTCTGGGTTCTGCTAACCCTCTGTTCTATTC
dB10	5'CCTCCCGCTCTGCCGCTCTGTGCGGCTCTCTATTTATC

6.7 Additional IFFL3 experiments

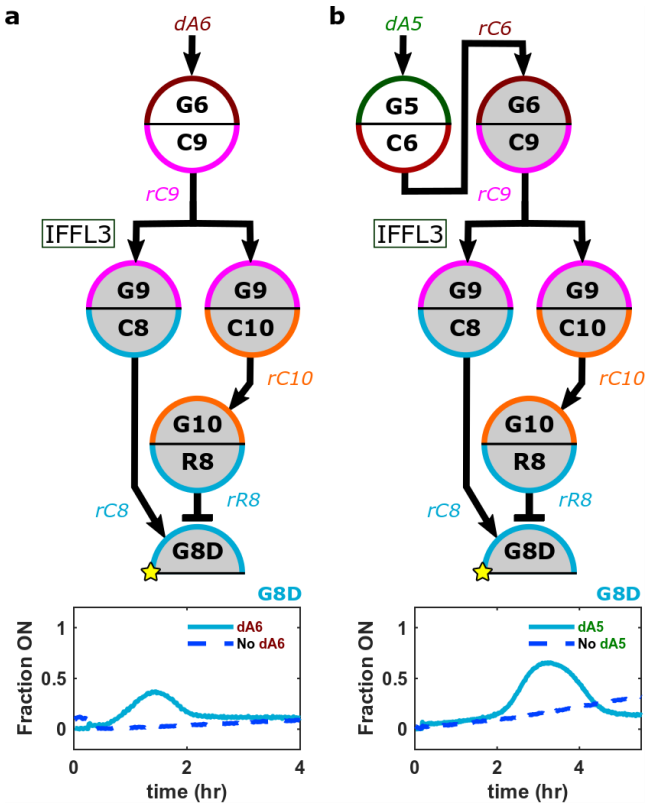

Supplementary Figure 31 | Using a transcriptional cascade to activate IFFL3. (**a**) Schematic of the G6C9_IFFL3 and the normalized activation levels of G8D with (solid) and without the addition of 250 nM dA6. [G6C9] = 25 nM, [G9C8] = 15 nM, [dB9-2omR] = [dB10-2omR] = 150 nM, [dB8-2omR] = 250 nM. The rest of the concentrations were as presented in Supplementary Table 11. (**b**) Schematic of the G5C6_G6C9_IFFL3 and the normalized activation levels of G8D with (solid) and without the addition of 250 nM dA5. [G5C6] = 5 nM, [G6C9] = 10 nM, [dA6] = 125 nM, [dA9] = 125 nM, [dB9-2omR] = 250 nM, [dB6] = [dB10-2omR] = [dB10-2omR] = 150 nM. The rest of the concentrations were as presented in Supplementary Table 11. The 2' methylated version of dB9 was used in these experiments (Supplementary Table 1). The sequences of species for this network are in Supplementary Table 15.

Supplementary Table 15 | Sequences of the strands used for the extended IFFL3 networks. Non-template and template strands of genelets are labeled with -nt and -t, respectively. The sequences of the rest of the IFFL3 genelet sequences were as in Supplementary Table 14. The sequences of the G5C6 node were the same as in the IFFL2 in Supplementary Table 13. All activator, blocker, and dummy node sequences are Supplementary Table 1.

GENELETS	
G6C9-nt	5'CCAACCTACTCTGCCGTTCCATACGGCTCCTAATACGACTCACTATA GGGAGATTCGTCTCCCAACCAACTACCTCTGACTGTAACCCAGTCTCTCGCCC
*G11C9-nt	5'CCACGGCTCGTCAAGAGCCACCTAATACGACTCACTATA GGGAGATTCGTCTCCCAACCAACTACCTCTGACTGTAACCCAGTCTCTCGC
*G11C5-nt	5'CCACGGCTCGTCAAGAGCCACCTAATACGACTCACTATA GGGAGATTCGTCTCCCATCTCTTACCCACGCTCGTCCTCCGAGCCTCCACA

7. Transcription of free blocker strands can cause node autoactivation

In our initial IFFL1b module experiments, we found that the BLK G3bR1 node slowly turned ON over the course of the experiment (Supplementary Figure 32b). We reasoned that the leak was not from the G2C3 node activating BLK G3R1, given OFF genelets do not exhibit appreciable transcription (Supplementary Figure 13), but rather from the BLK G3R1 node turning itself ON. Indeed, we found that the blocked G3bR1 node was able to turn itself ON when incubated in isolation in transcription conditions with enzymes present and that higher blocker concentrations resulted in faster activation (Supplementary Figure 32c). Since the rate of autoactivation increased with higher blocker concentrations, we hypothesized that the free blocker strand (dB3) was being transcribed to produce an RNA coactivator that removed the blocker from the blocked G3 domain. T7 RNAP is known to initiate transcription at single-stranded DNA 3' ends[3,16] and we have previously reported that such transcription can produce RNA molecules that affect genelet activation[4]. Given this hypothesized mechanism, we reasoned that changing the single-stranded 3' end of dB3 to RNA would prevent the undesired transcription reaction from occurring. To test this hypothesis, we ordered a dB3 variant that possessed 2' methylated RNA instead of DNA for the last twelve 3' bases on the blocker (dB3-2omR). We chose 2'methylated RNA to prevent the RNA portion of the blocker from being degraded by RNase H when bound to its target genelet[21]. The dB3-2omR variant prevented blocked G3R1 from turning ON at both blocker concentrations tested (Supplementary Figure 32d).

Although autoactivation does not affect what output is produced by the IFFL1 network, the propensity of G3 for autoactivation can change the outputs of longer cascades, where leaks can propagate. For example, a G2C3_G3bR1_IFFL2o network with a completely DNA dB3 strand for the G3bR1 node produced a pulse in the G4oS1 node even when no input trigger is provided to the network. This leak is suppressed if the G3bC5 node is replaced by a G3C5 node that uses the dB3-2omR variant (Supplementary Figure 33a). We therefore used the dB3-2omR variant in all subsequent networks using the IFFL1 network (IFFL1_2 and BS_IFFL1|2 networks).

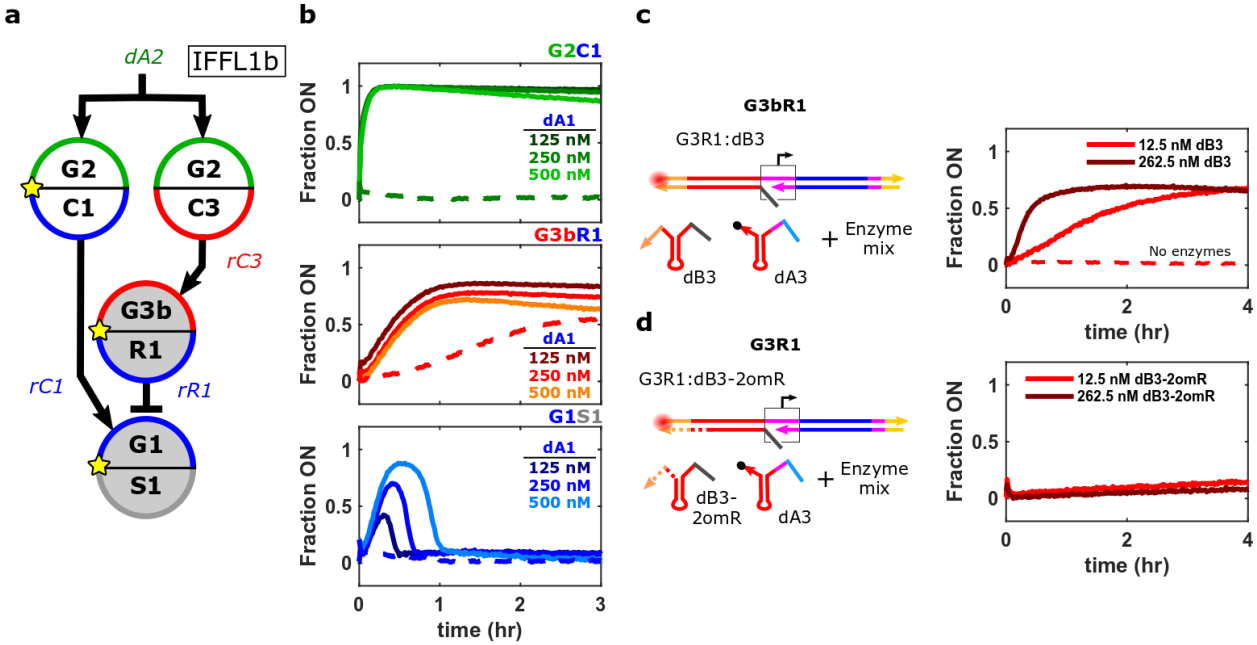

Supplementary Figure 32 | There is a slight leak in G3bR1 coactivation in the IFFL1b network, likely due to transcription of excess dB3. (**a**) Schematic of the IFFL1b network. (**b**) Normalized activation levels of network nodes during G1S1 pulses with varying dA1 concentrations. In the absence of the dA2 input (dashed lines) the G3bR1 node still turns on 50% over 3 hours ([dA1] = 250 nM). (**c**) Normalized activation levels of the G3bR1 node (species shown above the plot) during incubation with the enzyme mix used for circuit operation (T7 RNAP, RNase H, and YIPP) with different concentrations of excess dB3. Adding 250 nM dB3 increases the rate of spurious coactivation. Dashed lines are a control where enzymes were not added with 12.5 nM excess dB3. (**d**) Normalized activation levels of the G3R1 node (species shown above the plot) during incubation with the enzyme mix used for circuit operation (T7 RNAP, RNase H, and YIPP) with different concentrations of excess dB3-2omR variant. Reactions were otherwise conducted as described in Supplementary Section 6.2. For (c) and (d), 250 nM of dA3 was used. Sequences in Supplementary Table 12.

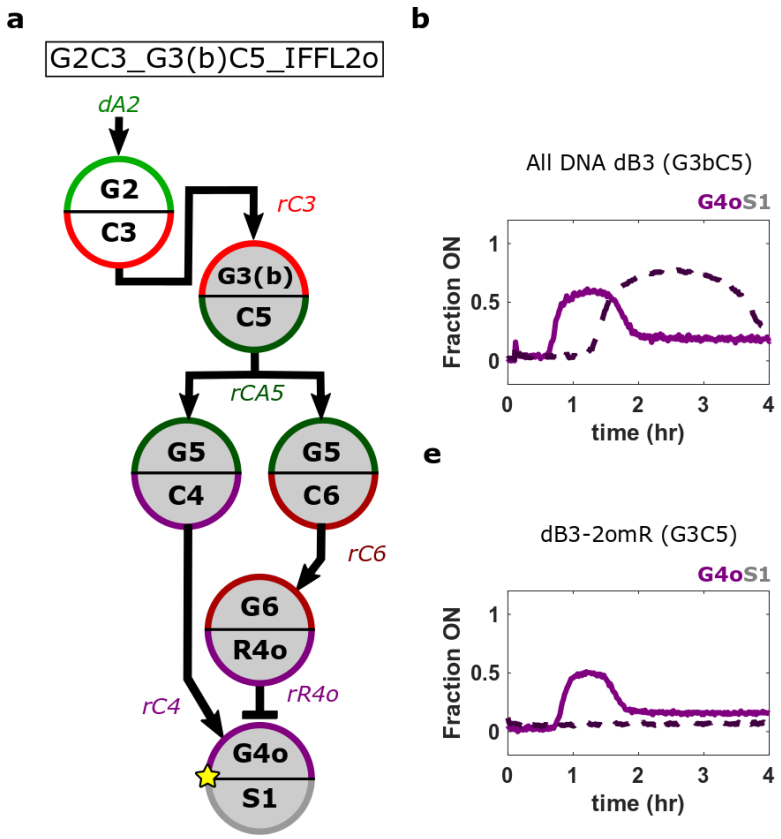

Supplementary Figure 33 | Spurious coactivation of G3 nodes causes a leak in the G2C3_G3bC5_IFFL2o network (**a**). (**b**) Normalized G4oS1 activation levels during experiments using the network in a, in which the pulse is initiated by the addition of dA2 with a G3bC5 node possessing dB3, which is composed entirely of DNA. In the absence of the dA2 input (dashed line), a pulse in G4oS1 is still observed. (**c**) Normalized G4oS1 activation levels during pulse experiments initiated by the addition of dA2 with a G3C5 node possessing dB3-2omR, which is modified to have the last 12 bases of its 3' be 2' methylated RNA. Replacing the blocker dB3 with the dB3-2omR variant prevents a pulse in G4oS1 activation in the absence of the dA2 input (dashed line). Reactions were otherwise conducted as described in Supplementary Section 8.2. Sequences in Supplementary Tables 12, 13, and 16.

We also found a prototype IFFL3 network (IFFL3b) using completely DNA versions dB8 and dB10 had a few leaks also likely related to transcription of free blocker stands. For example, a small pulse was still produced by the network in the absence of the input activator (Supplementary Figure 34a). We theorized this leak might be due to the blocked G8Db and G10bR8 nodes turning themselves ON *via* transcription of the free blocker strands, given that this transcription of blockers was also seen for the G3bR1 node in Supplementary Figure 32. Indeed, we found that the blocked G8Db node was able to turn itself ON when incubated in isolation in transcription conditions with enzymes present and that higher blocker concentrations resulted in faster activation (Supplementary Figure 34b). Additionally, blocked G10bR8 was able to repress G8D when incubated in transcription conditions with enzymes and this repression occurred more rapidly the higher the free blocker concentration (Supplementary Figure 34c). To suppress these leaks, we created dB8 and dB10 variants that possessed 2' methylated RNA instead of DNA for their last twelve 3' bases (dB8-2omR and dB10-2omR, respectively). These blocker variants prevented blocked G8D from turning itself ON (Supplementary Figure 34d) and G10R8 from repressing G8D (Supplementary Figure 34e).

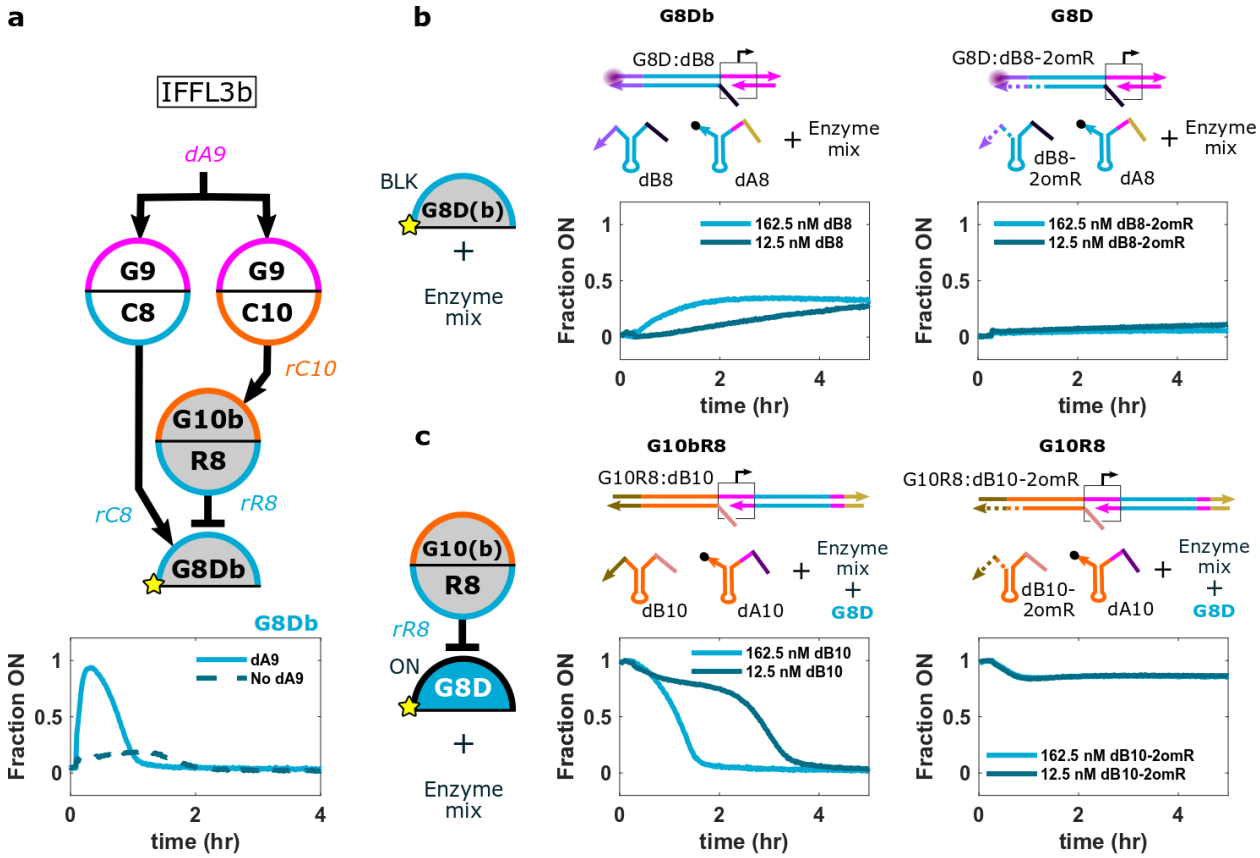

Supplementary Figure 34 | Suppressing spurious coactivation in the IFFL3b network. (**a**) Schematic of the IFFL3b and normalized kinetic data showing a pulse in G8Db activation in the absence of the network input dA9 (dashed line). (**b**) Normalized activation levels of the G8D(b) node (species shown above the plot) during incubation with the enzyme mix used for circuit operation (T7 RNAP, RNase H, and YIPP) using dB8 variants without (left, G8Db) and with (right, G8D) methylated RNA 3' ends. The dB8-2omR variant suppresses spurious coactivation of the G8D node. (**c**) Normalized activation levels of the G8D node during incubation with the enzyme mix used for circuit operation (T7 RNAP, RNase H, and YIPP) and the G10(b)R8 node (species shown above the plot) using dB10 variants without (left, G10bR8) and with (right, G10R8) methylated RNA 3' ends. The dB10-2omR variant suppresses spurious repression of the G8D node. Experiments otherwise conducted as described in Supplementary Section 6.2. Sequences are in Supplementary Table 14.

The untriggered activation identified for the blocked G3bR1, G8Db, and G10bR8 nodes appears to be due to spurious transcription of these nodes' free blocker strands. Thus, if the G3, G8, and G10 input domains are to be used in networks their blocker strands should have methylated RNA as the last 12 bases on their 3' ends to prevent autoactivation. In all experiments we will use G3b, G8b, and G10b to denote when these nodes were used with all DNA blockers rather than the methylated blocker versions. We did not observe any behavior consistent with autoactivation for the other input domains used in this study (G1, G2, G4, G5, G6, G9) so the blockers for these nodes likely do not need the methylated RNA modifications to function as designed, DNA versions of these blockers were used in all experiments in this work unless otherwise stated.

8. Design and characterization of the IFFL1_2 network

8.1 Design of the IFFL1_2 network

With successful pulses achieved for the IFFL1, IFFL2, and IFFL3 modules (Supplementary Section 6), we next set out to assemble a two-stage pulse network, in which the IFFL1 network was connected to the IFFL2 network to produce two sequential pulses. We termed this network the IFFL1_2. To connect the IFFL1 and IFFL2 networks, we designed an additional node with the G3 input domain and the C5 output domain that connects the IFFL1 and IFFL2 modules together. Simulations predicted that when the IFFL1 and IFFL2 networks were connected by this new node, triggering the IFFL1 network would produce sequential pulses in the activation levels of the output nodes of the IFFL1 and IFFL2 modules (Fig. 3e of the main text). The sequences of the G3C5 node that connects IFFL1 and IFFL2 is in Supplementary Table 16 below. These sequences were combined with the sequences for the IFFL1 and IFFL2 which are listed in Supplementary Tables 12 and 13, respectively.

Supplementary Table 16 | DNA oligonucleotides synthesized for the IFFL1_2 network. Non-template and template strands of genelets are labeled with -nt and -t, respectively. All strands were ordered from Integrated DNA Technologies, Inc (IDT) and the modifications marked with / / are labeled as defined by IDT.

GENELETS	
G3C5-nt	5’GAAGATGAAGGTGTACCGTATAGGTACTAGTAATACGACTCACTATA GGGAGATTCGTCTCCCATCTCTTACCCACGCTCGTCCTCCGAGCCTCCACACT
C5-t	5’ GTAGTGTGGAGGCTCGGAGGACGAGCGTGGGTAAGAGATGGGAGACGAATCTCCCTATAGTGAGTCG

8.2 IFFL1_2 experimental methods

Experiments to characterize the pulse behavior of the IFFL1_2 in response to an input trigger were conducted in a similar manner to the IFFL experiments (Supplementary Section 6.2). The concentrations of the components are listed in Supplementary Table 17, except where different concentrations of components are explicitly stated in figure captions. “Additional blocker strands” refer to additional blocker that was added beyond the 50% excess blocker all of the blocked genelets were annealed with.

Supplementary Table 17 | Concentrations of the components used in the IFFL1_2 experiments.

Component #	Component	Concentration
1	G2C1	25 nM
2	G2C3	5 nM
3	G3R1	25 nM
4	G1S1	25 nM
5	dA2	250 nM
6	dA3	125 nM
7	dA1	250 nM
8	Added dB1	0 nM
9	Added dB3-2omR	0 nM
10	G5C4	25 nM
11	G5C6	5 nM
12	G6R4 (or G6R4o)	25 nM
13	G4S1	25 nM
14	dA5	250 nM
15	dA6	250 nM
16	dA4 (or dA4o)	250 nM
17	Added dB4	150 nM
18	Added dB5	150 nM
19	Added dB6	150 nM
20	YIPP	1.35×10^{-3} U/µL
21	RNase H	8.92×10^{-3} U/µL
22	T7 RNAP	3.57 U/µL

8.3 IFFL1_2 simulations

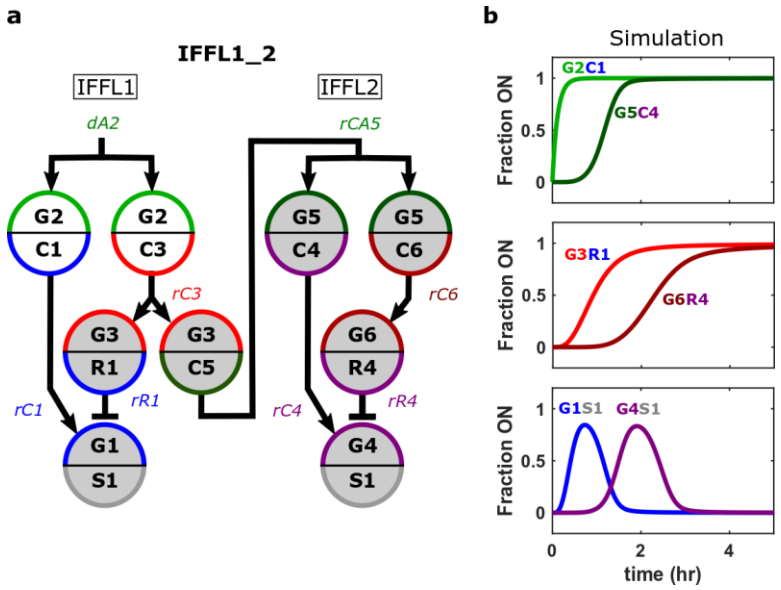

Supplementary Figure 35 | Kinetic simulations of the IFFL1_2 predict that the network should produce sequential pulses of G1S1 and G4S1 after the addition of an input trigger (dA2). (**a**) Schematic of the IFFL1_2 network. (**b**) Normalized activation levels of network nodes during kinetic simulations of the IFFL1_2 network. Simulations were otherwise conducted as described in Supplementary Section 5 with the concentrations of species in Supplementary Table 17.

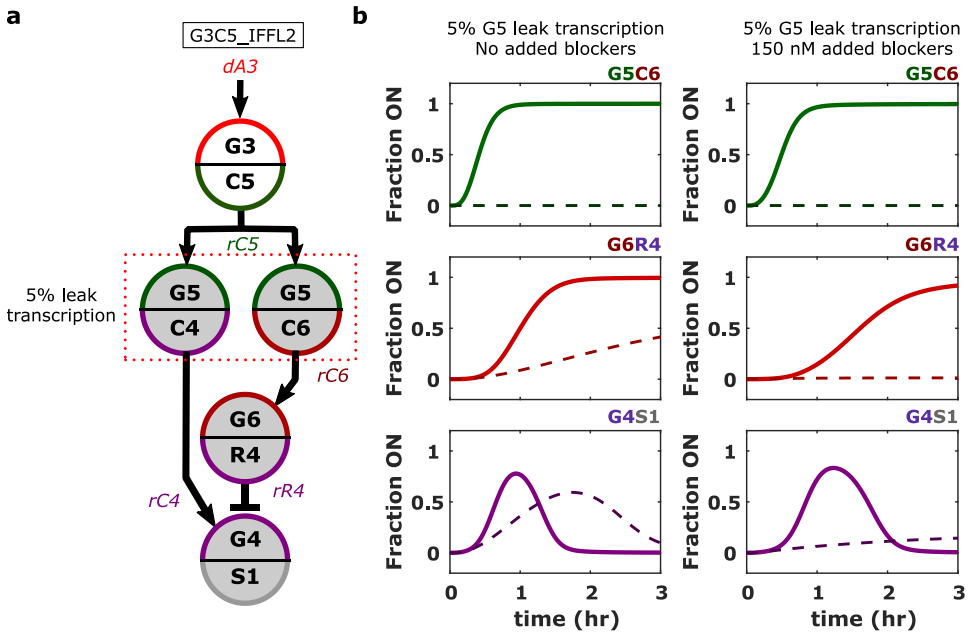

Supplementary Figure 36 | Kinetic simulations of the G3C5_IFFL2 network with 5% leak transcription from BLK G5C4 and BLK G5C6. (**a**) Schematic of the G3C5_IFFL2 network. (**b**) Normalized activation levels of network nodes during kinetic simulations without any added dB4, dB5, and dB6 (left) and with 150 nM of added dB4, dB5, and dB6. Dashed lines in the plots represent simulations where dA3 was not added at the beginning of the simulation. With 5% leak transcription from BLK G5C4 and BLK G5C6, G4S1 pulses even in the absence of input (left). Adding 150 nM additional dB4, dB5, and dB6 suppresses the spurious pulse without input (right). These results are in line with our experimental results in Supplementary Figure 38. Simulations were otherwise conducted as described in Supplementary Section 5 with the concentrations of species in Supplementary Table 17.

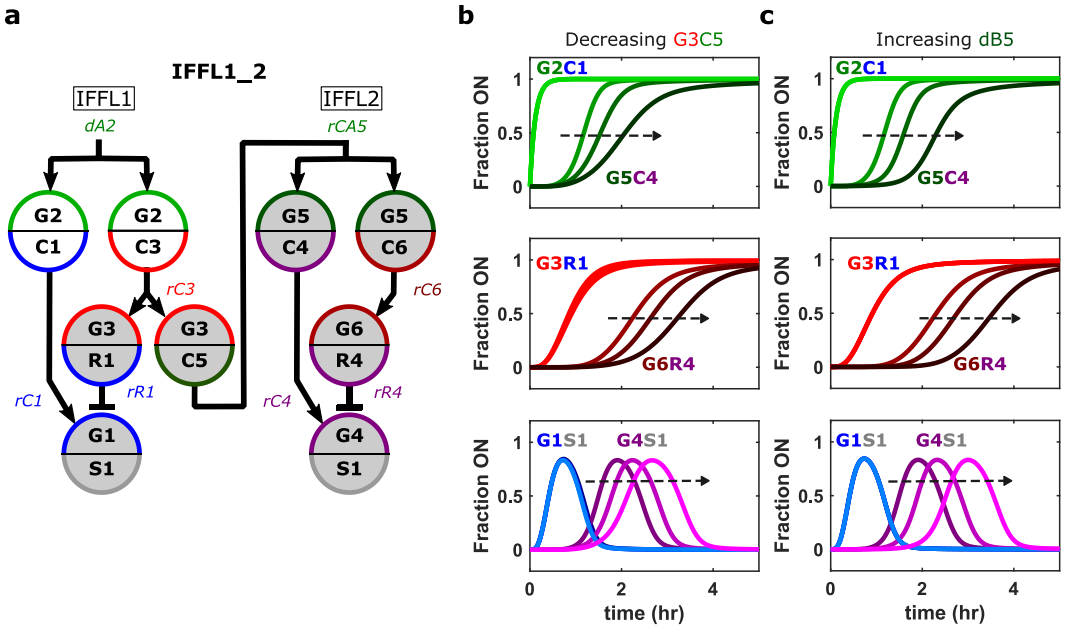

Supplementary Figure 37 | Kinetic simulations of the IFFL1_2 predict the G4S1 pulse can be delayed relative to the G1S1 pulse by changing the concentration of G3C5 or dB5. (**a**) Schematic of the IFFL1_2 network. (**b**) Normalized activation levels of network nodes during kinetic simulations of the IFFL1_2 network with decreasing concentrations of G3C5 (25 nM, 10 nM, 5 nM). (**c**) Normalized activation levels of network nodes during kinetic simulations of the IFFL1_2 network with increasing concentrations of added dB5 (150 nM, 500 nM, 1000 nM). Dashed arrows in plots indicate either a decrease in G3C5 (b) or increase in dB5 concentration (c). Both changes delay the triggering of the IFFL2 module without influencing the pulse dynamics of the IFFL1 module within the IFFL1_2. Simulations were otherwise conducted as described in Supplementary Section 5 with the concentrations of species in Supplementary Table 17.

8.4 Reducing leaks and unintended side reactions in the IFFL1_2 network

To construct the IFFL1_2, we started by adding the OFF G3C5 node into the network, which would serve as the connecting node between IFFL1 and the IFFL2 in IFFL1_2 network (Figure 3e of the main text). We then tested whether the activation of this node could produce a pulse in the level of G4oS1 activation (Supplementary Figure 38c). While activation of the G3C5 node did produce a pulse in the activation level of G4oS1, a pulse was also observed in the absence of G3C5 activation (Supplementary Figure 38d). We attributed this spurious pulse to a low level of transcription occurring either from the OFF G3C5 node or the BLK G5 nodes. We reasoned that the leak was likely not due to OFF G3C5 as genelets in their OFF state exhibit no detectible transcription and further since OFF G3C5 does not have blocker or activator present, autoactivation is not possible. In contrast, genelets in their BLK state incubated with their corresponding activators can exhibit leak of up to 10% transcriptional activity compared to their active state (Supplementary Figure 13). Thus, we hypothesized that a small transcriptional leak from the BLK G5 caused the G3C5_IFFL2o network to pulse without the input trigger. We tested this prediction by adding an additional 150 nM of each blocker in the IFFL2o network. With this change, the network produced a pulse in the level of G4oS1 activation only when G3C5 was activated (Supplementary Figure 38e).

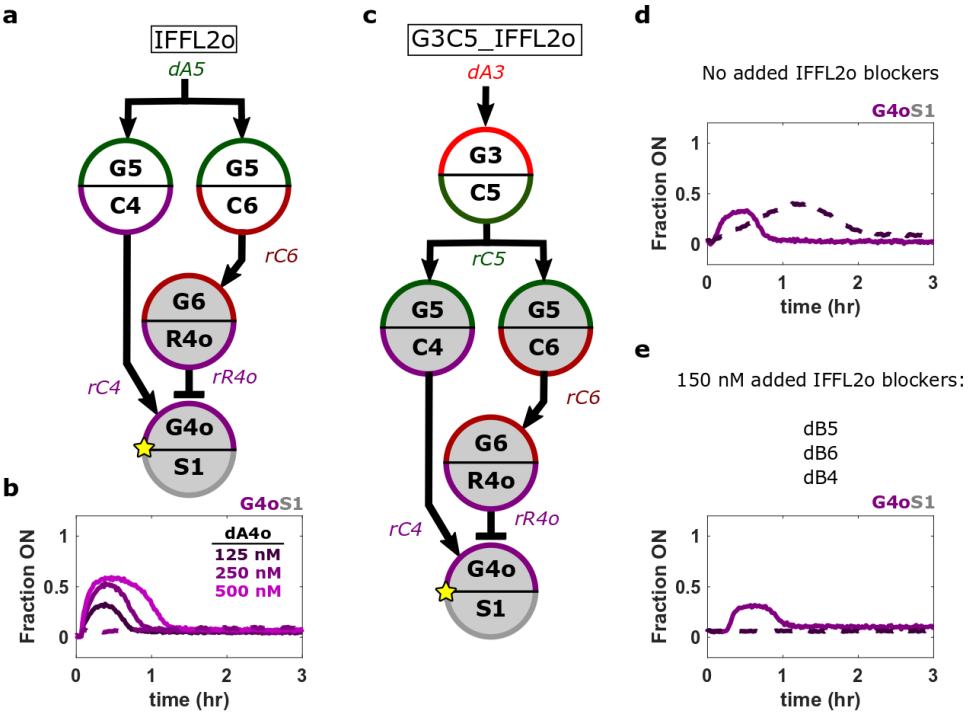

Supplementary Figure 38 | Suppressing leaks in transcriptional coactivation cascades. (**a**) Schematic of the IFFL2o network. (**b**) Normalized activation levels of the G4oS1 node during pulse experiments initiated by the addition of dA5 to the network depicted in (a). Dashed line represents a control where dA5 was not added. In these reactions no additional blocker was added. (**c**) Schematic of the G3C5_IFFL2o network, in which an upstream node triggers the IFFL2o. (**d**-**e**) Normalized activation levels of the G4oS1 node during pulse experiments initiated by the addition of dA3 to the network depicted in (a) both without (d) and with (e) 150 nM additional blocker strands for all the nodes in the IFFL2. Dashed line represents a control where dA3 was not added. Without the added IFFL2o blocker strands, G4oS1 pulses in the absence of the dA3 input. Concentrations of species varied in each experiment are shown in plots. Reactions were otherwise conducted as described in Supplementary Section 6.2. Sequences are in Supplementary Tables 12 and 14.

After suppressing the transcriptional leak in the G3C5_IFFL2o network, we next expanded this network to include the G2C3 node (Figure 3e of the main text) and tested whether activation of this node could trigger pulses in G4oS1 expression. We found activation of the G2C3 node resulted in pulses of G4oS1 activation without any leak if the variant of dB3 with 3' methylated RNA was used (dB3-2omR) (Supplementary Figure 33).

We next set out to assemble the whole IFFL1_2o network (Supplementary Figure 39a) and test whether it could produce sequential pulses in G1S1 then G4oS1 activation levels. Connecting these two networks together did result in sequential pulses as intended, however, the G1S1 node as not able to stay repressed during the pulse in G4oS1 activation (Supplementary Figure 39b). Given that G1S1 starts to turn back ON as soon as G4oS1 begins to get repressed, we reasoned the perhaps rR1 and rR4o were interacting in an undesired way. Analysis of minimum free energy structures with NUPACK[14] revealed that 80% of an equimolar mixture of rR1 and rR4o was predicted to be a dimer at 37°C (Supplementary Figure 39c, left). This likely causes G1S1 to turn ON as rR4o begins to accumulate and sequester rR1. We believe this undesired interaction was the result of an error in our sequence design workflow where rR1 was accidently excluded as a sequence to design against. To reduce the interaction between rR1 and rR4o we changed on base of the rR4o (G->C in Supplementary Figure 39c, left). This single base change reduced the predicted concentration of rR1:rR4 dimer to be less than 8% of an equimolar (1 μM) mixture of the two species (Supplementary Figure 39c, right). Importantly, the single base change was in the repression toehold region of rR4o, so the same G4 input domain could be used with the new activator. Reassembling the IFFL1_2 network with the new rR4 sequence resulted in the desired sequential pulses in G1S1 and G4S1 activation levels and G1S1 stayed repressed over the course of the experiment (Supplementary Figure 39d). Based on these results the new rR4 sequence was used in all subsequent networks that were assembled. All nodes that are labeled with a "o" after the 4 refer to the rR4o/dA4o sequences described in Supplementary Section 4 (i.e., G4oS1 uses the dA4o activator, G6R4o encodes the rR4o repressor sequence). All nodes **without** the "o" after the 4 refer to the new rR4/dA4 sequences described here. The rR4o/dA4o sequences are in Supplementary Table 13 and the rR4/dA4 sequences are in Supplementary Table 1.

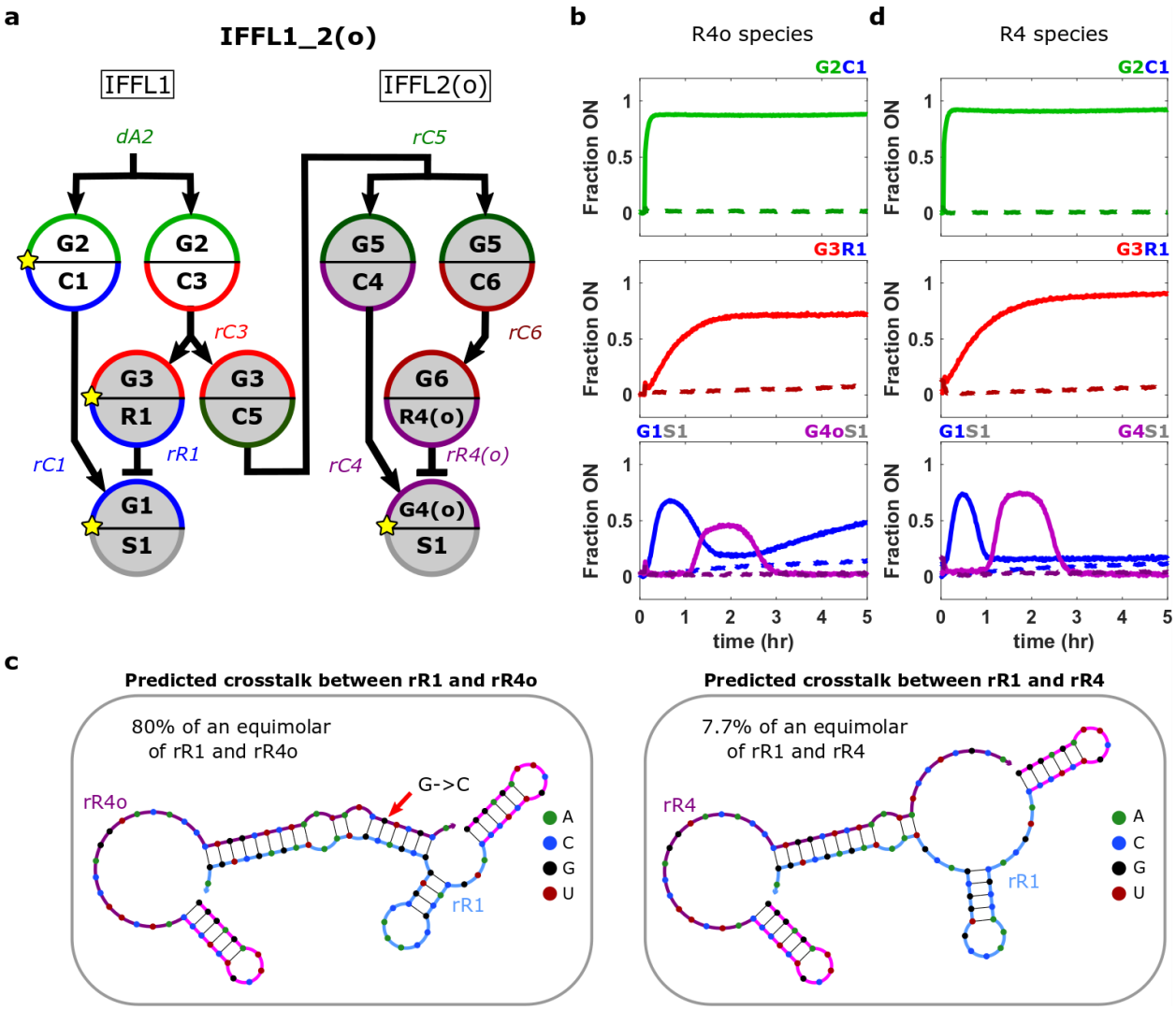

Supplementary Figure 39 | Identifying and removing crosstalk between rR1 and rR4o in the IFFL1_2o network. (**a**) Schematic of the IFFL1_2(o) network. Whether there is an "(o)" or not after a species name indicates whether the species was one of two designs *i.e.* rR4(o) was either rR4o or rR4 in subsequent experiments. (**b**) Normalized activation levels of IFFL1_2 network nodes during pulse experiments initiated by the addition of dA2 using R4o species. Dashed lines are controls where dA2 was not added. Note G1S1 begins to turn back ON after the G4oS1 pulse completes. (**c**) Left: NUPACK predicted secondary structure of the rR1 and rR4o species. NUPACK predicts this structure will be 80% of an equimolar mixture of rR1 and rR4o. The red arrow indicates where a guanine base was changed to a cytosine base to destabilize this secondary structure. Right: the NUPACK predicted secondary structure of rR1 and the rR4o variant (termed rR4) that has the G->C change indicated in the left panel. With this sequence change, NUPACK only predicts 7.7% of an equimolar mixture of rR1 and rR4 will adopt this undesired structure. (**d**) Normalized activation levels of IFFL1_2 network nodes during pulse experiments initiated by the addition of dA2 using R4 species. Dashed lines are controls where dA2 was not added. The redesigned R4 species remove the crosstalk between the G1S1 and G4S1 pulses. Reactions were conducted as described in Supplementary Section 8.2 with dB3-2omR. Sequences are in Supplementary Tables 12, 13 and 16.

8.5 Additional IFFL1_2 experiments

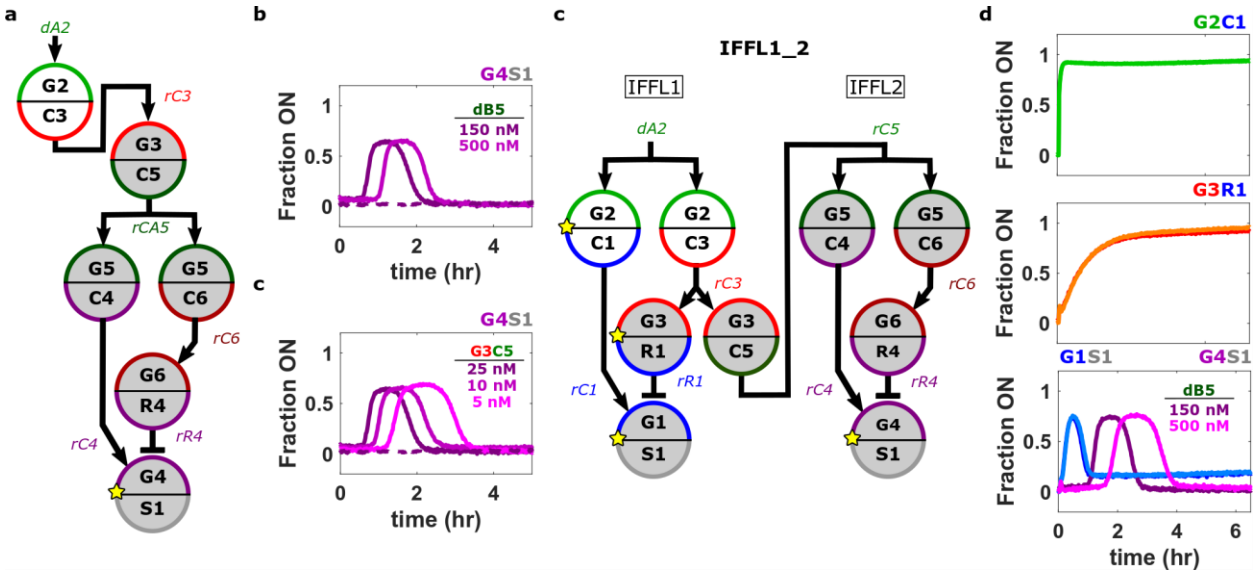

Supplementary Figure 40 | The timing of the IFFL2 pulse can be delayed by changing the concentrations of added dB5 or the G3C5 genelet. (**a**) Schematic of an expanded IFFL2 network used in the experiments in (b) and (c). (**b**-**c**) Normalized activation levels of the G4S1 node during pulse experiments initiated by the addition of dA2 to the network depicted in (a). Experiments were conducted with different concentrations of dB5 (b) or the G3C5 node (c). (**a**) Schematic of the IFFL1_2 network. (**b**-**c**) Normalized activation levels of IFFL1_2 network nodes during pulse experiments with different concentrations of dB5. Concentrations of species varied in each experiment are shown in plots. Reactions were otherwise conducted as described in Supplementary Section 8.2 with dB3-2omR. Sequences are in Supplementary Tables 12, 13 and 16.

9. Design and characterization of the tri-stable network (TSN)

9.1 Design of the TSN

To design the TSN, we selected three input domains (G1, G2, and G4) that all exhibited fast transcriptional repression kinetics from the standardized domains we identified in Supplementary Section 4.3. These nodes were chosen because we had also done experiments in which we had observed that each of these nodes could repress one another in isolation (Supplementary Figure 23). We used these 3 input domains to design a mutually repressive network (Supplementary Figure 41). The TSN uses the dA4 sequence, which differs by one base from dA4o presented in Supplementary Section 4.3. The dA4 variant was designed to prevent spurious hybridization with dR1 (Supplementary Figure 39c,d).

As the TSN only employs repression reactions, no DNA blockers were necessary and HPC5o genelets which lack the 5' blocking toehold (BTH) were used (Supplementary Figure 1). This change was made because shorter genelets were less expensive to synthesize and the shorter genelets were, in the context of a TSN, fully functional. Nodes with the HPC5o design that lacks the blocking toehold are marked with a * in subsequent tables and figures. Sequences specific to the TSN experiments are presented below in Supplementary Table 18.

The inducer RNAs were designed using a previously described method[4]. Briefly, the inducer RNAs are designed to have partial complementarity to their target RNA repressors. Inducer RNA binding sequesters the 8-base domain on an RNA repressor that facilitates the strand displacement of the repressor's target activator from a genelet, thereby inhibiting the repression reaction (Supplementary Figure 42a). The inducer RNAs are designed to be only partially complementary, rather than fully complementary, to the RNA repressors to prevent the inducer RNAs from binding the input domains of the genelets they are designed to activate (Supplementary Figure 42b). Schematics of the inducer RNAs bound to their target RNA repressors are presented in Supplementary Figure 42c.

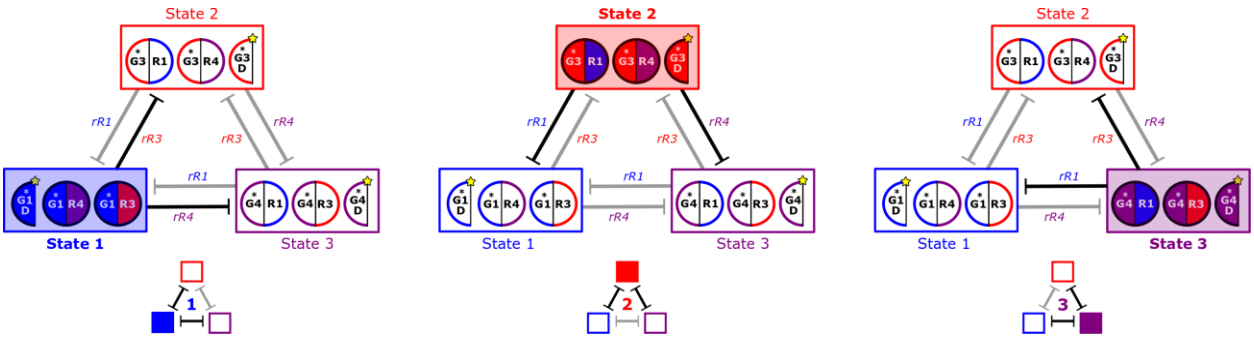

Supplementary Figure 41 | Schematic of the TSN. Shaded boxes indicate the nodes that are ON in each stable state.

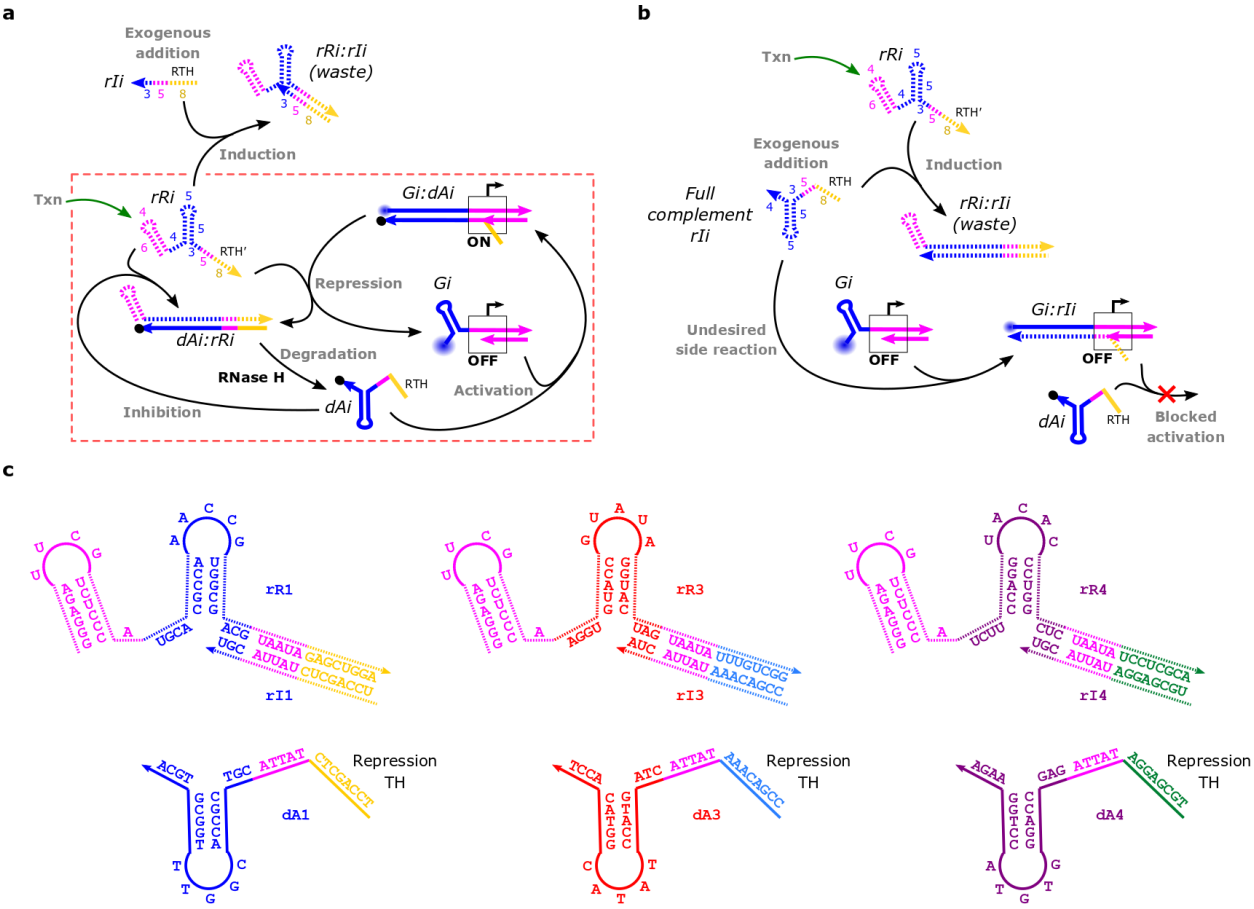

Supplementary Figure 42 | Inducer RNA designs. (**a**) Schematic of the induction reactions used to change states in the TSN. Reactions in the red box depict the genelet reactions in the absence of an inducer RNA. Once the inducer RNA is added, it sequesters its target rRi by preventing the rRi from binding to the repression toehold of its target activator. As rRi bound to dAi is degraded by RNase H, there is then no new rRi to bind to the activator. The dAi is then free to activate its target genelet. (**b**) Schematic of an undesired reaction that can arise if the inducer RNAs were designed to be fully complementary to their target RNA repressors. Such inducer RNAs would have the same sequence as the DNA activator of the genelet they are designed to turn ON and thus the inducers could bind the genelets and prevent them from being activated. (**c**) Sequence schematics of the TSN RNA repressors bound to their inducer RNAs (top). A bound inducer RNA prevents a repressor from binding the repression toehold of its target activator (bottom).

Supplementary Table 18 | DNA and RNA oligonucleotides synthesized for the TSN. Non-template and template strands of genelets are labeled with -nt and -t, respectively. All strands were ordered from Integrated DNA Technologies, Inc (IDT) and the modifications marked with / / are labeled as defined by IDT. The RNAs were ordered unpurified. * indicates the HPC5o genelet design where the BTH at the 5' end of the input domain was removed. All other activators, template and dummy node strands are presented in Supplementary Table 1.

GENELETS	
*G1R3-nt	5'TGCACGCCAAACCGTGGCGACGTAATACGACTCACTATA GGGAGATTCGTCTCCCAAGGTGTACCGTATAGGTACTAGTAATATTTGTCG
*G1R4-nt	5'TGCACGCCAAACCGTGGCGACGTAATACGACTCACTATA GGGAGATTCGTCTCCCATCTTCCAGGTACACCCTGGCTCTAATATCCTCGC
*G3R1-nt	5'AGGTGTACCGTATAGGTACTAGTAATACGACTCACTATA GGGAGATTCGTCTCCCATGCACGCCAAACCGTGGCGACGTAATAGAGCTGG
*G3R4-nt	5'AGGTGTACCGTATAGGTACTAGTAATACGACTCACTATA GGGAGATTCGTCTCCCATCTTCCAGGTACACCCTGGCTCTAATATCCTCGC
*G4R1-nt	5'TCTTCCAGGTACACCCTGGCTCTAATACGACTCACTATA GGGAGATTCGTCTCCCATGCACGCCAAACCGTGGCGACGTAATAGAGCTGG
*G4R3-nt	5'TCTTCCAGGTACACCCTGGCTCTAATACGACTCACTATA GGGAGATTCGTCTCCCAAGGTGTACCGTATAGGTACTAGTAATATTTGTCG
INDUCER RNAS	
rI1	5'rCrCrGrArCrArArArUrArUrUrArCrUrA
rI3	5'rUrCrCrArGrCrUrCrUrArUrUrArCrGrU
rI4	5'rUrGrCrGrArGrGrArUrArUrUrArGrArG
DNA REPRESSORS	
dR1	5'TGCACGCCAAACCGTGGCGACGTAATAGAGCTGGA
dR3	5'AGGTGTACCGTATAGGTACTAGTAATATTTGTCGG
dR4	5'TCTTCCAGGTACACCCTGGCTCTAATATCCTCGCA

9.2 TSN experimental methods

All genelet nodes were prepared by annealing corresponding -nt and -t strands at equimolar concentrations of 5 µM by heating to 90°C and then cooling from 90°C to 20°C at -1°C/min. All TSN experiments were conducted at 37°C in an Agilent Mx3005p qPCR with G1D tracked on the FAM channel, G3D tracked on the ROX channel, and G4D tracked on the HEX channel.

Samples for experiments were prepared by mixing all of the annealed genelets to the desired final concentrations (components 1-9 in Supplementary Table 19) together with the transcription mix components (Methods of the main text). To set the state of the network, only the activator that turns on the genelets of the desired initial state was added to each sample (dA1 was added to set the network in State 1, dA3 for State 2, or dA4 for State 3) and the other activators were left out of the mixture (Supplementary Figure 43). The samples were then added to the qPCR and an initial baseline fluorescence was measured to serve as a minimum for normalization. While the baseline readings were being taken, the enzyme mix was prepared (components 13-15 in Supplementary Table 19) and subsequently added to the samples in the qPCR (EM in Supplementary Figure 43). The samples were then incubated for 20 – 30 minutes in the qPCR. Note during this stage of the experiment only the genelets of the desired initial state are ON and these genelets are producing the RNAs that will repress the genelets of the other two states. After the 30-minute incubation, the activators for the other two states were added *i.e.* if the network was initially in State 1, then dA3 and dA4 were added (Supplementary Figure 43). The moment all the activators were added to the samples represented the start of an experiment (t = 0 in all the plots of all TSN experiments). Experiments were typically conducted for 16 – 24 hours. At the end of most experiments, to obtain a maximum fluorescence value

for normalization, the DNA repressors (dR1, dR3, dR4) were added in great excess (typically >2.5 µM) of their corresponding activators to remove the activators from each node. The normalization procedure for the TSN experiments is presented in Supplementary Section 13.2.

To trigger single state changes in the TSN, 10 µM of the inducer RNA of the repressor of the desired new state was added. In double state change experiments, the timing of the second state change depends on the concentration of inducer RNA added for the first state change: the more inducer RNA added for the first state change, the longer the time required to complete the second state change[4] (Supplementary Fig. 47). Thus, for each of the double state change experiments presented in Figure 4 of the main text, a set of inducer RNA concentrations were tested for the first state change to find the lowest concentration of inducer RNA required to induce the first state change and thus allowing the second state change to complete quickly (Supplementary Fig. 47). The concentrations of the inducer RNAs used to induce the double state changes present in Figure 4 of the main text are in Supplementary Table 20.

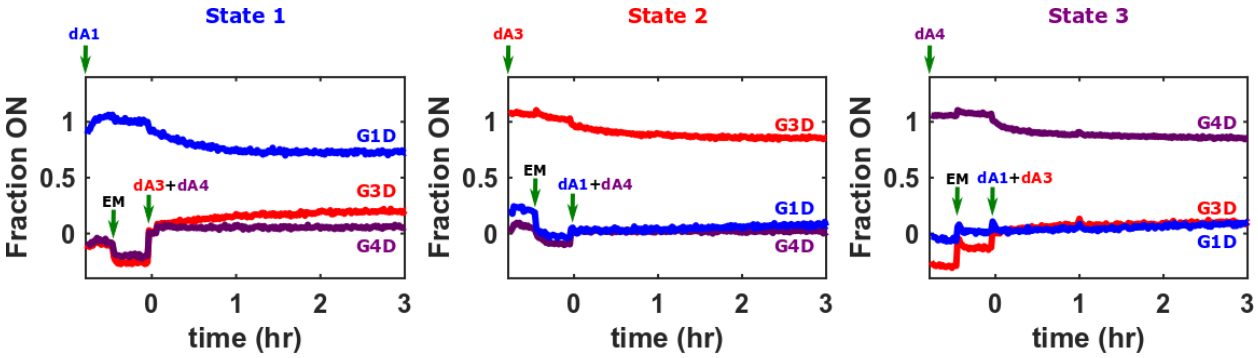

Supplementary Figure 43 | Representative data during experimental set up of the TSN experiments in each initial state. All samples initially contained components 1-9 in Supplementary Table 19 and the activator indicated with the pink arrows above the plots. The green arrows indicate when the enzyme mixture (EM) and non-initial state activators were added. Time = 0 for the experiments was defined as the time when the non-initial state activators were added. The experimental data after time = 0 is also presented in Figure 5b of the main text.

Supplementary Table 19 | Concentrations of the components used in the TSN experiments. Unless otherwise stated, all TSN experiments were conducted with these component concentrations.

Component #	Component	Concentration
1	*G1R3	50 nM
2	*G1R4	50 nM
3	*G3R1	50 nM
4	*G3R4	50 nM
5	*G4R1	50 nM
6	*G4R3	50 nM
7	*G1D	25 nM
8	*G3D	25 nM
9	*G4D	25 nM
10	dA1	250 nM
11	dA3	250 nM
12	dA4	250 nM
13	YIPP	1.35×10^{-3} U/µL
14	RNase H	8.92×10^{-3} U/µL
15	T7 RNAP	3.57 U/µL

Supplementary Table 20 | Concentrations of the inducer RNAs used in the double state change TSN experiments in Figure 5 of the main text.

State changes	Inducer RNA concentrations
1 to 2 to 3	rI3: 6 µM, rI4: 14 µM
1 to 3 to 2	rI4: 5 µM, rI3: 14 µM
2 to 1 to 3	rI1: 4 µM, rI4: 14 µM
2 to 3 to 1	rI4: 6 µM, rI1: 14 µM
3 to 1 to 2	rI1: 3 µM, rI3: 14 µM
3 to 2 to 1	rI3: 7 µM, rI1: 14 µM

9.3 Simulations and analysis of multi-stable networks

Here we explore the multi-stability of mutually repressive networks with simulations. We first explored the sensitivity to RNA repressor production and degradation rates of multi-stability in a two node mutually repressive network (*i.e.* a bi-stable network) as well as a three node mutually repressive network (*i.e.* a tri-stable network). Here, to emphasize qualitative changes in the character of the network over quantitative changes to particular concentrations in the system, we introduce a quantity that captures how effectively the network maintains a particular node at high concentration relative to the others when initialized in that state. This "multi-stability" quantity is computed as the ratio of the target genelet concentration (*i.e.* the network is initialized with this genelet's activator present) relative to the sum of the concentrations of all genelets, averaged over the different activator initial conditions. This quantity achieves a maximum value of 1 when the target state has much higher concentration than the other nodes in each initial condition and falls by 1/N (with N the number of states) if a particular initial condition ends with some other state having a much larger concentration. In these simulations, we follow a prescription similar to that presented in Supplementary Figure 46 where the system is initialized by only adding the activator corresponding to the set of genelets of the target state. Both a two node and three node mutually repressive networks exhibit regions of multi-stability for a range of RNA production and degradation rates, however moving to a three node network decreases the phase space where the maximum number of stable states can be achieved (Supplementary Figure 44).

To further explore the effect of increasing the number of mutually repressive nodes in a network on the robustness to kinetic parameter variation, we ran similar multi-stability analyses for systems with N=2, 3, 4, 5, 6, and 7 nodes. Instead of analyzing dependence on any particular rate constant or rate constant combination, we created random rate constant sets (drawn from Gaussian distributions centered on the base parameter values assumed in the general genelet model) and computed the multi-stability metric over increasing standard deviation of these rate constant distributions. In Supplementary Figure 45 we plot the fraction of simulations (*i.e.* rate constant parameter sets) where the multi-stability metric dropped below (N-1)/N (*i.e.* corresponding to the network effectively losing one stable state). These results show a modest drop in the robustness of a three node mutually repressive network compared to a two node network.

We further explored the sensitivity of the TSN to rate constant variations with systematic perturbations in these kinetic parameters. The TSN involves 5 types of reactions - repression, inhibition, RNA production, RNA degradation, and genelet activation. In Supplementary Figure 47, we show the results for modifications to kinetic parameters involved in each type of process when individually modified (excluding inhibition which had no qualitative effect and genelet activation which only alters the time

required to set the initial state) and when modified in pairs (Supplementary Figure 48 and Supplementary Figure 44) for select rate constant combinations.

Finally, we use simulations to explore two different mechanisms to switch the tri-stable network that have both been previously used to switch the state of a two node mutually repressive bi-stable network (Supplementary Figures 49 and 50).

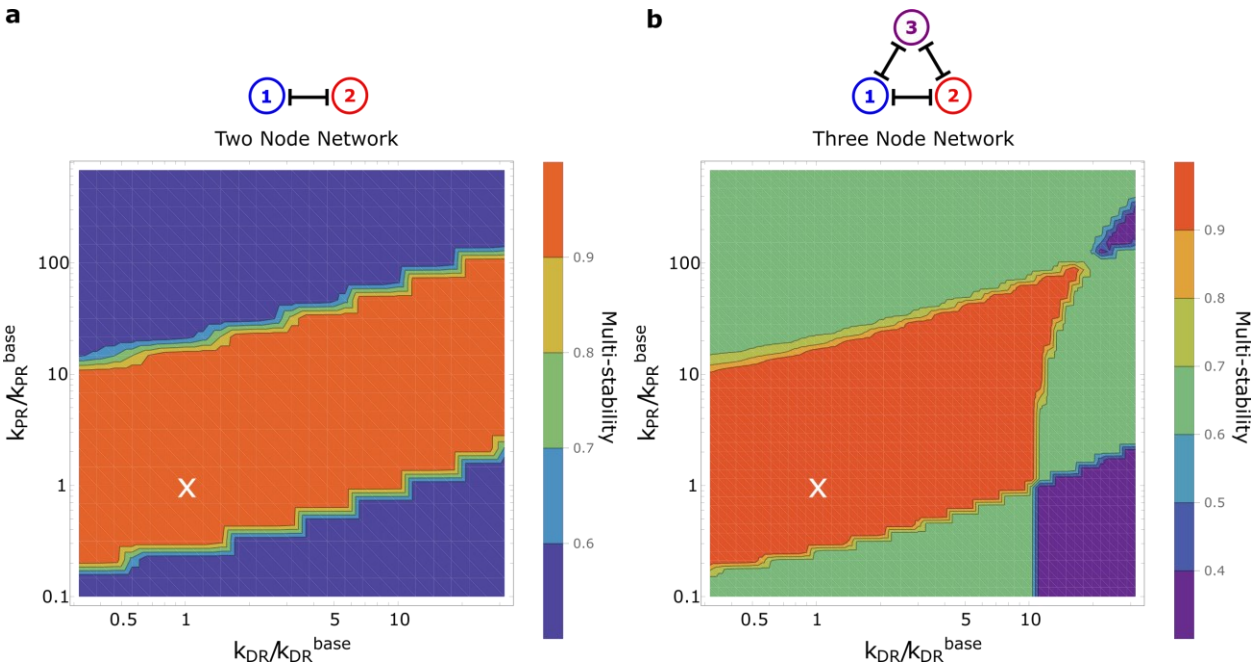

Supplementary Figure 44 | The phase space of multi-stability with respect to RNA repressor production and degradation rates is smaller for a three node mutually repressive network than a two node mutually repressive network**.** Contour plots for multi-stability computed over a grid of parameter values for the repressor production rate (for the repressor of Node 1 produced by Node 2) and the degradation rate of this repressor surrounding the assumed values from the general genelet model (indicated by the white "x"). **a**, For a mutually repressive 2 node network, the system maintains bi-stability (red) to larger values of the repressor degradation rate, but shows a sensitivity to the repressor production rate leading to mono-stability (blue). **b**, For the TSN system, tri-stability (red) is observed over a large region around experimental values with bi-stable regions (green) and mono-stable regions (purple) for extreme values of the production rate and large values of the degradation rate respectively. Simulations were otherwise conducted as described in Supplementary Figure 46.

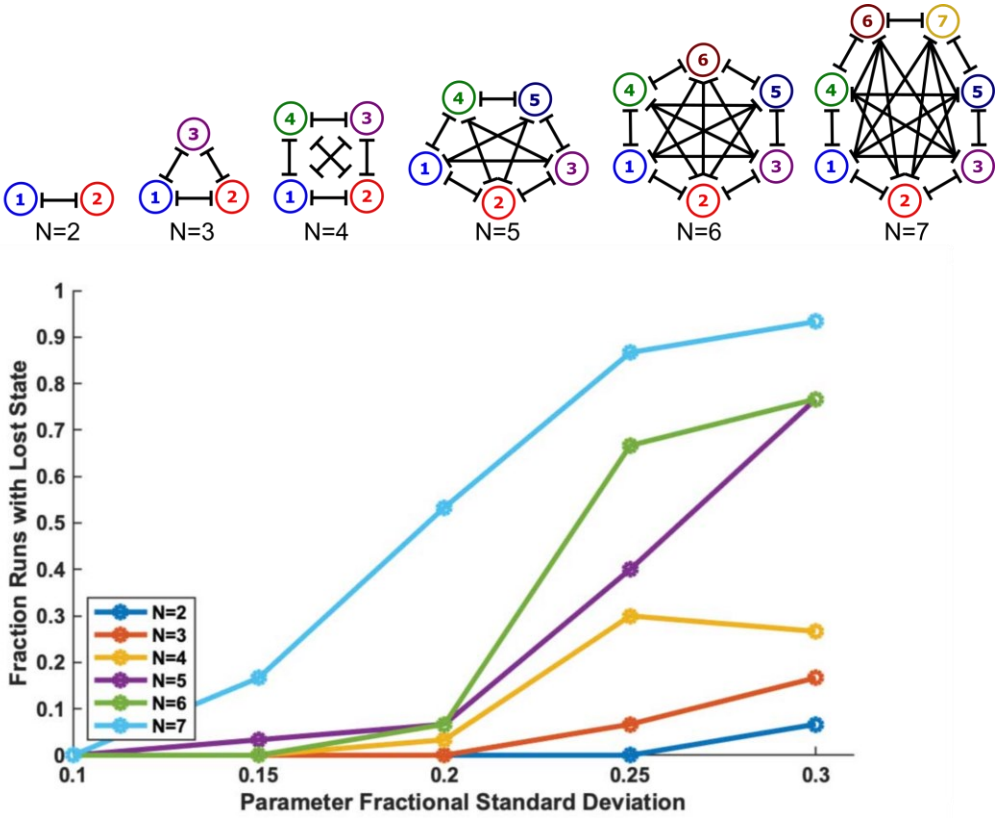

Supplementary Figure 45 | Fraction of random parameter sets (out of 30 total sets for each value of N) where at least one of the stable states is effectively lost (inferred from multi-stability values <=(N-1)/N). Parameters were drawn from a Gaussian centered on the base parameter values (Supplementary Table 8) with standard deviation varied from 10% to 30% of the base value. Simulations were otherwise conducted as described in Supplementary Figure 46.

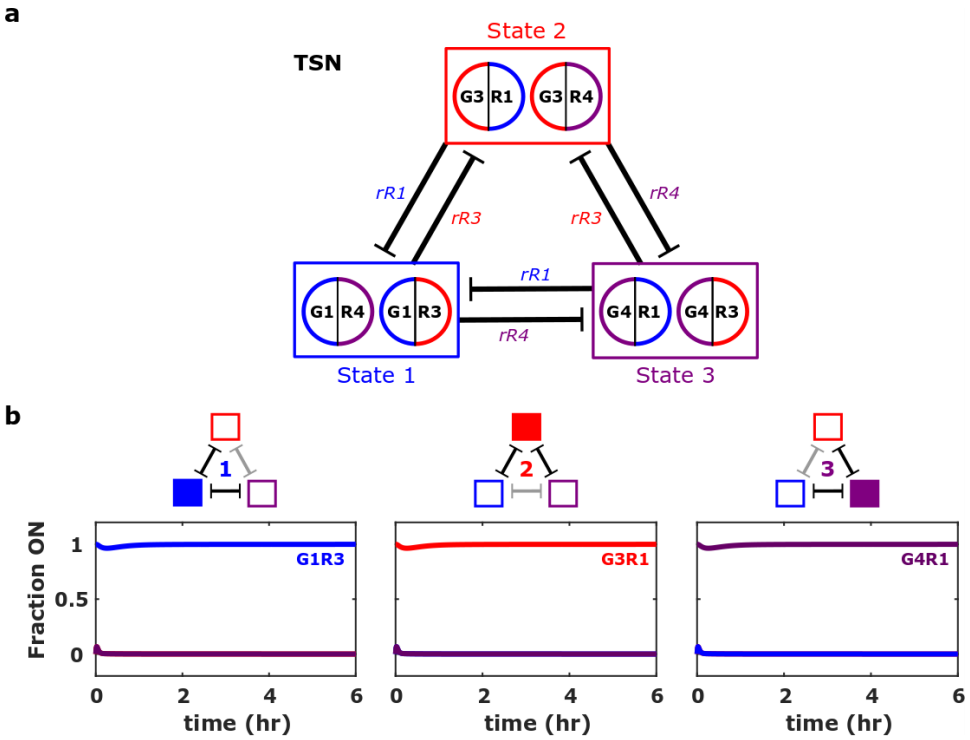

Supplementary Figure 46 | Kinetic simulations of the TSN predicts tri-stability. (**a**) Schematic of the network used in the simulations. (**b**) Simulated normalized activation levels of network nodes initialized in each stable state. Simulations were conducted using the generalized genelet model presented in Supplementary Section 5 with the component concentrations in Supplementary Table 19. The simulations were conducted in two stages similarly to how the experiments were conducted (Supplementary Section 9.2). Initially, only the activator of the initial state was present and the simulation was conducted for 30 minutes so that the repressors of the undesired states could accumulate. The activators of the other network states were then introduced into the simulations; this addition represents time = 0 in the plots.

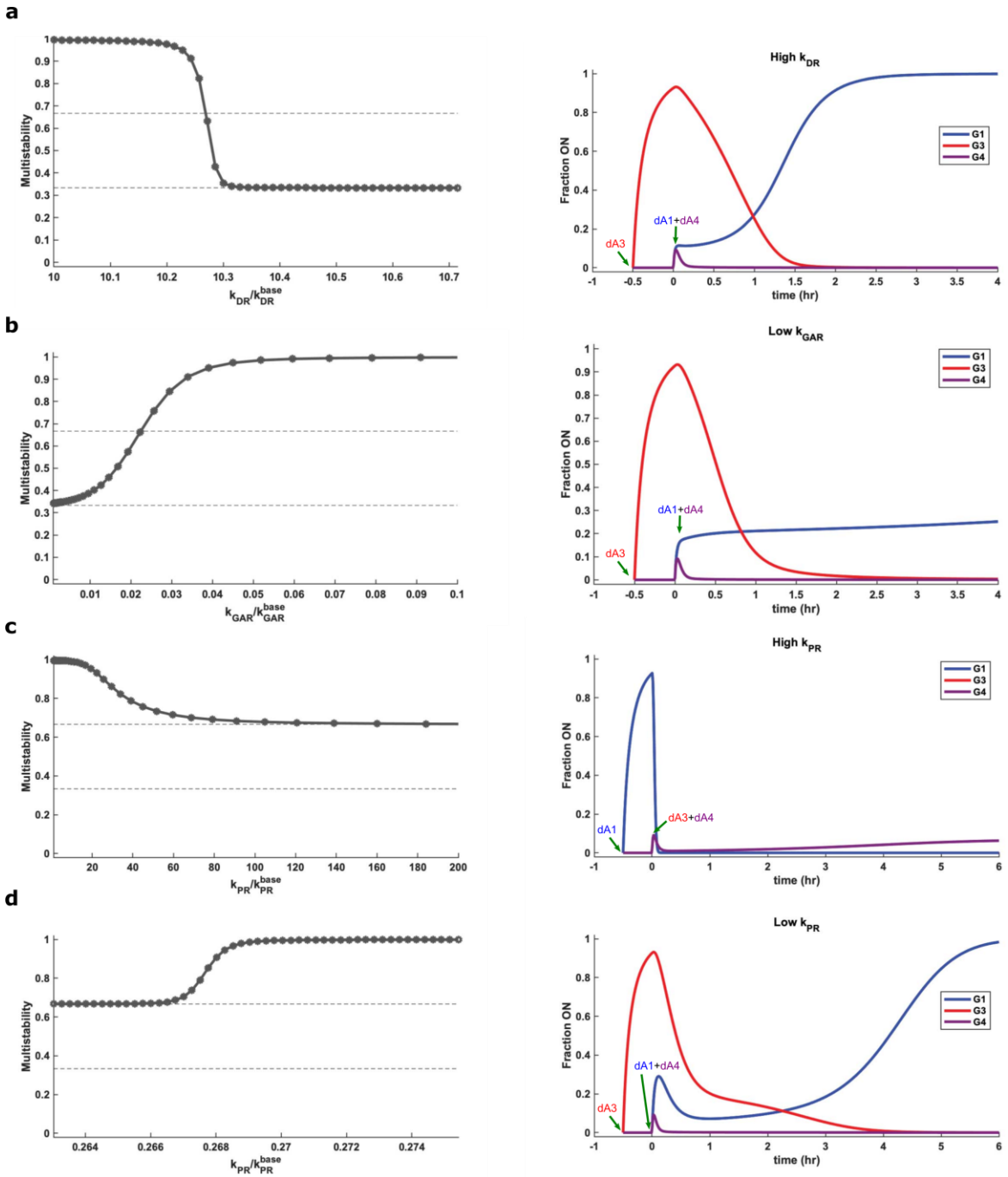

Supplementary Figure 47 | Sensitivity of tri-stability to variations in single reaction rate constants. **a**, Large values for G1's repressor degradation rate destabilizes the other stable states in the system. (Left) Multi-stability drops to ~1/3 (*i.e.* two stable states are lost) when the repressor degradation rate is increased by more than ~10.3x. (Right) Simulation trajectory shows the failure mode. For small values of the degradation rate, even when the TSN is initialized with G3 ON, G1 overtakes the initial condition at long times due to the increased steady state value of its associated activator. **b**, Small values for the repression rate constant of G1 results in a loss of multi-stability (left). When initialized with G3 ON, the low repression rate of G1 prevents G3 from keeping G1 OFF (right). **c**,**d**, Small and large repressor production rates lead to loss of stable state. Multi-stability plots for high (c, left) and low (d, left) production rate constants for the repressor of G1 produced by G3. At large repressor production rates, the initial accumulation of G1 ON is insufficient to overcome the strength of the suppression from G3 (c, right). For small values, G3 is unable to effectively suppress G1 when the system is initialized with G3 ON (d, right). Simulations were otherwise conducted as described in Supplementary Figure 46.

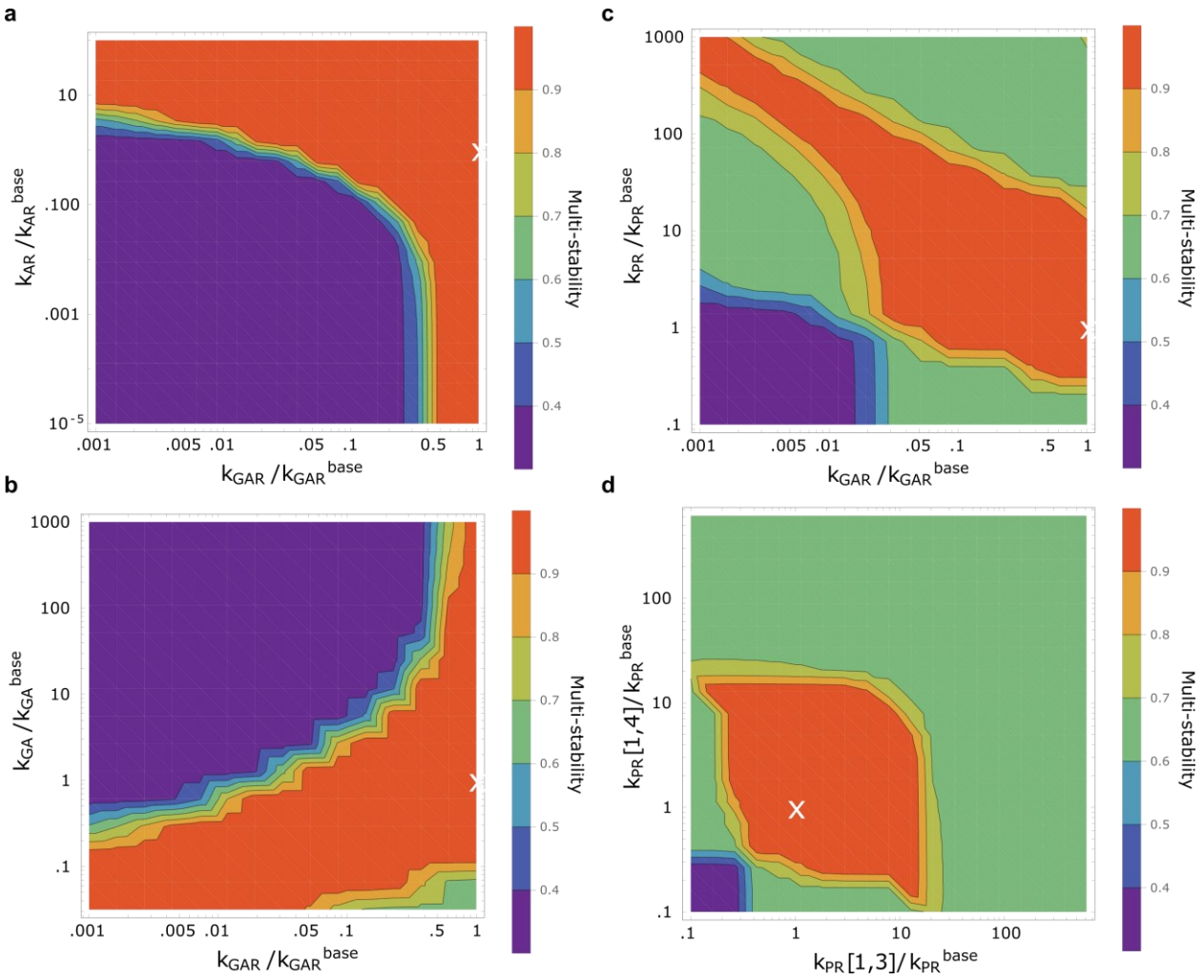

Supplementary Figure 48 | Contour plots for multi-stability computed over a grid of reaction rate constant values for the surrounding the assumed values of the general genelet model (indicated by the white "x"). **a**, Multi-stability phase space for variations in k_{AR} and k_{GAR} for one node in the tri-stable network. **b**, Multi-stability phase space for variations in k_{GA} and k_{GAR} for one node in the tri-stable network. **c**, Multi-stability phase space for variations in k_{PR} and k_{GAR} for one node in the tri-stable network. **d**, Multi-stability phase space for variations in k_{PR} for two nodes producing the repressor of the third node in the tri-stable network. Red regions indicate three stable states, green regions indicate only two stable states (loss of one state), blue regions indicate only one stable state (loss of two states). Simulations were otherwise conducted as described in Supplementary Figure 46.

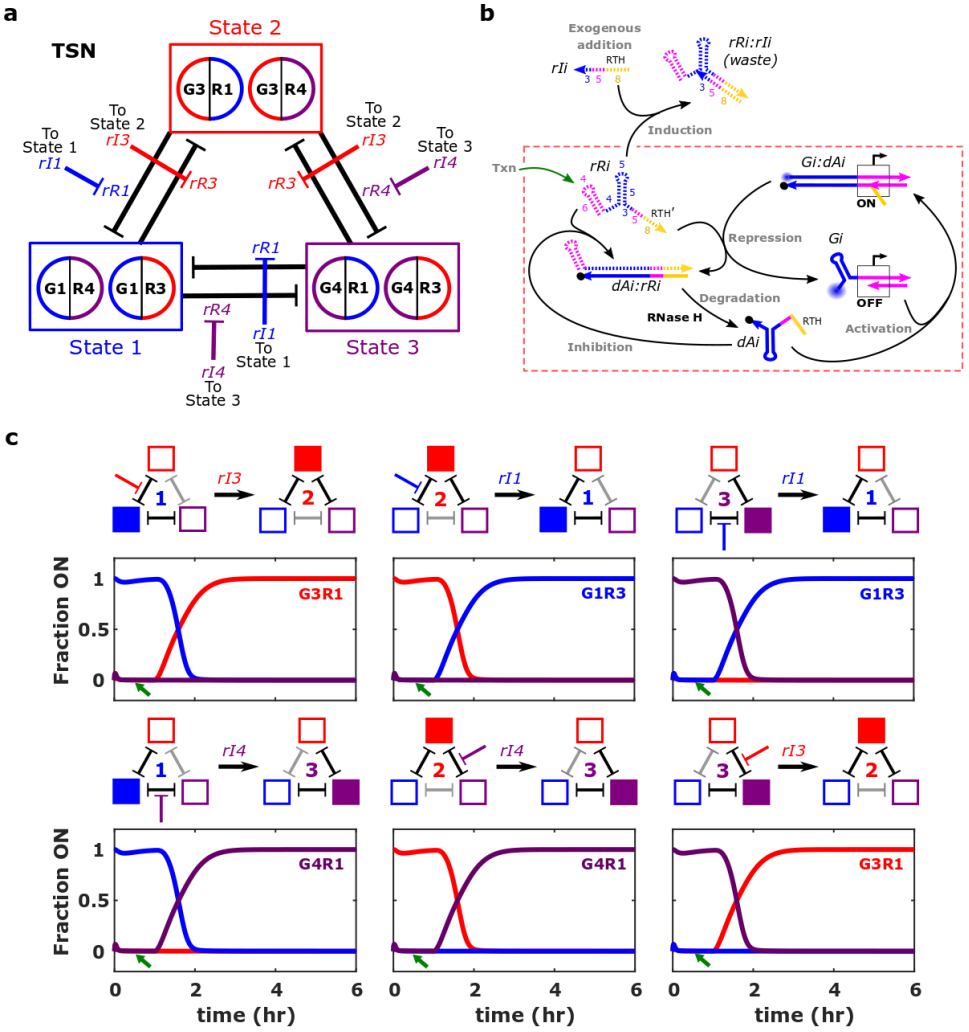

Supplementary Figure 49 | Analysis of state changes with inducer RNAs. (**a**) Schematic of the TSN showing the three inducer RNAs for changing states. (**b**) Schematic of the induction reactions used to change states in the TSN. Reactions in the red box depict the genelet reactions in the absence of an inducer RNA. Once the inducer RNA is added, it removes rRi from the reaction, allowing dAi to be freed by degradation to activate the target genelets. (**c**) Kinetic simulations of all six possible state changes of the TSN *via* the addition of the inducer RNAs that sequester the RNA repressors. The inducer RNAs were introduced into the simulations after 30 minutes in the initial state (green arrows) to a final concentration of 10 µM. Simulations were otherwise conducted as described in Supplementary Figure 46.

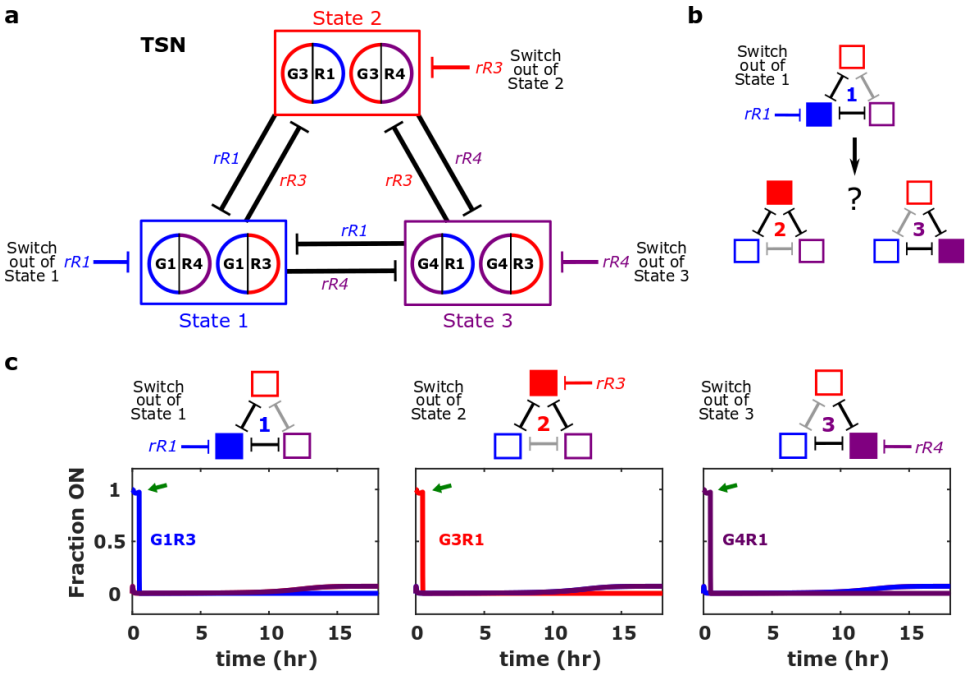

Supplementary Figure 50 | Simulations of attempted state changes *via* repression of the network nodes ON in the initial state. (**a**) Schematic of the TSN with additional repressor interactions indicating RNA repressors that could be exogenously added to the system to potentially change states. (**b**) Schematic of an attempted state change out of State 1. Repression of the State 1 nodes does not tell the system which state to switch into. (**c**) Kinetic simulations of attempted state changes out of State 1, 2, and 3 *via* the addition of rR1, rR3, and rR4, respectively. The RNA repressors were introduced into the simulations after 30 minutes in the initial state (green arrows) to a final concentration of 10 μM. Simulations were otherwise conducted as described in Supplementary Figure 46.

9.4 Additional TSN experiments

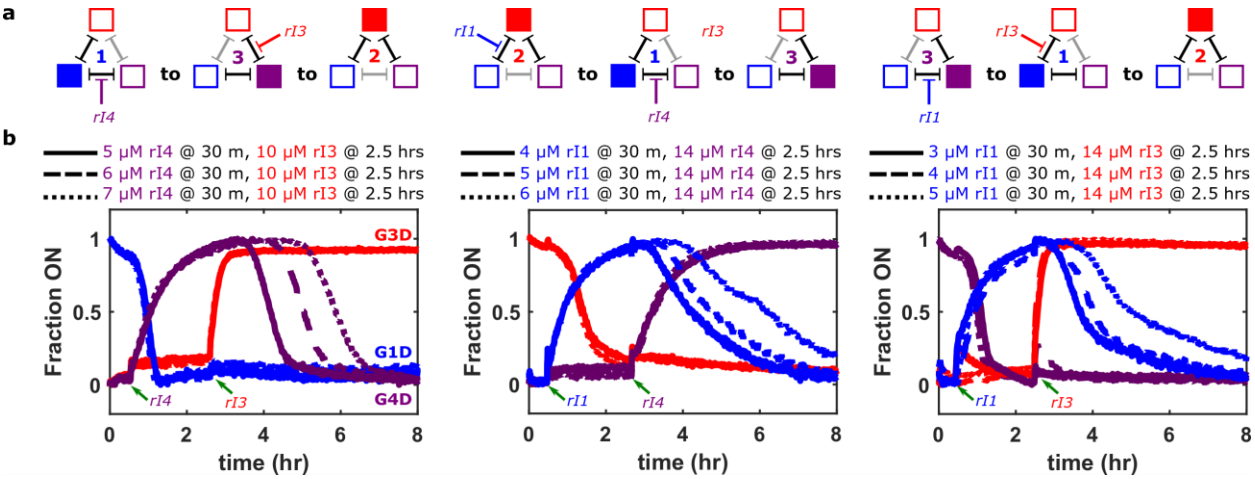

Supplementary Figure 51 | The timing of the second state change depends on the concentration of the inducer RNA used to orchestrate the first state change. (**a**) Schematics of the double state changes executed for the results in (b). (**b**) Normalized activation levels of network reporting nodes during the state changes depicted in (a). The concentrations and times of addition of each inducer RNA are depicted above the plot. Reactions otherwise conducted as described in Supplementary Section 9.2. The higher the concentration of inducer RNA used to induce the first state change, the longer the delay before the network switches states after the addition of the second inducer RNA. The delay is the result of excess inducer RNA left over from the first state change blocking the repression of new state after the second inducer RNA is added. All of the excess inducer RNA from the first state change must be removed before the second state change can begin.

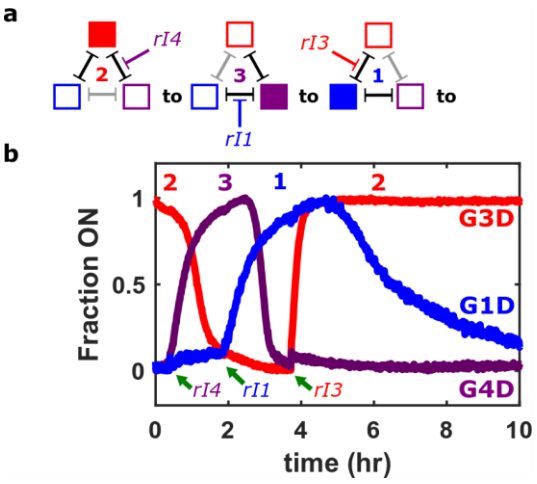

Supplementary Figure 52 | A triple state change. (**a**) The mechanism for switching the TSN from State 2 to State 3 to State 1 and back to State 2. (**b**) Normalized activation levels of network reporting nodes during the state changes depicted in (a). rI4, rI1, and rI3 were added at the times indicated by the green arrows in the plot to final concentrations of 4 μM, 7 μM, and 14 μM, respectively. Reactions otherwise conducted as described in Supplementary Section 9.2.

10. Design and characterization of the BS_IFFL1|2, I_ BS_IFFL1|2, and I_BS_IFFL1|2_FB1 networks

10.1 Design of the BS_IFFL1|2

To build the BS_IFFL1|2, we combined the IFFL1 and IFFL2 and created a new bistable switch module (BSM4). To build the BSM4, we selected two additional input domains (G7 and G8) that exhibited fast transcriptional repression kinetics from the standardized domains we identified in Supplementary Section 4.3. As with the TSN (Supplementary Section 9.1), only repression reactions are present in the BSM4 so no DNA blockers were necessary and HPC5o genelets which lack the 5' blocking toehold (BTH) were used (Supplementary Figure 1). The sequences and nodes that do not have BTH domains are denoted with a * below. The sequences of the IFFL1 and IFFL2 from Supplementary Tables 12 and 13 were used in the BS_IFFL1|2 experiments in addition to the sequences presented below in Supplementary Table 21. From the IFFL1 network, dB3-2omR was used in IFFL1 of this network. The inducer RNAs for changing the states of the BSM4 were designed using the same principles as of the inducer RNAs used to change states in the TSN. Sequence schematics of the inducer RNAs are presented in Supplementary Figure 53. Before assembling the full BS_IFFL1|2, we confirmed that the G7 and G8 bi-stable module exhibited bi-stability and could be induced to switch states (Supplementary Figure 54).

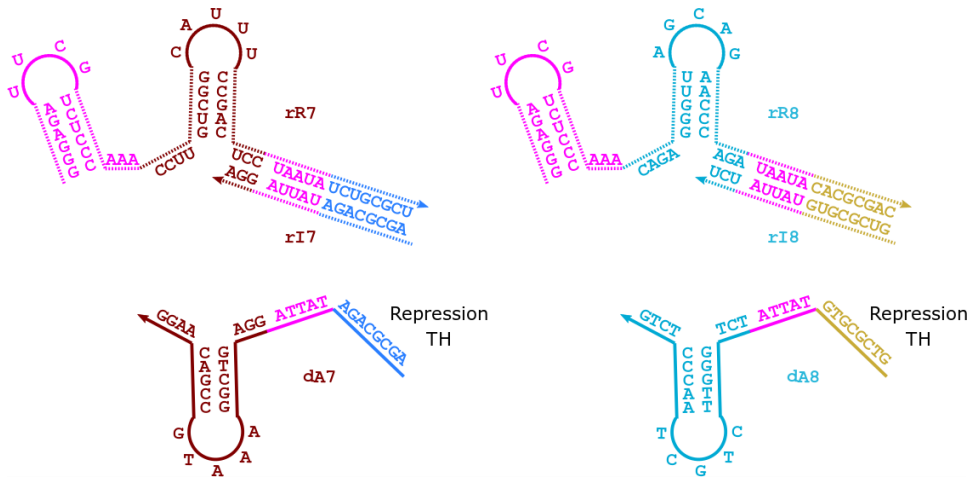

Supplementary Figure 53 | Sequence schematics of the RNA repressors from the bi-stable module (BSM4) of the BS_IFFL1|2 bound to their inducer RNAs (top). A bound inducer RNA prevents a repressor from binding the repression toehold of its target activator (bottom).

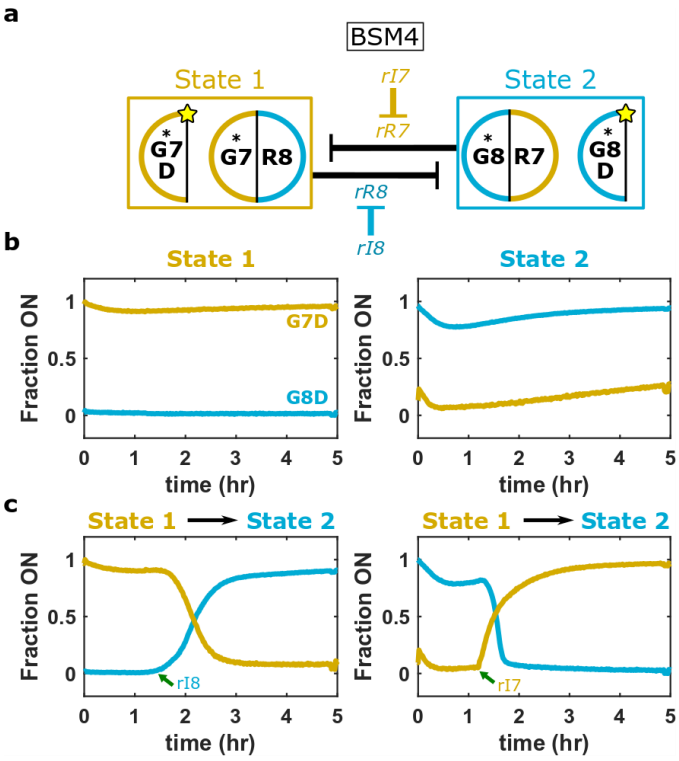

Supplementary Figure 54 |The bi-stable module (BSM4) of the BS_IFFL1|2 works as designed in isolation. (**a**) Schematic of the bi-stable module. (**b**) Normalized activation levels of reporting nodes after initialization in either State 1 or State 2. (**c**) Normalized activation levels of reporting nodes during state changes from State 1 to State 2 (left) or State 2 to State 1 (right). Inducer RNAs were added at the times indicated by the green arrows in the plots to final concentrations of 10 µM. Experiments otherwise conducted as described in Supplementary Section 10.2 using components 1-6 in Supplementary Table 22 with the exception that *G7R8 was at 50 nM. YIPP = 1.35 x 10^{-3} U/µL, RNase H = 8.89 x 10^{-3} U/µL, T7 RNAP = 3.57 U/µL. Sequences in Supplementary Table 21.

Supplementary Table 21 | DNA and RNA oligonucleotides synthesized for the BS_IFFL1|2. Non-template and template strands of genelets are labeled with -nt and -t, respectively. All strands were ordered from Integrated DNA Technologies, Inc (IDT) and the modifications marked with / / are labeled as defined by IDT. * denotes the HPC5o genelet design where the BTH at the 5' end of the input domain was removed. The RNAs were ordered unpurified. All other activators, blockers, template and dummy genelet strands are presented in Supplementary Table 1.

GENELETS	
*G7R8-nt	5'CCTTGTCGGCATTTCCGACTCCTAATACGACTCACTATA GGGAGATTCGTCTCCCAAACAGAGGGTTAGCAGAACCCAGATAATACACGC
*G8R7-nt	5'CAGAGGGTTAGCAGAACCCAGATAATACGACTCACTATA GGGAGATTCGTCTCCCAAACCTTGTCGGCATTTCCGACTCCTAATATCTGC
*G7C2-nt	5'CCTTGTCGGCATTTCCGACTCCTAATACGACTCACTATA GGGAGATTCGTCTCCCAAAGCCAAGATTAAGGTCAATAAGTGACCAAGCGTACACC
*G8C5-nt	5'CAGAGGGTTAGCAGAACCCAGATAATACGACTCACTATA GGGAGATTCGTCTCCCATCTCTTACCCACGCTCGTCCTCCGAGCCTCCACACT
G2C1-nt	5'AGCCAAGATTCAGGTCAATAAGTGACCAAGTAATACGACTCACTATA GGGAGATTCGTCTCCCAAATCCTTCCATGAACGCCAAACCGTGGCGACG
G3R1-nt	5'GAAGATGAAGGTGTACCGTATAGGTACTAGTAATACGACTCACTATA GGGAGATTCGTCTCCCATGCACGCCAAACCGTGGCGACGTAAT
INDUCER RNAS	
rI7	5'rArGrCrGrCrArGrArUrArUrUrArGrGrA
rI8	5'rGrUrCrGrCrGrUrGrUrArUrUrArUrCrU
RNA REPRESSORS	
dR7	5'rCrCrUrUrGrUrCrGrGrCrArUrUrUrCrCrGrArCrUrCrCrUrArArUrArUrCrUrGrCrGrCrU
dR8	5'rCrArGrArGrGrGrUrUrArGrCrArGrArArCrCrCrArGrArUrArArUrArCrArCrGrCrGrArC

10.2 Design of the I_BS_IFFL1|2 and I_BS_IFFL1|2_FB1 networks

To design the I_BS_IFFL1|2 and the I_BS_IFFL1|2_FB1 networks, we first selected two additional input domains (G9 and G10) that exhibited fast transcriptional coactivation kinetics from the library of standardized domains we identified in Supplementary Section 4.3 to create the induction module. The specific networks we were building only required transcriptional coactivation for the induction module nodes, so we selected nodes that met this criterion. Since the RNAs that switch the state of the bistable switch in the BS_IFFL1|2 (rI7 and rI8) were added directly to the solution containing the network, rather than being transcribed during the reaction, we used inducers without 5PSHP domains (Supplementary Section 1). The G9I8 and G10I7 nodes did include the 5PSHP domain at the 5' ends of the rI7 and rI8 transcripts. The additional non-template and template genelet sequences required for the I_BS_IFFL1|2 and the I_BS_IFFL1|2_FB1 networks are in Supplementary Table 22.

Supplementary Table 22 | DNA oligonucleotides synthesized for the I_BS_IFFL1|2 and I_BS_IFFL1|2_FB1 networks. Non-template and template strands of genelets are labeled with -nt and -t, respectively. All strands were ordered from Integrated DNA Technologies, Inc (IDT) and the modifications marked with / / are labeled as defined by IDT. All other activators, blockers, template and dummy genelet strands are presented in Supplementary Table 1.

GENELETS	
G9I8-nt	5'CCAACTACCTATGACTGTAACCCAGTCTCTTAATACGACTCACTATA GGGAGATTCGTCTCCCAGTCGCGTGTATTATCT
I8-t	5'AGATAATACACGCGACTGGGAGACGAATCTCCCTATAGTGAGTCG
G10I7-nt	5'GATAAATAGAGAGCCGCACAGAGCGGCAGATAATACGACTCACTATA GGGAGATTCGTCTCCCAAGCGCAGATATTAGGA
I7-t	5'TCCTAATATCTGCGCTTGGGAGACGAATCTCCCTATAGTGAGTCG
G1C9-nt	5'TCCTTCCATGCACGCCAAACCGTGGCGACGTAATACGACTCACTATA GGGAGATTCGTCTCCCAACCAACTACCTCTGACTGTAACCCAGTCTCTCGCCC

10.3 BS_IFFL1|2, I_ BS_IFFL1|2, and I_BS_IFFL1|2_FB1 experimental methods

Samples were prepared by mixing all but the last five components in Supplementary Tables 23 and 24 to the desired final concentrations. For experiments that began with a network initially in State 1, dA7 was added and for experiments that began with a network initially in State 2, dA8 was added. The samples were then placed in the qPCR and incubated at 37°C for 15 to 30 minutes to allow dA7 or dA8 to bind to their target genelets. Then the transcription mix components (YIPP, RNase H, T7 RNAP) were added along with pre-annealed dAi:rRi complexes to start the experiment. For experiments that began with the network initially in State 1, a pre-annealed dA8:rR8 complex was added alongside the experiments; for experiments that began with a network in State 2, a pre-annealed dA7:dR7 complex was added alongside the enzymes. The dA7:rR7 and dA8:rR8 were prepared by annealing the DNA activators with 50% excess of their corresponding RNA repressors 90°C to 20°C at -1°C/min. The concentrations of the components used in the experiments are presented in Supplementary Tables 23 and 24.

For all experiments, a reference well was also included for the fluorescently labeled nodes in the IFFL1 and IFFL2 (G1S1 and G4S1, respectively). Each reference well contained G1S1 or G4S1 initially in a blocked state without any enzymes and at the start of the experiment the DNA coactivator for each node was added to the reference well to obtain the minimum value for normalization (Supplementary Section 13.4).

Supplementary Table 23 | Concentrations of the components used in the BS_IFFL1|2 experiments. Unless otherwise stated, all BS_IFFL1|2 experiments were conducted with these component concentrations.

Component #	Component	Concentration
1	*G7R8	25 nM
2	*G8R7	50 nM
3	*G7D	25 nM
4	*G8D	25 nM
5	*G7C2	15 nM
6	*G8C5	25 nM
7	G2C1	15 nM
8	G2C3	5 nM
9	G3R1	25 nM
10	G1S1	25 nM
11	dA1	250 nM
12	dA2	250 nM
13	dA3	250 nM
14	dB1	250 nM
15	dB2	200 nM
16	dB3-2omR	50 nM
17	G5C4	25 nM
18	G5C6	5 nM
19	G6R4	25 nM
20	G4S1	25 nM
21	dA4	250 nM
22	dA5	250 nM
23	dA6	250 nM
24	dB4	150 nM
25	dB5	150 nM
26	dB6	150 nM
27	dA7 (or dA7:rR7)	150 nM
28	dA8 (or dA8:rR8)	250 nM
29	YIPP	1.35×10^{-3} U/µL
30	RNase H	3.57×10^{-2} U/µL
31	T7 RNAP	7.14 U/µL

Supplementary Table 24 | Concentrations of the components used in the I_BS_IFFL1|2 and the **I_BS_IFFL1|2_FB1** experiments. The components in bold **red** text were only added for the I_BS_IFFL1|2_FB1 experiments. Unless otherwise stated, all experiments were conducted with these component concentrations.

Component #	Component	Concentration
1	G9I8	175 nM
2	G10I7	175 nM
3	**dA9**	**750 nM**
4	**dB9-2omR**	**0 nM**
5	*G7R8	25 nM
6	*G8R7	50 nM
7	*G7D	25 nM
8	*G8D	25 nM
9	*G7C2	15 nM
10	*G8C5	25 nM
11	G2C1	15 nM
12	G2C3	5 nM
13	G3R1	25 nM
14	G1S1	25 nM
15	**G1C9**	**50 nM**
16	dA1	250 nM
17	dA2	250 nM
18	dA3	250 nM
19	dB1	250 nM
20	dB2	200 nM
21	dB3-2omR	50 nM
22	G5C4	25 nM
23	G5C6	5 nM
24	G6R4	25 nM
25	G4S1	25 nM
26	dA4	250 nM
27	dA5	250 nM
28	dA6	250 nM
29	dB4	150 nM
30	dB5	150 nM
31	dB6	150 nM
32	dA7 (or dA7:rR7)	150 nM
33	dA8 (or dA8:rR8)	250 nM
34	YIPP	1.35×10^{-3} U/µL
35	RNase H	5.36×10^{-2} U/µL
36	T7 RNAP	9.14 U/µL

10.4 Additional I_ BS_IFFL1|2 and I_BS_IFFL1|2_FB1 experiments and simulations

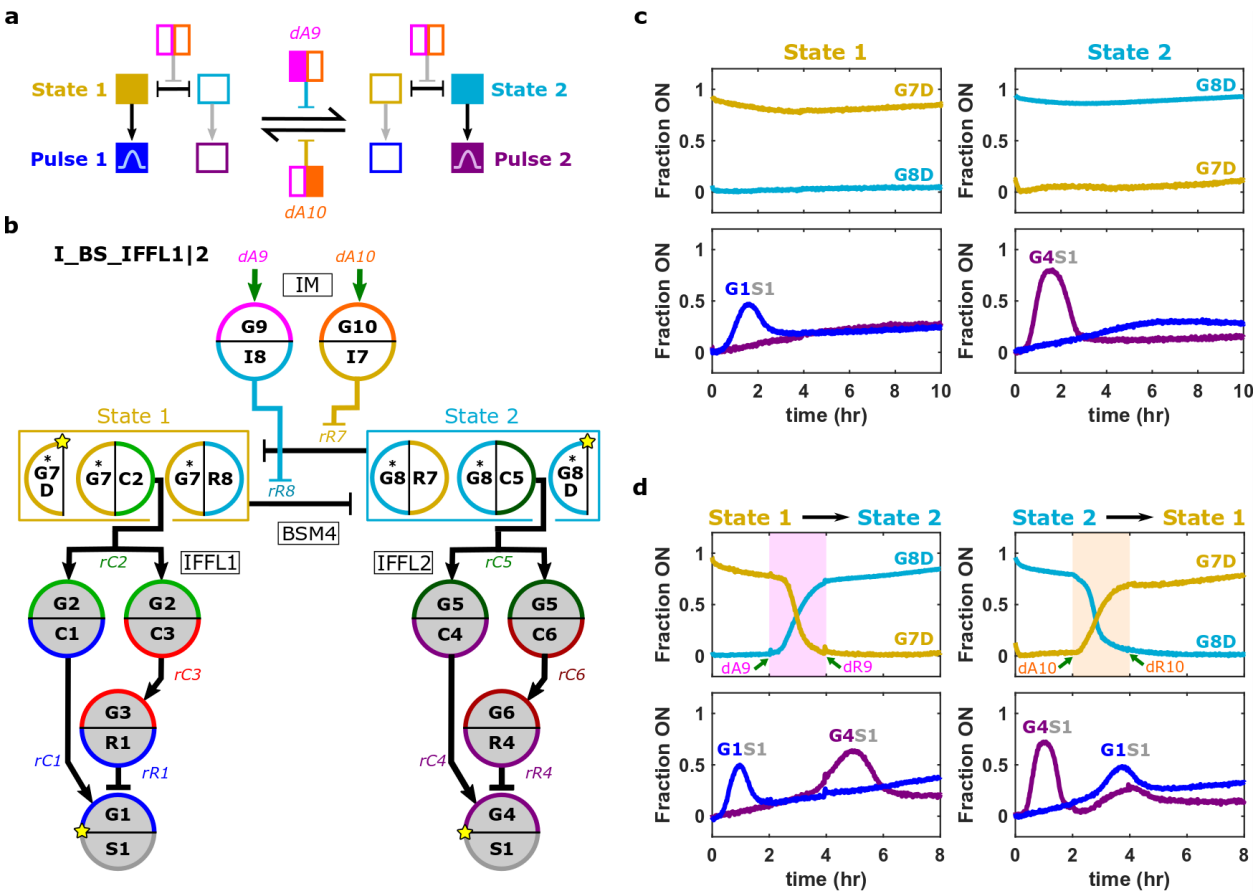

Supplementary Figure 55 | The BS_IFFL1|2 with an induction module for triggering state changes. (**a**) Schematic of the desired network behavior where unique pulses can be triggered based on the state of the network and state changes can be triggered by turning upstream nodes on/off. (**b**) The I_BS_IFFL1|2 network architecture where the BS_IFFL1|2 network is connected to an upstream induction module (IM) comprised of nodes that transcribe the inducer RNAs required to change states. * denotes nodes for which no DNA blockers were present and HPC5P genelets that did not possess the BTH domain were used. (**c**) Normalized activation levels of reporting nodes for the I_BS_IFFL1|2 network initialized in either initial state. (**d**) Normalized activation levels of reporting nodes during state changes of the I_BS_IFFL1_2 from either initial state via activation of G9I8 (left) or G10I7 (right). The shaded regions in the top plots indicate when the respective induction module nodes were ON during the experiments. The DNA activators and DNA repressors were added at the times indicated by the green arrows in the top plots to final concentrations of 0.75 µM and 1.5 µM, respectively. The I_BS_IFFL1|2 network design notes and sequences are in Supplementary Section 10.2. Experiments were conducted as described in Supplementary Section 10.3 except T7 RNAP was at 7.14 U/µL for the experiments in (c).

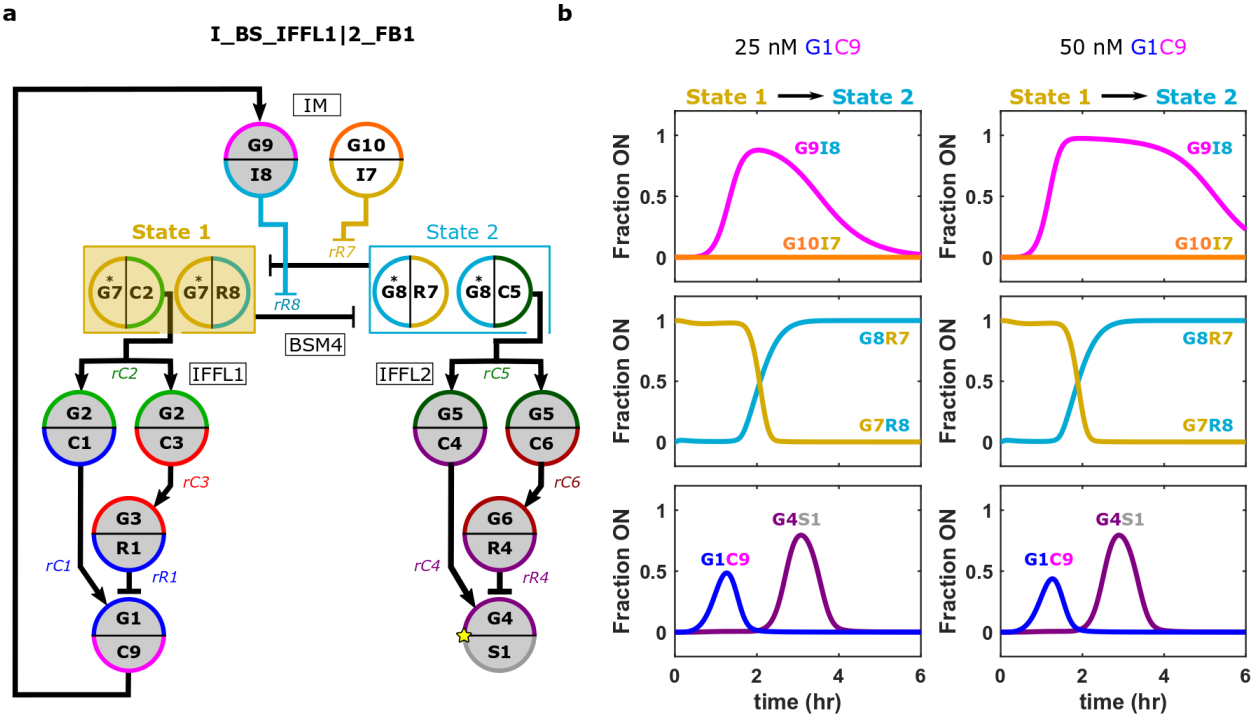

Supplementary Figure 56 | Simulations of the I_BS_IFFL1|2_FB1 network. (**a**) The I_BS_IFFL1|2_FB1 network used in the simulation. (**b**) Simulated normalized activation levels of network nodes after initialization of the I_BS_IFFL1|2_FB1 network in State 1. The pulse in G1C9 (bottom plot) triggers a pulse in the activation of G9I8 (top plot) which triggers the BSM4 to switch to State 2. Note that G9I8 eventually resets which would allow this network to be switched back to State 1 to orchestrate the same program again. Simulations were conducted as described in Supplementary Section 5 using the concentrations of species presented in Supplementary Table 24.

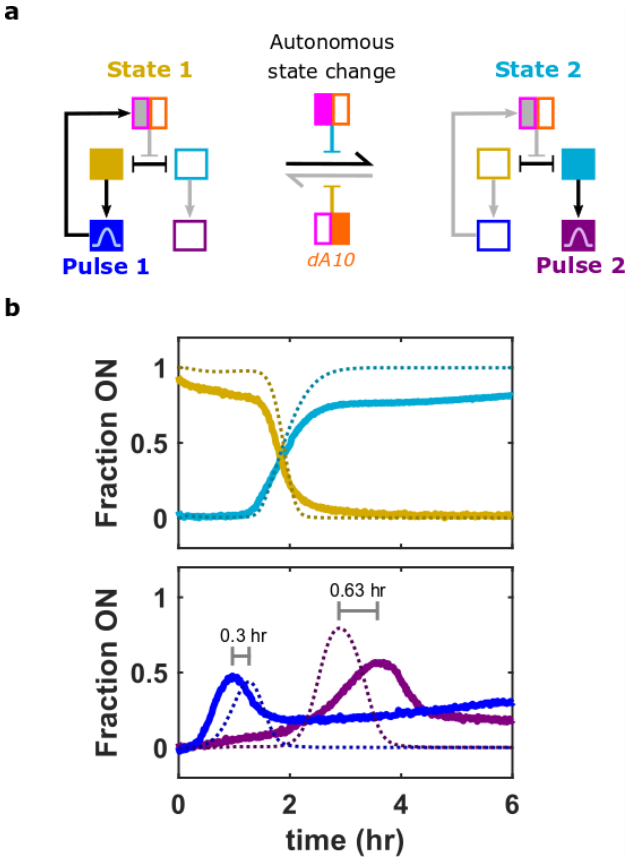

Supplementary Figure 57 | Comparison of the I_BS_IFFL1|2_FB1 network dynamics in simulation and in experiments. (**a**) Schematic of the desired I_BS_IFFL1|2_FB1 network behavior. (**b**) Normalized activation levels of network nodes in simulations (dashed lines) or in experiments (solid lines) after initialization of the I_BS_IFFL1|2_FB1 network in State 1. The timing of the autonomous state change (top plot) is nearly identical in simulation and in experiment. The time the max IFFL1 and IFFL2 outputs reach max height differs by less than an hour in simulation and in experiment (bottom plot). Simulations were conducted as described in Supplementary Section 5 using the concentrations of species presented in Supplementary Table 24.

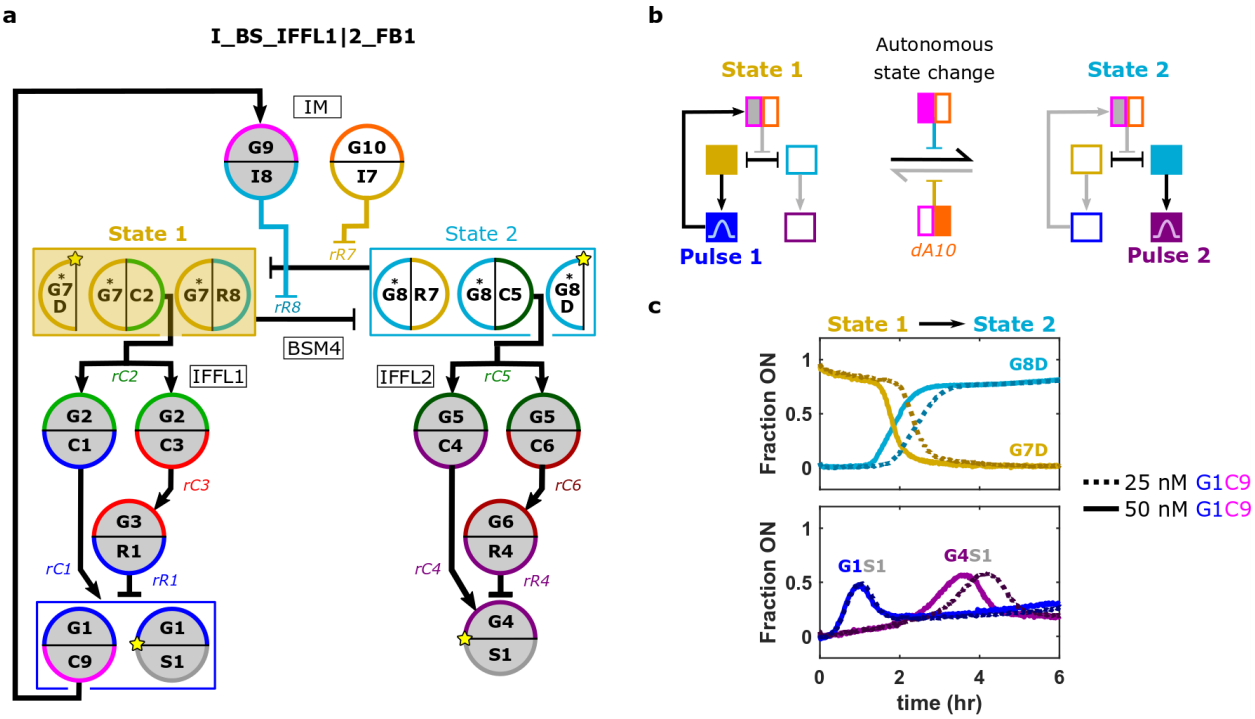

Supplementary Figure 58 | Tuning the timing of state changes in the I_BS_IFFL1|2_FB1. (**a**) The I_BS_IFFL1|2_FB1 network. * denotes nodes for which no DNA blockers were present and HPC5P genelets that did not possess the BTH domain were used. (**b**) Schematic of the desired network behavior. (**c**) Normalized activation levels of reporting nodes for the I_BS_IFFL1|2_FB1 network initialized in State 1 with 50 nM (solid lines) or 25 nM (dashed lines) of the G1C9 genelet. Decreasing the concentration of G1C9 increases the time spent in State 1 (top plot) and delays the IFFL2 pulse relative to the IFFL1 pulse. The I_BS_IFFL1|2_FB1 network design notes and sequences are in Supplementary Section 10.2. Experiments were otherwise conducted as described in Supplementary Section 10.3.

11. A second round of screening identifies more standardized nodes for network engineering

11.1 Screening results

In Supplementary Section 4 we developed a two-stage screening protocol for identifying standardized genelet input domains for network assembly. In the initial round of screening we tested a total of 37 potential sequences and identified 11 standardized sequences that we used to build a variety of regulatory networks. Given the success of our first round of screening we wanted to investigate whether we could use the same screening protocol to find more standardized sequences.

To conduct a second round of screening, we used the same NUPACK design protocol described in Supplementary Section 4.1 to design 24 new genelet sequences. In addition to being designed to have minimal crosstalk among themselves, the new sequences were also designed to have minimal crosstalk with the 11 standardized node sequences presented in Supplementary Table 1.

We next evaluated the DNA activation kinetics of the 24 new genelet sequences using the high-throughput screening assay described in Supplementary Section 4.2 and Supplementary Figure 14. Of the 24 genelet:activator pairs, we found 13 that activated to 90% in less than an hour. We then screened nine of these genelet sequences for their transcriptional coactivation and repression kinetics using the high-throughput assay described in Supplementary Section 4.3 and Supplementary Figure 19. Despite all nine nodes exhibiting fast coactivation and repression kinetics when DNA coactivators / repressors were used, only one node exhibited both fast transcriptional coactivation and repression and another five nodes exhibited fast transcriptional coactivation but slow or incomplete transcriptional repression (Supplementary Figure 59).

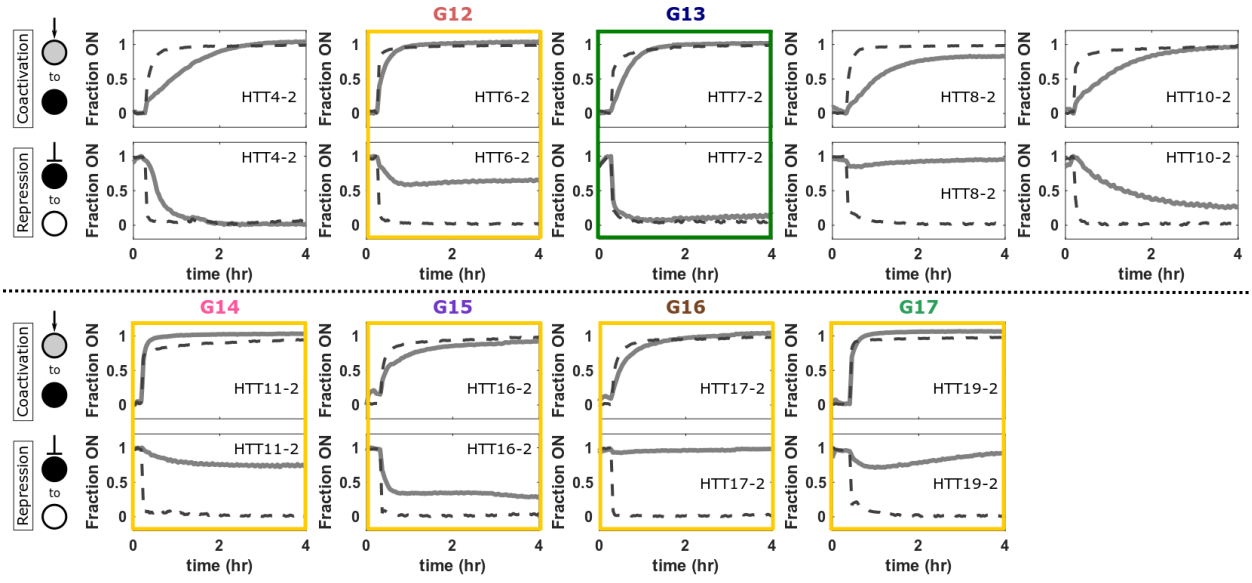

Supplementary Figure 59 | Results from a second round of transcriptional coactivation and repression screening. Plots show the normalized node activation levels during transcriptional coactivation and repression (solid lines). Dashed lines represent control experiments where DNA coactivators or repressors (-nt strands from Supplementary Table 24) were added to samples in the absence of enzymes. DNA coactivators and repressors were added to a final concentration of 500 nM and 1000 nM, respectively. Reactions were conducted under the conditions described in the Methods of the main text with DNA activator complexes at 250 nM, genelet complexes at 25 nM, and transcription templates at 25 nM, and [RNase H] = 3.57 x 10^{-2} U/µL, [YIPP] = 1.35 x 10^{-3} U/µL, [T7 RNAP] = 3.57 U/µL. Experiments were otherwise conducted as described for Supplementary Figure 19. Sequences are in Supplementary Table 25.

Supplementary Table 25 | Sequences of the strands used for the second round of HTT transcriptional coactivation and repression screening (Supplementary Figure 59). The At quencher strand was ordered HPLC purified and all other strands were ordered unpurified from IDT.

GENELETS	
Gt HTT4-2	/56-FAM/ TGCAAGCCCAGTACGGTCTTGACGACCGGTGTAATA CGACTCACTATAGGGAGA
Gt HTT6-2	/56-FAM/ TGCCCTCGACAATCCAAGCAACTCTTGGTACTAATA CGACTCACTATAGGGAGA
Gt HTT7-2	/56-FAM/ TGTCCATATCTAGACCGTCTGACACGGTGCGTAATA CGACTCACTATAGGGAGA
Gt HTT8-2	/56-FAM/ TGTCGTCAGCTTCATCCAGATGGGATGTCGTAATA CGACTCACTATAGGGAGA
Gt HTT10-2	/56-FAM/ TGGTAAAGCGAGTACTGGTTCATCCAGTCCCTAATA CGACTCACTATAGGGAGA
Gt HTT11-2	/56-FAM/ TGGATAGTATGGAGTAAGGCATTCTTACCGGTAATA CGACTCACTATAGGGAGA
Gt HTT16-2	/56-FAM/ CATGCTTAGATTCACAAGACCATTGTGACGTAATA CGACTCACTATAGGGAGA
Gt HTT17-2	/56-FAM/ CATGCCTAACCTGTTCCGATTTGGAACCTCTAATA CGACTCACTATAGGGAGA
Gt HTT19-2	/56-FAM/ TGGACGCACGCAAAGCTATCGGATAGCTATCTAATA CGACTCACTATAGGGAGA
universal-t	5'TCTCCCTATAGTGAGTCG
ACTIVATORS	
At HTT4-2	5'TGTACACCTATTACACCGGTCGTCAAGACCGTACT ACACCACCAAACTTCATCTCA
At HTT6-2	5'TTATCGAGTATTAGTACCAAGAGTTGCTTGGATTG ACACCACCAAACTTCATCTCA
At HTT7-2	5'TCTCCGGCTATTACGCACCGTGTCAGACGGTCTAG ACACCACCAAACTTCATCTCA
At HTT8-2	5'TTCTAGTCTATTACGACATCCCATCTGGATGAAGC ACACCACCAAACTTCATCTCA
At HTT10-2	5'AAAGTTTCTATTAGGGACTGGATGAACCAGTACTC ACACCACCAAACTTCATCTCA
At HTT11-2	5'TAGGGATCTATTACCGGTAAGAATGCCTTACTCCA ACACCACCAAACTTCATCTCA
At HTT16-2	5'CTCTCGTGTATTACGTCACAATGGTCTTGTGAATC ACACCACCAAACTTCATCTCA
At HTT17-2	5'CGTGCTAGTATTAGAGGTTCCAAATCGGAACAGGT ACACCACCAAACTTCATCTCA
At HTT19-2	5'AAGCCACCTATTAGATAGCTATCCGATAGCTTTGC ACACCACCAAACTTCATCTCA
At quencher	5'TGAGATGAAGTTTGGTGGTG/3IAbRQSp/
BLOCKERS	
Bt HTT4-6	5'TTCAGAGTCACCGGTCGTCAAGACCGTACTGGGCTTGC
Bt HTT6-2	5'CATCCACCGTACCAAGAGTTGCTTGGATTGTCGAGGGC
Bt HTT7-2	5'AAGAGCTCCGCACCGTGTCAGACGGTCTAGATATGGAC
Bt HTT8-9	5'CAACTGCTCGACATCCCATCTGGATGAAGCTGACGACA
Bt HTT10-2	5'CACATCATGGGACTGGATGAACCAGTACTCGCTTTACC
Bt HTT11-2	5'AGCGGTTTCCGGTAAGAATGCCTTACTCCATACTATCC
Bt HTT16-2	5'TGATTGCGCGTCACAATGGTCTTGTGAATCTAAGCATG
Bt HTT17-2	5'TTCTGGGCGAGGTTCCAAATCGGAACAGGTTAGGCATG
Bt HTT19-2	5'GGTGCGTTGATAGCTATCCGATAGCTTTGCGTGCGTCC
TRANSCRIPTION TEMPLATES	
C-HTT4-2-nt	5'GGAGA TTGC TCTCCC AAA GCAAGCCCAGGACGGTCTTGACGACCGGTGACTCTGAA
C-HTT4-2-t	5'TTCAGAGTCACCGGTCGTCAAGACCGTCCTGGGCTTGC TTTGGGAGAGCAATCTCCCTATAGTGAGTCGTATTAGAA
R-HTT4-2-nt	5'GGAGA TTGC TCTCCC AAA AGTACGGTCTTGACGACCGGTGTAATAGGTGTACA
R-HTT4-2-t	5'TGTACACCTATTACACCGGTCGTCAAGACCGTACT TTTGGGAGAGCAATCTCCCTATAGTGAGTCGTATTAGAA
C-HTT6-2-nt	5'GGAGA TTGC TCTCCC AAA GCCCTCGACACTCCAAGCAACTCTTGGTACGGTGGATG
C-HTT6-2-t	5'CATCCACCGTACCAAGAGTTGCTTGGAGTGTCGAGGGC TTTGGGAGAGCAATCTCCCTATAGTGAGTCGTATTAGAA
R-HTT6-2-nt	5'GGAGA TTGC TCTCCC AAA CAATCCAAGCAACTCTTGGTACTAATACTCGATAA
R-HTT6-2-t	5'TTATCGAGTATTAGTACCAAGAGTTGCTTGGATTG TTTGGGAGAGCAATCTCCCTATAGTGAGTCGTATTAGAA
C-HTT7-2-nt	5'GGAGA TTGC TCTCCC AAA GTCCATATCTCGACCGTCTGACACGGTGCGGAGCTCTT
C-HTT7-2-t	5'AAGAGCTCCGCACCGTGTCAGACGGTCGAGATATGGAC TTTGGGAGAGCAATCTCCCTATAGTGAGTCGTATTAGAA
R-HTT7-2-nt	5'GGAGA TTGC TCTCCC AAA CTAGACCGTCTGACACGGTGCGTAATAGCCGGAGA
R-HTT7-2-t	5'TCTCCGGCTATTACGCACCGTGTCAGACGGTCTAG TTTGGGAGAGCAATCTCCCTATAGTGAGTCGTATTAGAA
C-HTT8-2-nt	5'GGAGA TTGC TCTCCC AAA TGTCGTCAGCGTCATCCAGATGGGATGTCGAGCAGTTG
C-HTT8-2-t	5'CAACTGCTCGACATCCCATCTGGATGACGCTGACGACA

	TTTGGGAGAGCAATCTCCCTATAGTGAGTCGTATTAGAA
R-HTT8-2-nt	5′GGAGA TTGC TCTCCC AAA GCTTCATCCAGATGGGATGTCGTAATAGACTAGAA
R-HTT8-2-t	5′TTCTAGTCTATTACGACATCCCATCTGGATGAAGC TTTGGGAGAGCAATCTCCCTATAGTGAGTCGTATTAGAA
C-HTT10-2-nt	5′GGAGA TTGC TCTCCC AAA GGTAAAGCGATTACTGGTTCATCCAGTCCCATGATGTG
C-HTT10-2-t	5′CACATCATGGGACTGGATGAACCAGTAATCGCTTTACC TTTGGGAGAGCAATCTCCCTATAGTGAGTCGTATTAGAA
R-HTT10-2-nt	5′GGAGA TTGC TCTCCC AAA GAGTACTGGTTCATCCAGTCCCTAATAGAAACTTT
R-HTT10-2-t	5′AAAGTTTCTATTAGGGACTGGATGAACCAGTACTC TTTGGGAGAGCAATCTCCCTATAGTGAGTCGTATTAGAA
C-HTT11-2-nt	5′GGAGA TTGC TCTCCC AAA GGATAGTATGAAGTAAGGCATTCTTACCGGAAACCGCT
C-HTT11-2-t	5′AGCGGTTTCCGGTAAGAATGCCTTACTTCATACTATCC TTTGGGAGAGCAATCTCCCTATAGTGAGTCGTATTAGAA
R-HTT11-2-nt	5′GGAGA TTGC TCTCCC AAA TGGAGTAAGGCATTCTTACCGGTAATAGATCCCTA
R-HTT11-2-t	5′TAGGGATCTATTACCGGTAAGAATGCCTTACTCCA TTTGGGAGAGCAATCTCCCTATAGTGAGTCGTATTAGAA
C-HTT16-2-nt	5′GGAGA TTGC TCTCCC AAA CATGCTTAGACTCACAAGACCATTGTGACGCGCAATCA
C-HTT16-2-t	5′TGATTGCGCGTCACAATGGTCTTGTGAGTCTAAGCATG TTTGGGAGAGCAATCTCCCTATAGTGAGTCGTATTAGAA
R-HTT16-2-nt	5′GGAGA TTGC TCTCCC AAA GATTCACAAGACCATTGTGACGTAATACACGAGAG
R-HTT16-2-t	5′CTCTCGTGTATTACGTCACAATGGTCTTGTGAATC TTTGGGAGAGCAATCTCCCTATAGTGAGTCGTATTAGAA
C-HTT17-2-nt	5′GGAGA TTGC TCTCCC AAA CATGCCTAACGTGTTCCGATTTGGAACCTCGCCCAGAA
C-HTT17-2-t	5′TTCTGGGCGAGGTTCCAAATCGGAACACGTTAGGCATG TTTGGGAGAGCAATCTCCCTATAGTGAGTCGTATTAGAA
R-HTT17-2-nt	5′GGAGA TTGC TCTCCC AAA ACCTGTTCCGATTTGGAACCTCTAATACTAGCACG
R-HTT17-2-t	5′CGTGCTAGTATTAGAGGTTCCAAATCGGAACAGGT TTTGGGAGAGCAATCTCCCTATAGTGAGTCGTATTAGAA
C-HTT19-2-nt	5′GGAGA TTGC TCTCCC AAA GGACGCACGCTAAGCTATCGGATAGCTATCAACGCACC
C-HTT19-2-t	5′GGTGCGTTGATAGCTATCCGATAGCTTAGCGTGCGTCC TTTGGGAGAGCAATCTCCCTATAGTGAGTCGTATTAGAA
R-HTT19-2-nt	5′GGAGA TTGC TCTCCC AAA GCAAAGCTATCGGATAGCTATCTAATAGGTGGCTT
R-HTT19-2-t	5′AAGCCACCTATTAGATAGCTATCCGATAGCTTTGC TTTGGGAGAGCAATCTCCCTATAGTGAGTCGTATTAGAA
Mod-T7-5p1+	5′TTCTAATACGACTCACTATAG

11.2 Assembling an IFFL4 from the nodes identified in the second round of screening

The six new node sequences identified in this second round of screening could be used to assemble new regulatory networks. To validate that some of these nodes could be reliably used for network construction we designed another feedforward loop (IFFL4) using three of the nodes identified in Supplementary Figure 60. Since G13 exhibited both fast transcriptional coactivation and repression, we selected this input domain for the node that would be pulsed ON and OFF in IFFL4. We then selected G15 and G17 as the other two input domains in the network as they both only needed to be activated in IFFL4 (Supplementary Figure 60). Sequences for the IFFL4 are in Supplementary Table 26. Using the same reaction conditions as those of the IFFL1, IFFL2, and IFFL3 (Supplementary Table 27), we were able to obtain pulses in G13 activation levels for the IFFL4 as designed (Supplementary Figure 60). These results indicate that our genelet sequence screening procedure can be used to identify more standardized genelet sequences for network construction as needed.

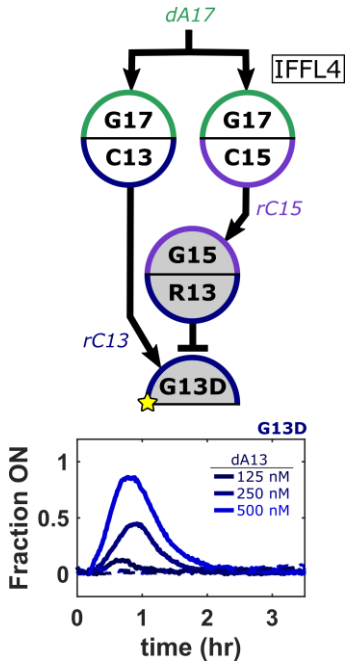

Supplementary Figure 60 | Another IFFL network (IFFL4) constructed from standardized nodes identified in the second round of screening. The plot shows normalized activation levels of G13D during experiments with varying concentrations of dA13. Dashed lines represent controls where dA17 was not added. Reactions were otherwise conducted as described in Supplementary Section 6.2 and the concentrations of all species are presented in Supplementary Table 26.

Supplementary Table 26 | Sequences of the strands used for the IFFL4. Non-template and template strands of genelets are labeled with -nt and -t, respectively. The universal-t strand was the template strand for G13D.

GENELETS	
G13D-nt	/56-Cy5/TGTCCATATCTAGACCGTCTGACACGGTGCGTAATACGACTCACTATAGGGAGA
universal-t	5'TCTCCCTATAGTGAGTCG
G17C13-nt	5'GGACGCACGCAAAGCTATCGGATAGCTATCTAATACGACTCACTATA GGGAGATTGCTCTCCCGTCCATATCTCGACCGTCTGACACGGTGCGGAGCTCT
C13-t	5'AAGAGCTCCGCACCGTGTCAGACGGTCGAGATATGGACGGGAGAGCAATCTCCCTATAGTGAGTCG
G17C15-nt	5'GGACGCACGCAAAGCTATCGGATAGCTATCTAATACGACTCACTATA GGGAGATTGCTCTCCCACATGCTTAGACTCACAAGACCATTGTGACGCGCAAT
C15-t	5'TGATTGCGCGTCACAATGGTCTTGTGAGTCTAAGCATGTGGGAGAGCAATCTCCCTATAGTGAGTCG
G15R13-nt	5'CATGCTTAGATTCACAAGACCATTGTGACGTAATACGACTCACTATA GGGAGATTGCTCTCCCACTAGACCGTCTGACACGGTGCGTAATAGCCGGAGA
R13-t	5'TCTCCGGCTATTACGCACCGTGTCAGACGGTCTAGTGGGAGAGCAATCTCCCTATAGTGAGTCG
ACTIVATORS	
dA13	5'TCTCCGGCTATTACGCACCGTGTCAGACGGTCTAG/3IABkFQ/
dA15	5'CTCTCGTGTATTACGTCACAATGGTCTTGTGAATC
dA17	5'AAGCCACCTATTAGATAGCTATCCGATAGCTTTGC
BLOCKERS	
dB13-2omR	5'AAGAGCTCCGCACCGTGTCAGACGGTmCmUmAmGmAmUmAmUmGmGmAmC
dB15-2omR	5'TGATTGCGCGTCACAATGGTCTTGTGmAmAmUmCmUmAmAmGmCmAmUmG

Supplementary Table 27 | Concentrations of the components used in the IFFL4 experiments. In these experiments, the blockers both had methylated RNA for the last 12 bases at their 3' ends as we found this removed the possibility for autoactivation (Supplementary Section 7).

Component #	Component	Concentration
1	G17C13	25 nM
2	G17C15	5 nM
3	G15R13	25 nM
4	G13	25 nM
5	dA13	250 nM
6	dA15	250 nM
7	dA17	250 nM
8	Added dB13-2omR	0 nM
9	Added dB15-2omR	0 nM
10	YIPP	1.35×10^{-3} U/µL
11	RNase H	8.92×10^{-3} U/µL
12	T7 RNAP	3.57 U/µL

12. Summary of all standardized input/output domain combinations tested

Supplementary Table 28 | All input/output combinations tested. Each input domain and output domain has an associated weight, I(C|R)W and O(C|R)W, respectively. These weights are computed based on the total number of successful combinations in which the input or output domain has been previously used. Each combination that was using in an actual network in the main text was given a weight of 2 and if the combination was only used in the experiments in Supplementary Section 4.5 it was given a weight of 1. All these weights were summed to score each unique input/output domain. Across all experiments, 42/187 (23%) input/output combinations were tested.

RNA coactivators

	C1	C2	C3	C4	C5	C6	C7	C8	C9	C10	C11	ICW
G1	i								g			3
G2	a		a									4
G3	i	i		i	d							5
G4									j	j		2
G5				b		b						4
G6									k			1
G7		f										2
G8					f							2
G9								c		c		4
G10												0
G11					j				j			2
OCW:	4	3	2	3	5	2	NA	2	5	3	NA	

RNA repressors

	R1	R2	R3	R4	R5	R6	R7	R8	R9	R10	R11	IRW	ICRW
G1		h	e	e				h				6	**8**
G2	h		g									2	**6**
G3	e	g		e				h				6	**11**
G4	e		e					h				5	**7**
G5	h											1	**5**
G6				e								2	**3**
G7								f			h	3	**5**
G8	h		h	h			f					5	**7**
G9												0	**4**
G10								c				2	**2**
G11							h					1	**3**
ORW:	7	2	6	7	0	NA	3	7	NA	NA	1		
OCRW:	**11**	**5**	**8**	**10**	**5**	**NA**	**NA**	**9**	**NA**	**NA**	**NA**		

ICW	Gi rC wt
OCW	rCi wt
IRW	Gi rR wt
ORW	rRi wt
ICRW	Gi rC+rR wt
OCRW	rCi+rRi wt

Key	Primary Use
a	IFFL1
b	IFFL2
c	IFFL3
d	IFFL1_2
e	TSN
f	BS_IFFL1|2
g	I_..._FB1
h	Supp Fig 23
i	Supp Fig 24
j	Supp Fig 25
k	Supp Fig 31

13. Normalization of fluorescence data

13.1 Default normalization procedure

For most genelet experiments where OFF genelets were activated *via* the addition of DNA activators or ON genelets were repressed a simple normalization procedure could be applied using the minimum and maximum fluorescence values of the experimental data (Eq. 11). For most reactions involving repression, an excess of the DNA repressor(s) of the node(s) was added at the end of the experiment to ensure a maximum fluorescence value was obtained.

$$(11)\ \text{Fraction ON} = 1 - \frac{\text{data} - \min(\text{data})}{\max(\text{data}) - \min(\text{data})}$$

13.2 Normalization of coactivating genelet data

For experiments where transcriptional genelet coactivation was employed there was no way to internally guarantee a minimum fluorescence value was obtained, especially for IFFL pulse data where the pulsing genelet does not reach full activation before it begins to shut off. Thus, a separate reference well was used to find the minimum fluorescence for normalization (Eq. 12). The reference well contained the isolated node of interest initially in a blocked state without any enzymes (Supplementary Figure 61a), the DNA coactivator of the node of interest was then added to the reference well to obtain the minimum value (Supplementary Figure 61b) and the minimum reference well value was used in the normalization (Eq. 12 and Supplementary Figure 61c). A reference well was used for all genelets that were transcriptionally coactivated in a given experiment even if they were not genelets that were pulsing ON and OFF (for example G3R1 in the IFFL1 and IFFL1_2 networks).

$$(12)\ \text{Fraction ON} = 1 - \frac{\text{data} - \min(\text{ref well})}{\max(\text{data}) - \min(\text{ref well})}$$

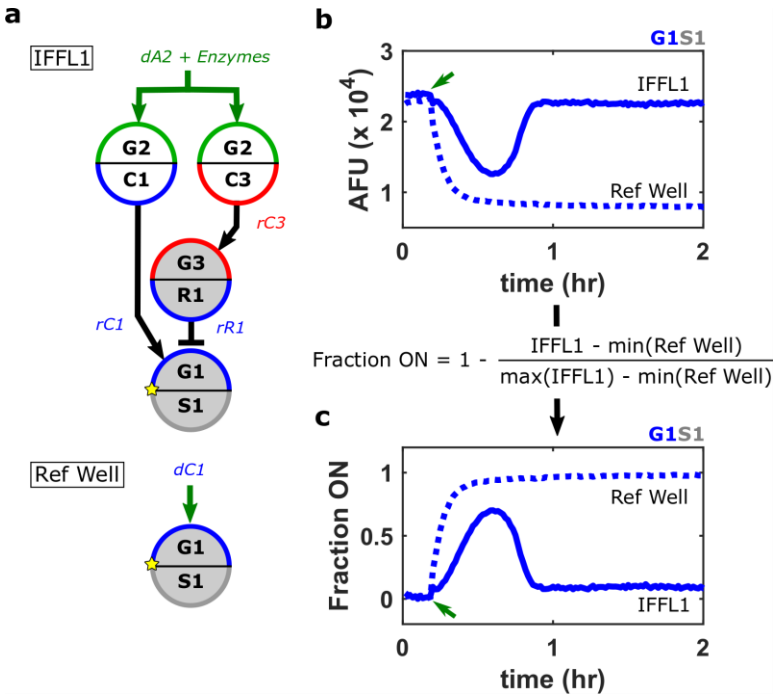

Supplementary Figure 61 | Normalization of pulse data. (**a**) Schematics of the nodes in an IFFL1 experiment and the corresponding reference well for normalizing G1S1. (**b**) Raw fluorescence data (arbitrary units) from the experiments in (**a**) depicting that G1S1 in the IFFL1 network does not reach the minimum value observed in the reference well. (**c**) Normalized activation levels of G1S1 using the minimum value obtained in the reference well. Green arrows indicate when the components above the green arrows in (a) were added to the samples. Experiments conducted as described for the IFFL1 with 250 nM of dA1.

13.3 Normalization of TSN data

Since not all of the activators were present at the beginning of the TSN experiments (Supporting Section 9.2), the data was normalized beginning at the time when all the activators were added.

For TSN experiments without state changes, a reference well containing all three reporting genelets and their activators was included in all of the experiments. This well was incubated in the qPCR in a quenched state over the course of the experiment to obtain a minimum fluorescence value for each reporting genelet. The reference well data was then used to find minimum fluorescence values of the reporting genelets that initially started in an OFF state in the experiments (Eq. 12).

For TSN experiments with a single state change, Eq. 11 was used for normalization.

For TSN experiments with more than one state change, data normalization was conducted in stages. This was done to account for changes in the minimum and maximum fluorescence values of the reporting nodes over the course of the experiments. In particular, the maximum fluorescence values of the reporting nodes that changed states more than once were always lower after the second state change than at the beginning of the experiments. The addition of excess DNA repressors in these experiments indicates that the maximum fluorescence values obtained after the second state changes correspond to the maximum fluorescence values of these nodes (Supplementary Figure 62a). The drop in maximum fluorescence could be due to dilution and DNA binding to the pipette tips from the numerous additions and mixing steps in these experiments and is consistent with previous observations[4,6,19]. To account for changes in the absolute range of fluorescence intensity in these experiments we normalized the

fluorescence data for the nodes that changed states more than once in two parts considering only the data of each state change in each normalization with Eq. 11. For example, the data in Region 1 in Supplementary Figure 62b for the reporting nodes that change states twice was normalized using only the data in that region (the *G1D data in the left plot and the *G4D data in the right plot). The data in Region 2 in Supplementary Figure 62b (corresponding to the rest of the experiment) for the reporting nodes that change states twice was then normalized using only the data in that region. This two-part normalization accounts for the change in absolute fluorescence values for nodes that change states multiple times (Supplementary Figure 62c).

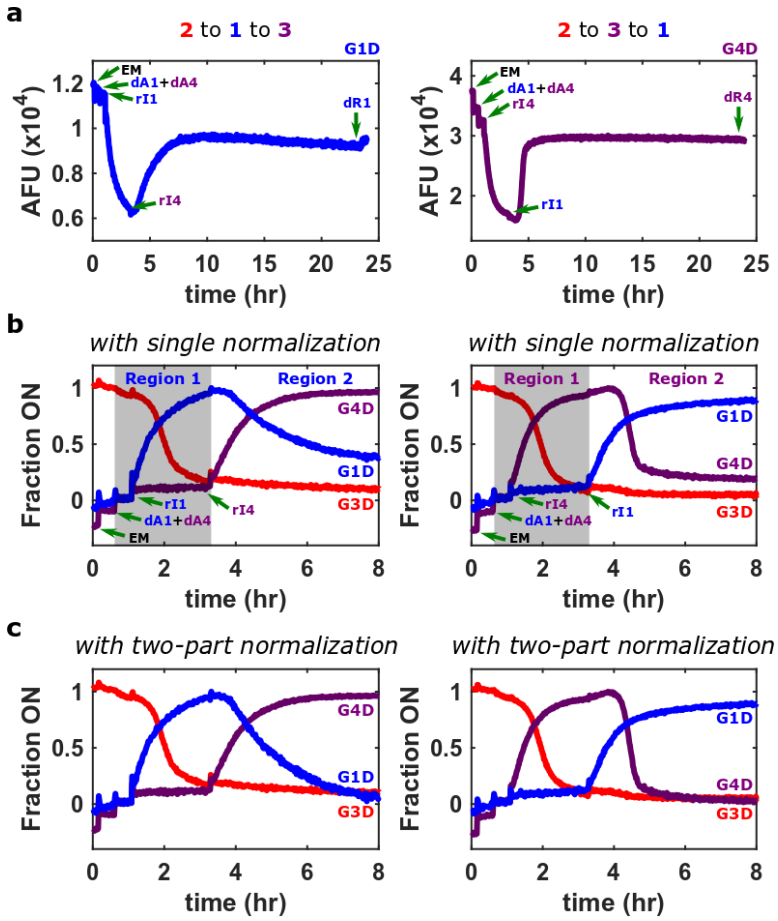

Supplementary Figure 62 | Representative normalization examples for nodes that change states multiple times in TSN experiments. (**a**) Raw fluorescence values (arbitrary units) of nodes that change states more than once in double state change experiments. Green arrows indicate the addition of different components. The enzyme mix (EM) for the reactions was added first to set the initial network states. The activators (dAi) of the other network states were then added which marks the beginning of the experiment. The inducer RNAs (rIi) that direct the state changes were then subsequently added. At the end of the experiments the DNA repressors for each reporting node were added (dRi). (**b**) The experimental results after a single normalization step using all of the data in Region 1 and Region 2. Region 2 also extends (**c**) The experimental results where the data of the nodes in (a) has been normalized in two parts (Region 1 then Region 2). Experiments were conducted as described in Figure 5 of the main text.

13.4 Normalization of BS_IFFL1|2, I_BS_IFFL1|2, and I_BS_IFFL1|2_FB1 data

The reporting nodes in the bi-stable module (*G7D and *G8D) were normalized as described for the TSN without state changes and with single state changes (Supplementary Section 13.3). The reporting nodes IFFL1 and IFFL2 (G1S1 and G4S1) were normalized as described in Supplementary Section 13.2 using reference wells for both the G1S1 and G4S1 nodes.

REFERENCES

1. Pleiss, J. A., Derrick, M. L. & Uhlenbeck, O. C. T7 RNA polymerase produces 5' end heterogeneity during in vitro transcription from certain templates. *RNA* **4**, 1313–1317 (1998).
2. Milligan, J. F., Groebe, D. R., Witherell, G. W. & Uhlenbeck, O. C. Oligoribonucleotide synthesis using T7 RNA polymerase and synthetic DNA templates. *Nucleic Acids Res.* **15**, 8783–8798 (1987).
3. Rong, M., Durbin, R. K. & McAllister, W. T. Template strand switching by T7 RNA polymerase. *J. Biol. Chem.* **273**, 10253–10260 (1998).
4. Schaffter, S. W. & Schulman, R. Building in vitro transcriptional regulatory networks by successively integrating multiple functional circuit modules. *Nature Chemistry* **11**, 829–838 (2019).
5. Schenborn, E. T. & Mierendorf, R. C. A novel transcription property of SP6 and T7 RNA polymerases: dependence on template structure. *Nucleic Acids Res.* **13**, 6223–6236 (1985).
6. Kim, J., White, K. S. & Winfree, E. Construction of an in vitro bistable circuit from synthetic transcriptional switches. *Mol. Syst. Biol.* **2**, 68 (2006).
7. Krupp, G. RNA synthesis: strategies for the use of bacteriophage RNA polymerases. *Gene* **72**, 75–89 (1988).
8. McGinness, K. E. & Joyce, G. F. Substitution of Ribonucleotides in the T7 RNA Polymerase Promoter Element. *Journal of Biological Chemistry* **277**, 2987–2991 (2002).
9. Kim, J. & Winfree, E. Synthetic in vitro transcriptional oscillators. *Mol. Syst. Biol.* **7**, 465 (2011).
10. Kuzmine, I., Gottlieb, P. A. & Martin, C. T. Binding of the priming nucleotide in the initiation of transcription by T7 RNA polymerase. *J. Biol. Chem.* **278**, 2819–2823 (2003).
11. Martin, C. T., Muller, D. K. & Coleman, J. E. Processivity in early stages of transcription by T7 RNA polymerase. *Biochemistry* **27**, 3966–3974 (1988).
12. Arnaud-Barbe, N., Cheynet-Sauvion, V., Oriol, G., Mandrand, B. & Mallet, F. Transcription of RNA templates by T7 RNA polymerase. *Nucleic Acids Res.* **26**, 3550–3554 (1998).
13. Kar, S. & Ellington, A. D. In vitro transcription networks based on hairpin promoter switches. *ACS Synth. Biol.* **7**, 1937–1945 (2018).
14. Zadeh, J. N. *et al.* NUPACK: Analysis and design of nucleic acid systems. *J. Comput. Chem.* **32**, 170–173 (2011).
15. Schneider, T. D. & Stephens, R. M. Sequence logos: a new way to display consensus sequences. *Nucleic Acids Res.* **18**, 6097–6100 (1990).
16. Krupp, G. Unusual promoter-independent transcription reactions with bacteriophage RNA polymerases. *Nucleic Acids Res.* **17**, 3023–3036 (1989).
17. Anderson-Lee, J. *et al.* Principles for Predicting RNA Secondary Structure Design Difficulty. *Journal of Molecular Biology* **428**, 748–757 (2016).
18. Kim, J., Hopfield, J. & Winfree, E. Neural network computation by in vitro transcriptional circuits. in *Advances in Neural Information Processing Systems 17* (eds. Saul, L. K., Weiss, Y. & Bottou, L.) 681–688 (MIT Press, Boston, MA, 2005).
19. Franco, E. *et al.* Timing molecular motion and production with a synthetic transcriptional clock. *Proc. Natl. Acad. Sci. USA* **108**, E784–E793 (2011).

20. Cuba Samaniego, C., Giordano, G., Kim, J., Blanchini, F. & Franco, E. Molecular titration promotes oscillations and bistability in minimal network models with monomeric regulators. *ACS Synth. Biol.* **5**, 321–333 (2016).
21. Lapham, J. & Crothers, D. M. RNase H cleavage for processing of in vitro transcribed RNA for NMR studies and RNA ligation. *RNA* **2**, 289–296 (1996).